

IBAAS-JNARDDC 2022 TECHNICAL LECTURE SERIES

REVIEW OF 50 YEARS OF HALL-HÉROULT CELL MODELS DEVELOPMENT



Dr. MARC DUPUIS
GENISM **HATCH**

About the Presenter

- **Name:** Dr. Marc Dupuis
- **Degrees and date earned:** Ph.D. Chemical Engineering 1984
- **Main affiliation:** GeniSim Inc. since 1994
- **Second affiliation:** Hatch since 2019
- **Present position:** Consultant since 1994
- **Work experience:** Mathematical modelling and design of H.H. cells dealing with thermo-electric, thermo-electro-mechanical, CFD and MHD phenomena.

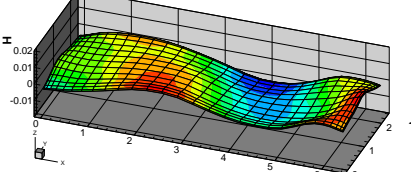
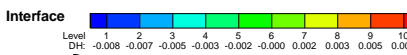
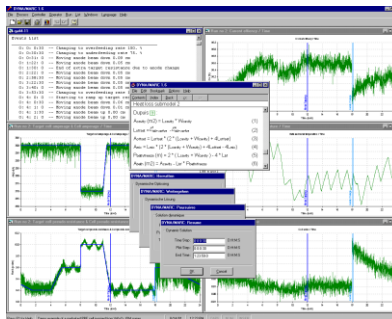
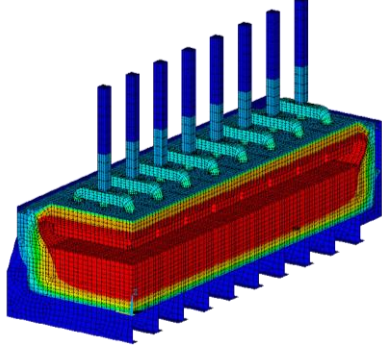
About the Presenter



GeniSim Inc.

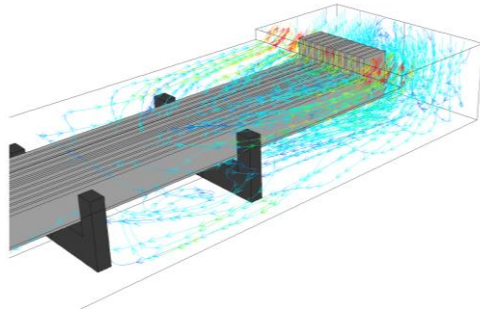
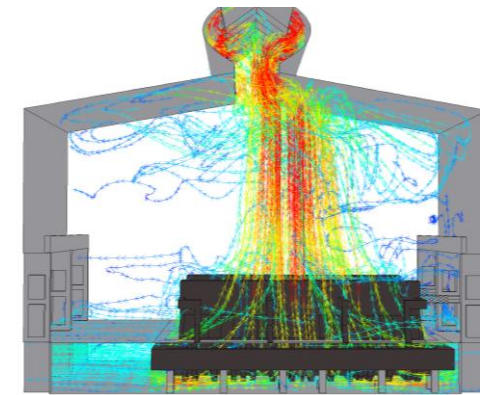
Clients list

- **3D ANSYS® T/E models:**
Alcan, Alumax, Reynolds, Hoogovens, Alcoa, Noranda, Sumitomo, Indal, Nalco, SAMI, Comalco, NEUI, Dubal, GAMI, Inalum
- **Dyna/Marc cell simulator:**
Alcan, Alusuisse, VAW, Alumax, Reynolds, Hoogovens, Hydro Aluminium, Alcoa, Rio Tinto
- **MHD-Valdis:**
SAMI, NEUI, Dubal, GAMI, Rusal, Hydro Aluminium, Inalum



Hatch's Center of Excellence for Aluminium

- Hatch is a leading company for the development, construction and expansion of aluminium smelters, and is involved daily in smelters operations support and sustaining capital projects.
- Hatch's expertise is anchored in process knowledge and experience covering all areas of the plant.
- To support its projects, Hatch has also developed specialized numerical tools of different aspects of the Reduction Area, including busbars thermo-electro-mechanical models, laminated flexibles mechanical models, anode beam mechanical system model, potroom ventilation models, potline and casthouse metal flow logistics models, relining operations logistics models, etc.



Plan of the Presentation

- The thermo-electric cell heat balance model
- The magneto-hydrodynamic (MHD) cell stability model
- The bath bubble flow driven CFD model
- The alumina dissolution, dispersion and consumption CFD model
- The multi-physic model that is a merge of the above 4 models
- The thermo-chemo-mechanical potshell deformation model
- The potroom ventilation CFD model

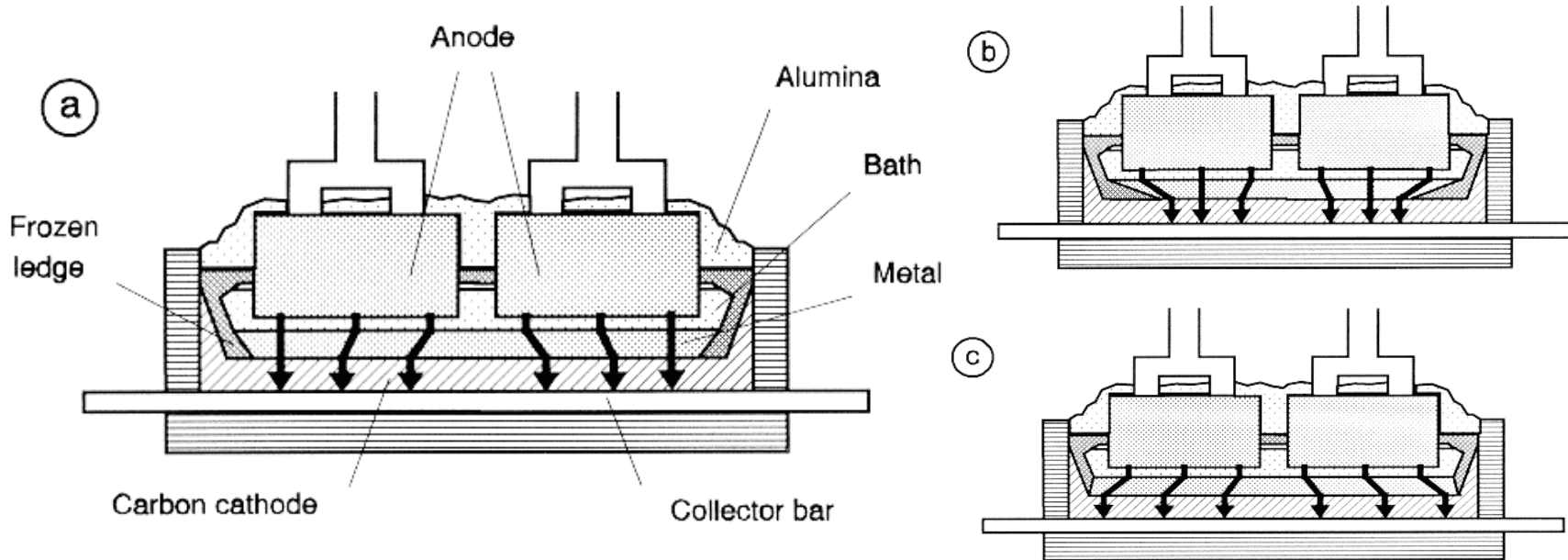


Plan of the Presentation

- The thermo-electro-mechanical anode and cathode models
- The transient thermo-electro-mechanical cathode preheating model
- The transient thermo-mechanical cathode cooling model
- The busbar and flexes thermo-electro-mechanical models
- The lump parameters dynamic cell simulator model
- The multi-zones dynamic cell simulator model
- The cell digital twin

Cell Heat Balance Model

- The cell heat balance model was developed to address this problem: you want a) not b) not c)

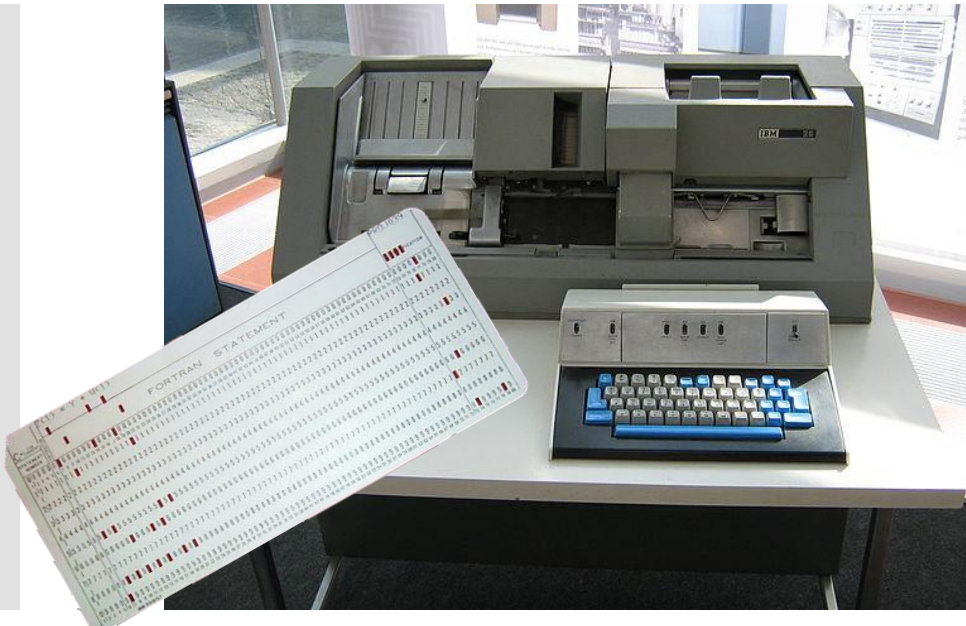


Cell Heat Balance Model

- Oldest type of cell mathematical model, this is a sample of Haupin's code from the 50's

```
HEAT BALANCE AND
C.E. COMPUTATION

7 0 FH=0.74+ 0.065*Z2
8 0 QA=(0.025*(AH-3.)+0.034*EL1+0.
8 1 15*Z1)*AN*FT*FH
9 0 QAS=0.0535*AAS*FT*FH
10 0 QC=(0.70/B+0.25/(B*B*B))1*(1.+0.
10 1 .09*EL1)*AC*FT*FH
11 0 QCO=(0.04*TB-26.0)*TO*A0/1440.
12 0 QB=(TB-TR)/(1897.0*RB)
13 0 QCB=0.0425*ACB*FT
```



Cell Heat Balance Model

- This is the time line of the development of Alcoa in house cell heat balance model: HTBAL

Calculating resistances of lanes.

$$R_a = l_{1a}/(k_{1a}W_{1a}P_{1a}) + l_{2a}/(k_{2a}W_{2a}P_{2a}) + l_{3a}/(k_{3a}W_{3a}P_{3a}) + l_{4a}/(k_{4a}W_{4a}P_{4a}) + 1/(h_sW_{4a}P_{4a}F_a)$$

Where k_i is thermal conductivity of material i , P is the perimeter around the cell at this position. h_s is the combined radiation and convection heat transfer coefficient of the shell. F_i takes care of the fin effect of struts and cell reinforcements:

$$F_i = 1 + E_f (A_F / A_S),$$

A_F is the surface area of fin like structures attached to the shell. A_s is the area of the shell, F_F is the fin efficiency

$$E_\varepsilon \equiv \{\tanh [(2h_s/k t_\varepsilon)^{0.5} W_\varepsilon]\} / [(2h_s/k t_\varepsilon)^{0.5} W_\varepsilon]$$

Where: t_f is the fin thickness, W_f is the average width (extending out from shell) of the fin, k is the thermal conductivity of steel.

R_+ and R_- are calculated similar to R_0 .

$$R_d = l_{1d} / (k_{1d} W_{1d} P_{1d}) + l_{2d} / (k_{2d} W_{2d} P_{2d}) + l_{3d} / (k_{3d} W_{3d} P_{3d}) + 1 / (h_s W_{3d} P_{3d} F_d) + l_{4d} / (k_{4d} W_{4d} P_{4d}) + l_{5d} / (k_{5d} W_{5d} P_{5d}) + l_{6d} / (k_{6d} W_{6d} P_{6d}) + 1 / (h_w W_{6d} P_{6d} F_d)$$

$$R_1 \equiv |z_1|/(k_1 \cdot W_1 \cdot P_{1-}) + |z_2|/(k_2 \cdot W_2 \cdot P_{2-}) + |z_3|/(k_3 \cdot W_3 \cdot P_{3-}) + 1/(h \cdot W_3 \cdot P_{3-} \cdot E_1)$$

$$R_f = l_{1f} / (k_{1f} W_{1f} P_{1f}) + l_{2f} / (k_{2f} W_{2f} P_{2f}) + l_{3f} / (k_{3f} W_{3f} P_{3f}) + 1 / (h_s W_{3f} P_{3f} F_f) + l_{4f} / (k_{4f} W_{4f} P_{4f}) + l_{5f} / (k_{5f} W_{5f} P_{5f}) + l_{6f} / (k_{6f} W_{6f} P_{6f}) + 1 / (h_c W_{c} P_c F_c)$$

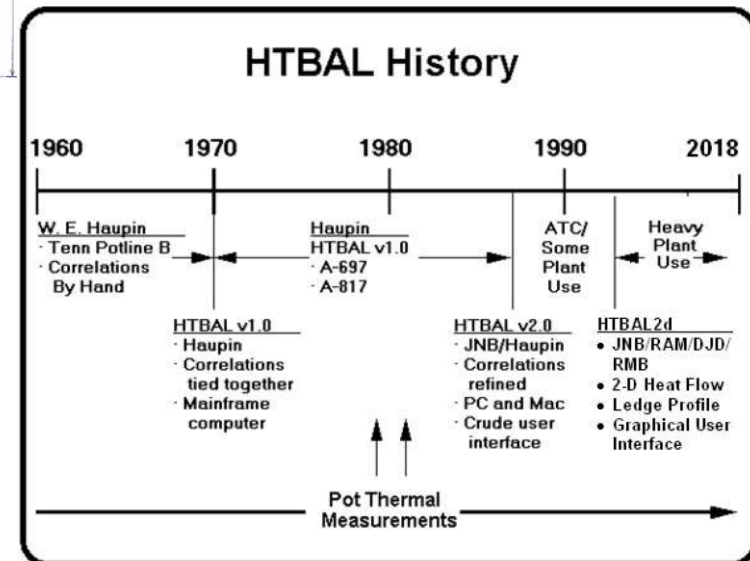
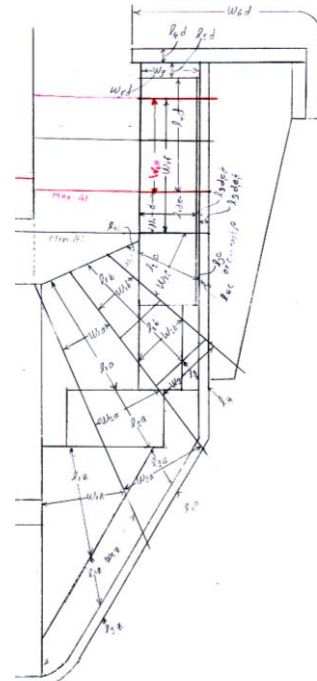


Figure 1.1: HTBAI Evolution Timeline



Cell Heat Balance Model

- This led to the 2D in-house TE model HTBAL 2D presented at the TMS 1990 by Jay Bruggeman:

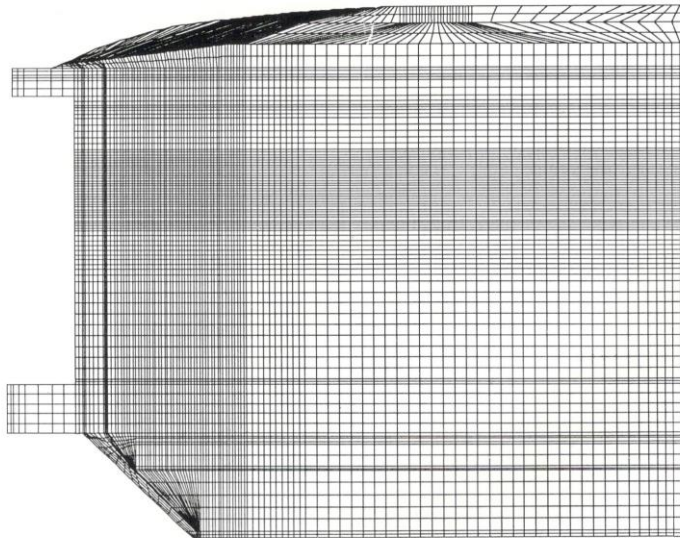


Figure 2: Finite element mesh for 2-D Hall-Heroult model.

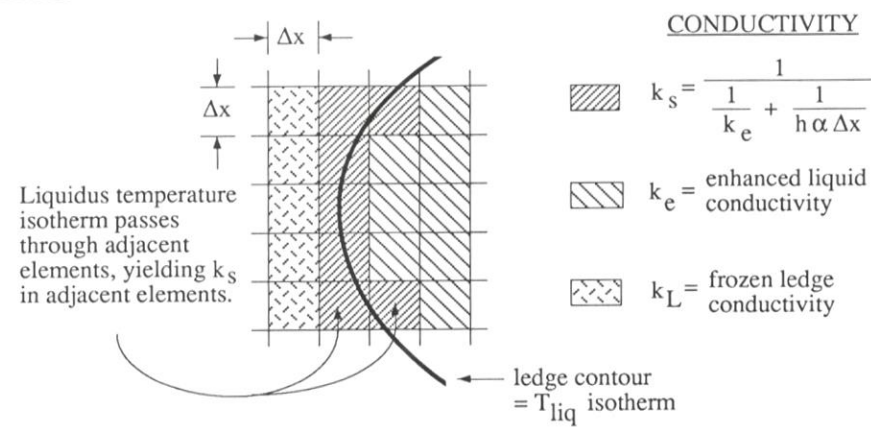
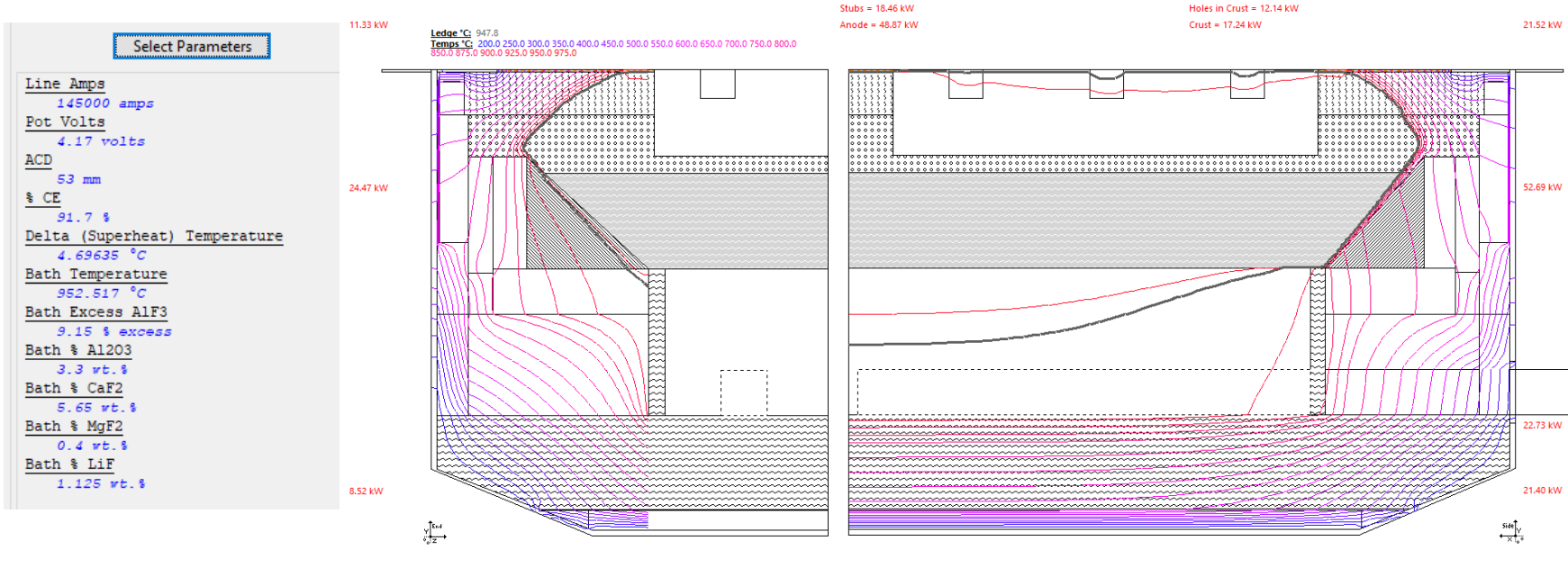


Figure 3: Element thermal conductivities in vicinity of ledge.

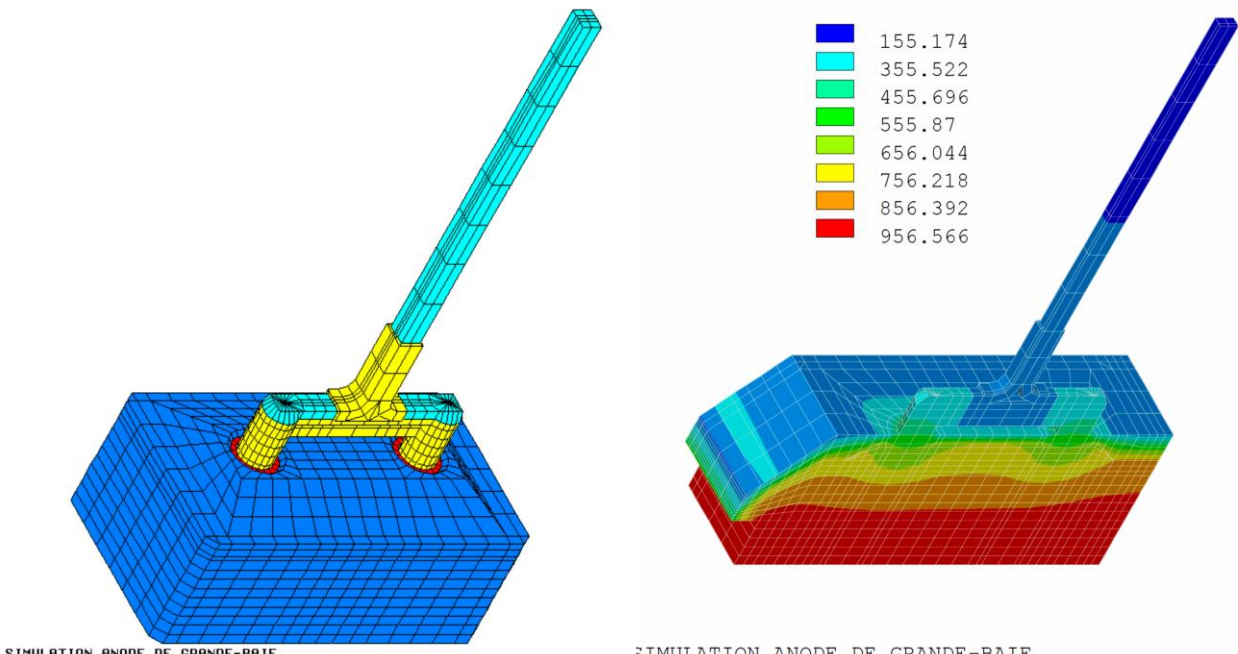
Cell Heat Balance Model

- HTBAL 2D is still in use in Alcoa smelters today:



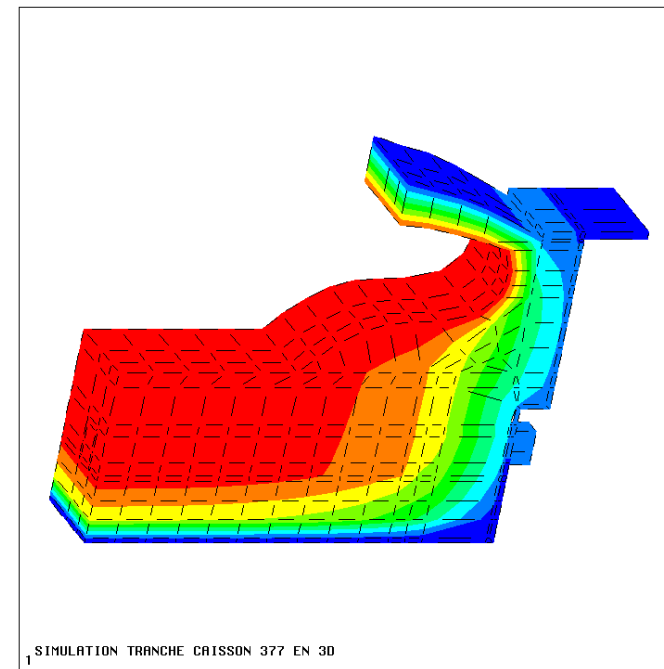
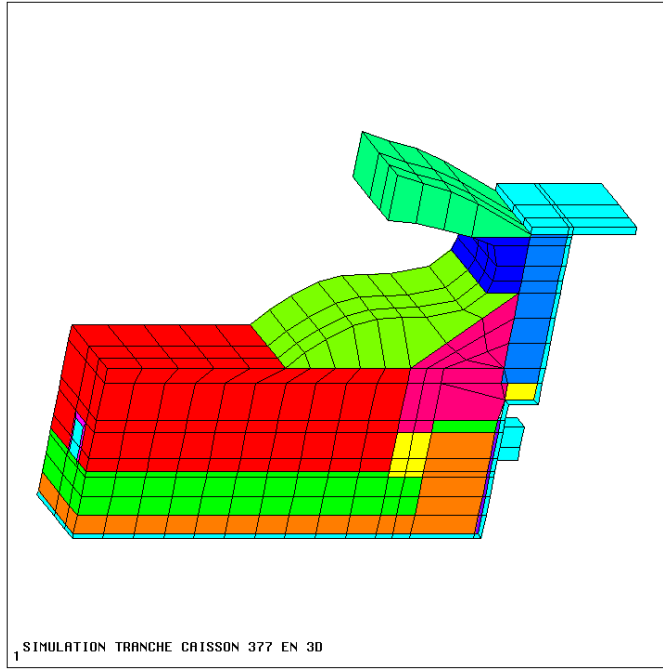
Cell Heat Balance Model

- I was hired by Alcan in 1984 to replace their 2D in house model called 2D Thermal by 3D ANSYS models



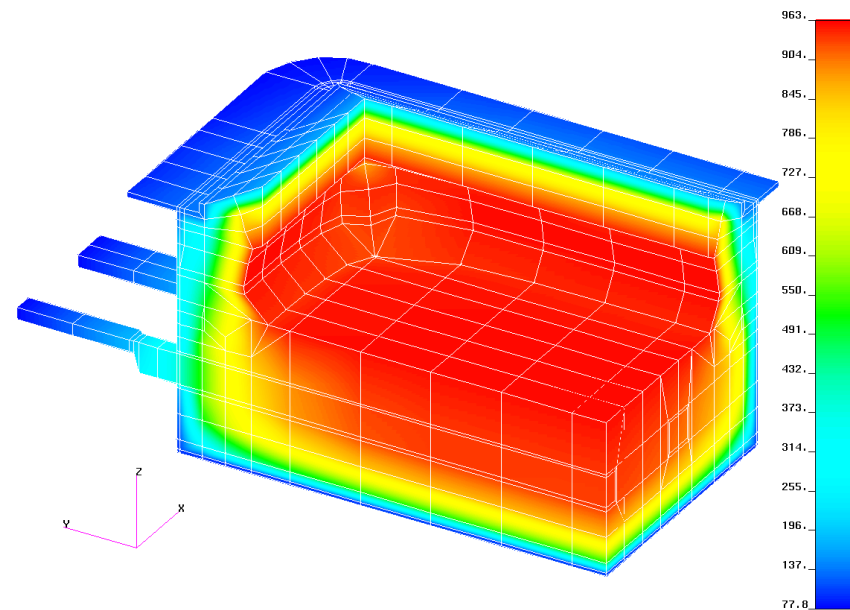
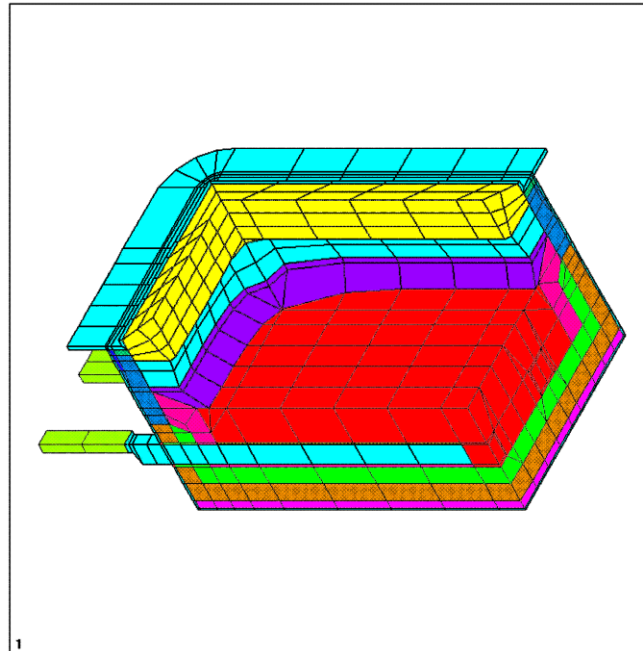
Cell Heat Balance Model

- I then developed the 3D TE cathode side slice model, here the Arvida step shell, side broken cell model



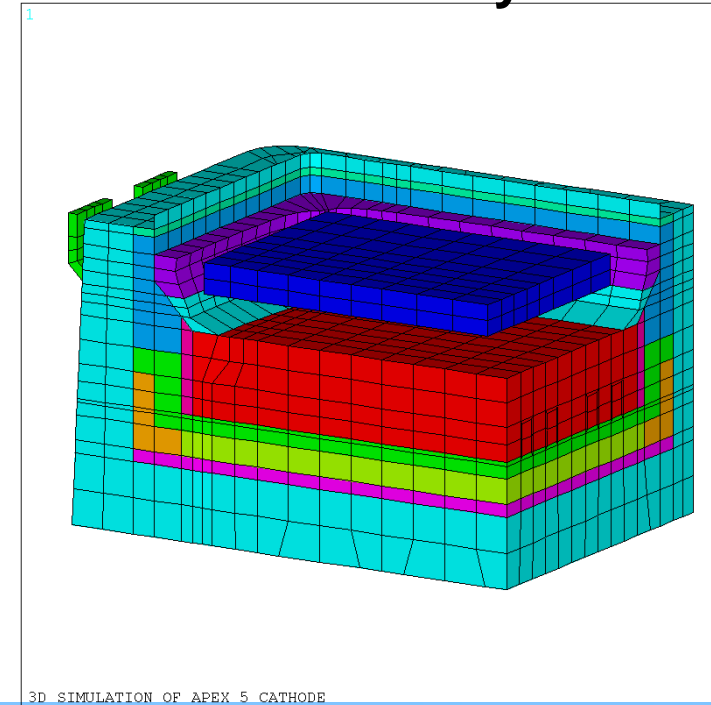
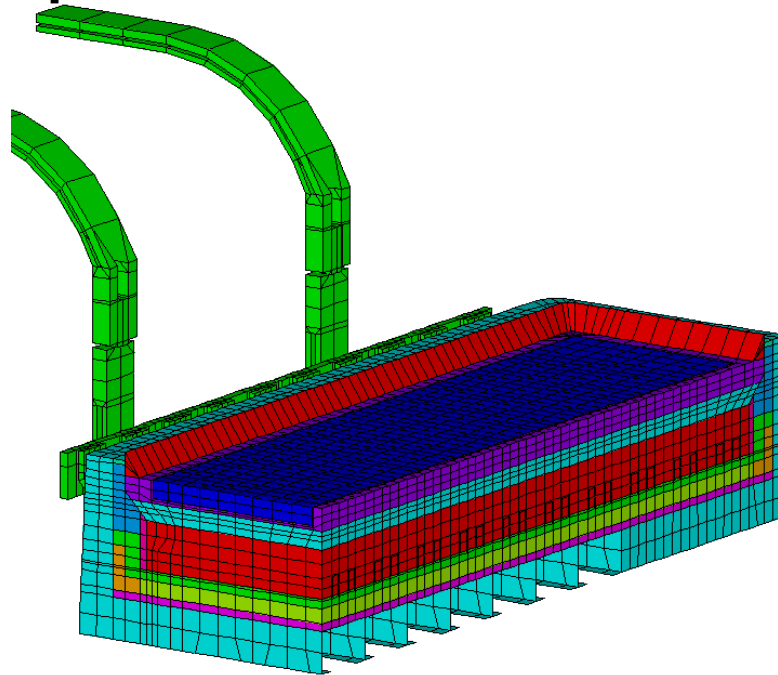
Cell Heat Balance Model

- Then the cathode corner model, notice that ledge profile convergence is part of the model solution



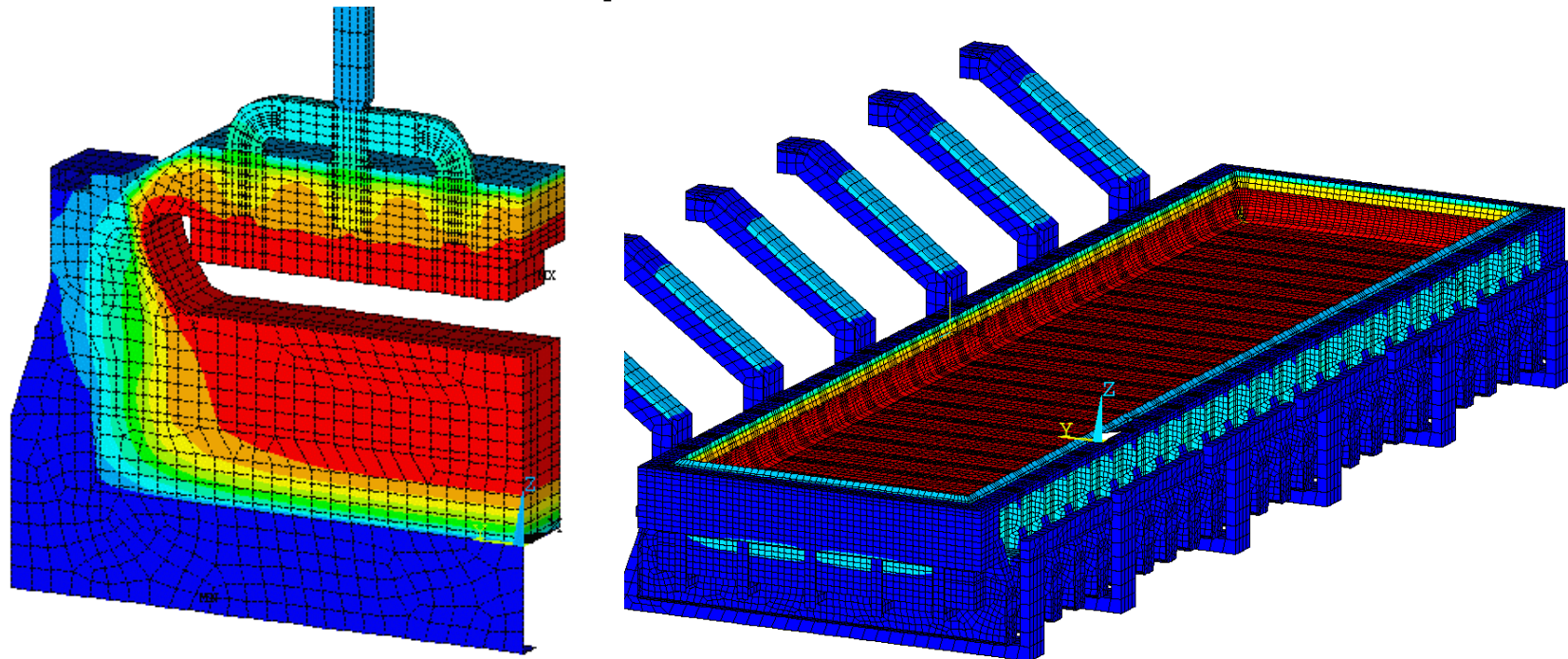
Cell Heat Balance Model

- Finally I developed the full 3D cell quarter model with liquid zone and busbar to compute current density



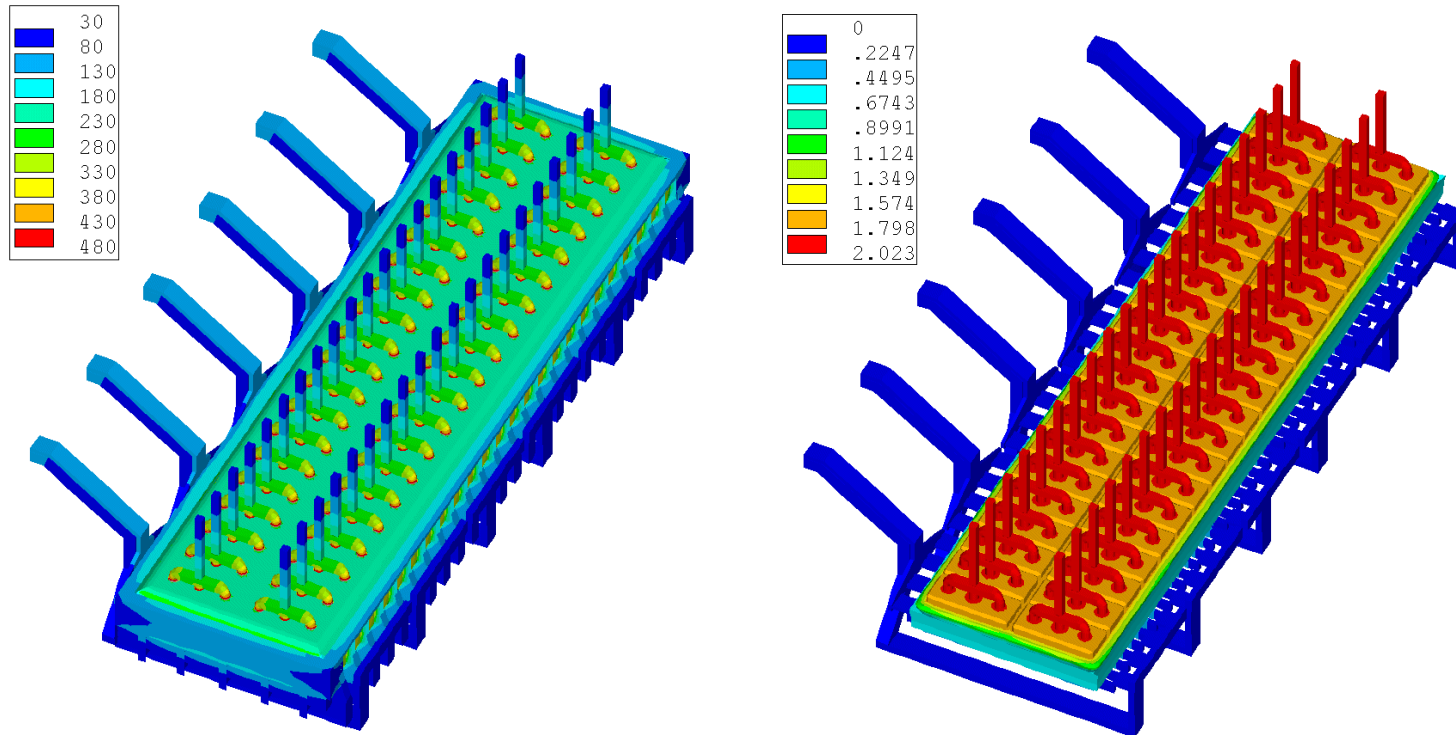
Cell Heat Balance Model

- Then as GeniSim, I developed the full cell slice and the full cell cathode with liquid zone and busbar



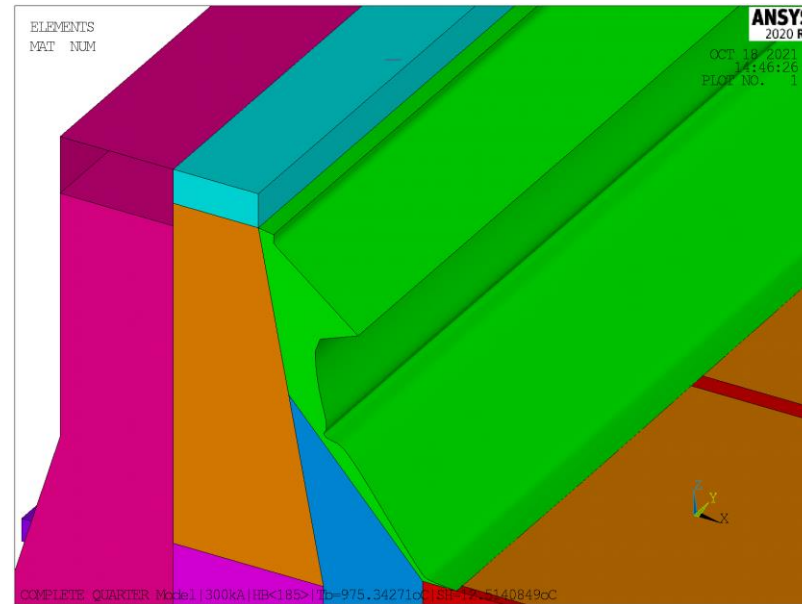
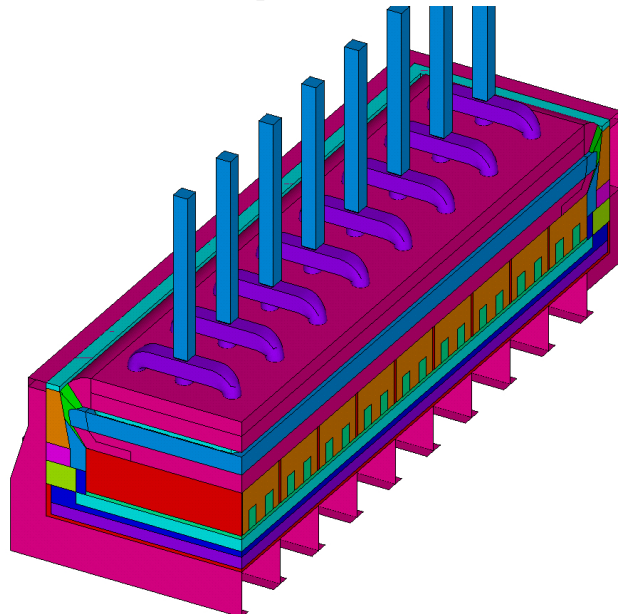
Cell Heat Balance Model

- And finally the full cell and busbar



Cell Heat Balance Model

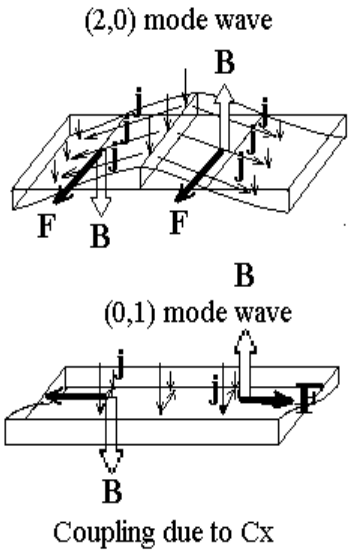
- All the previous models are based on MAPDL, very recently Hatch migrated the full cell quarter to ANSYS Workbench/SpaceClaim, with improved physics



Cell stability MHD Model

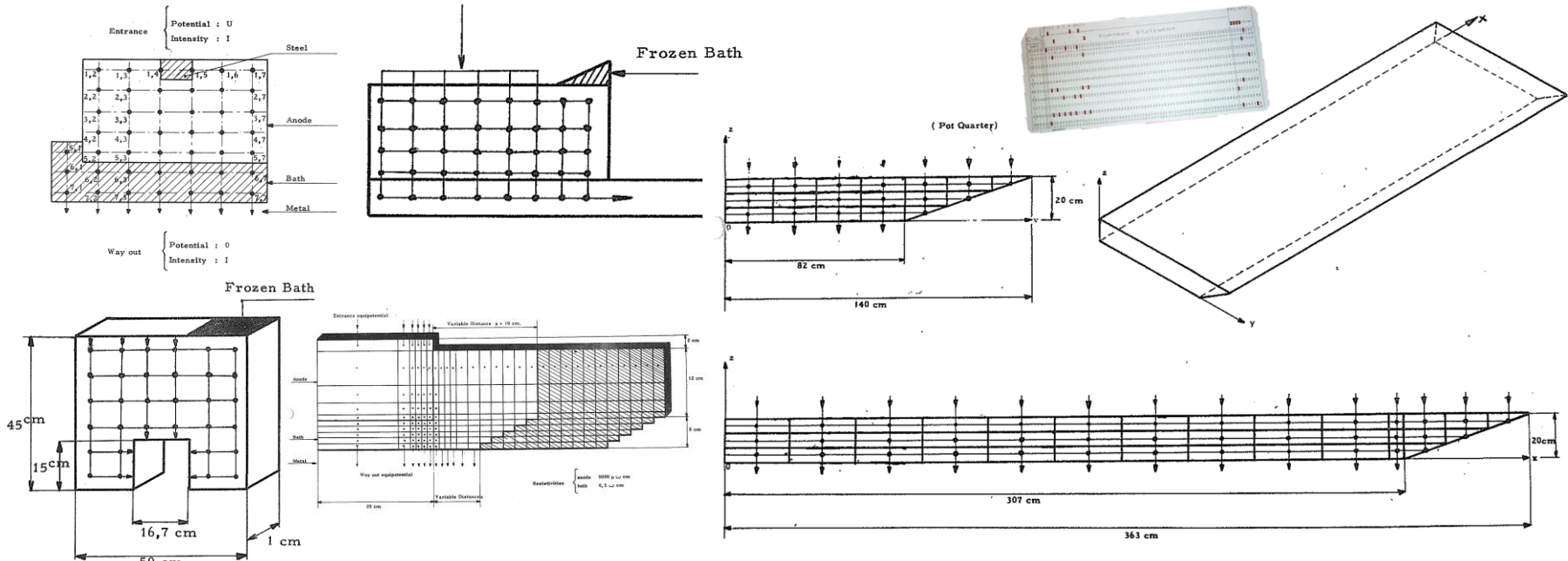
- The cell stability MHD model was developed to address this problem: you don't want this

- Cell stability influenced by C_x magnitude of B_z in metal pad
- B_z is the vertical component of the magnetic fields
- C_x is the gradient between the B_z positive value in one end of cell and the B_z negative value in the other end



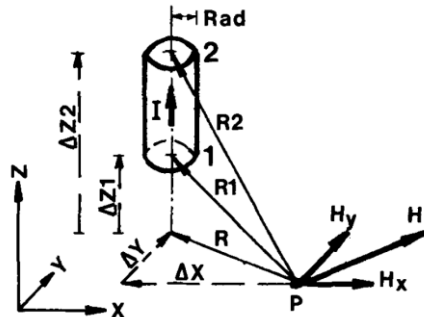
Cell stability MHD Model

- All MHD cell stability models start with current density calculation. Jivry (TMS 1965) was the



Cell stability MHD Model

- Then follows magnetic field calculation. Sele (TMS 1975) was a pioneer proposing to use dipoles.



$$H_x = \frac{\Delta Y \cdot I}{R} = \frac{\Delta Y \cdot I}{R^2} \left(\frac{\Delta Z_2}{R_2} - \frac{\Delta Z_1}{R_1} \right)$$

$$H_y = -\frac{\Delta X \cdot I}{R} = -\frac{\Delta X \cdot I}{R^2} \left(\frac{\Delta Z_2}{R_2} - \frac{\Delta Z_1}{R_1} \right)$$

$$\text{If } R < \text{Rad} : H = \frac{R}{\text{Rad}} \cdot H_{\text{Rad}}$$

Fig. 3—Magnetic field from current carrying conductor.

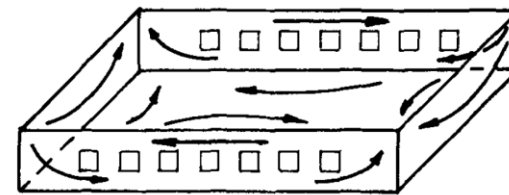


Fig. 6—Main magnetic flux in bottom shell.

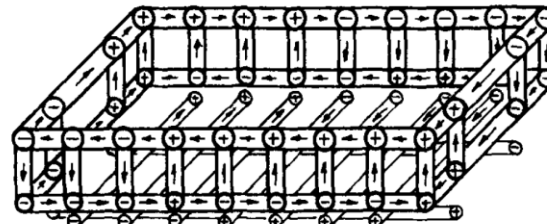
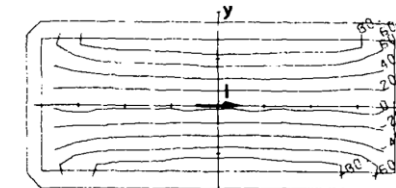
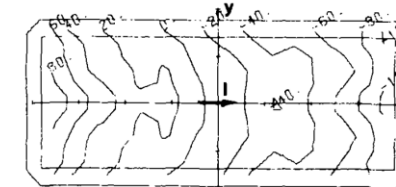


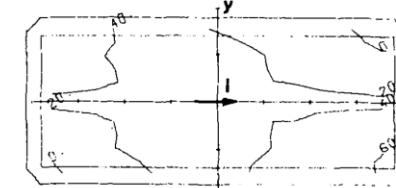
Fig. 7—Dipole model of bottom shell and support beams.



a) X-component.



b) Y-component.

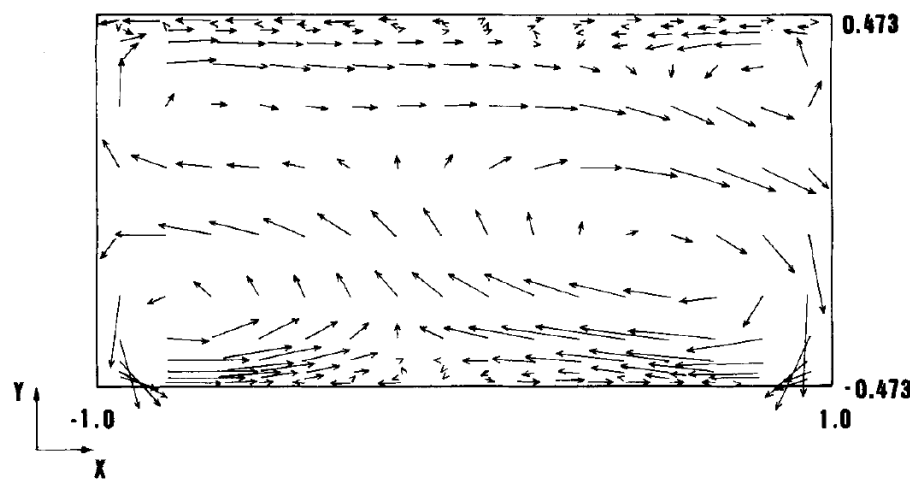
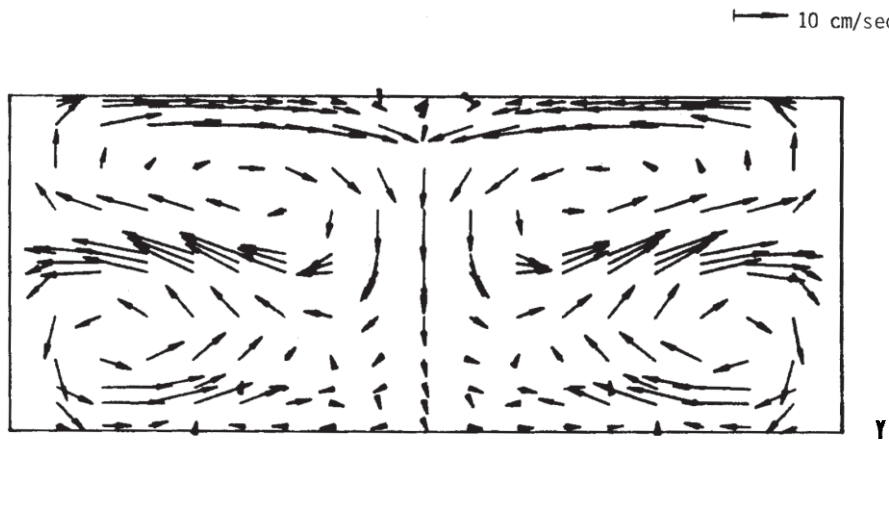


c) Z-component.

Fig. 8—Magnetic field in 150 kA cell.

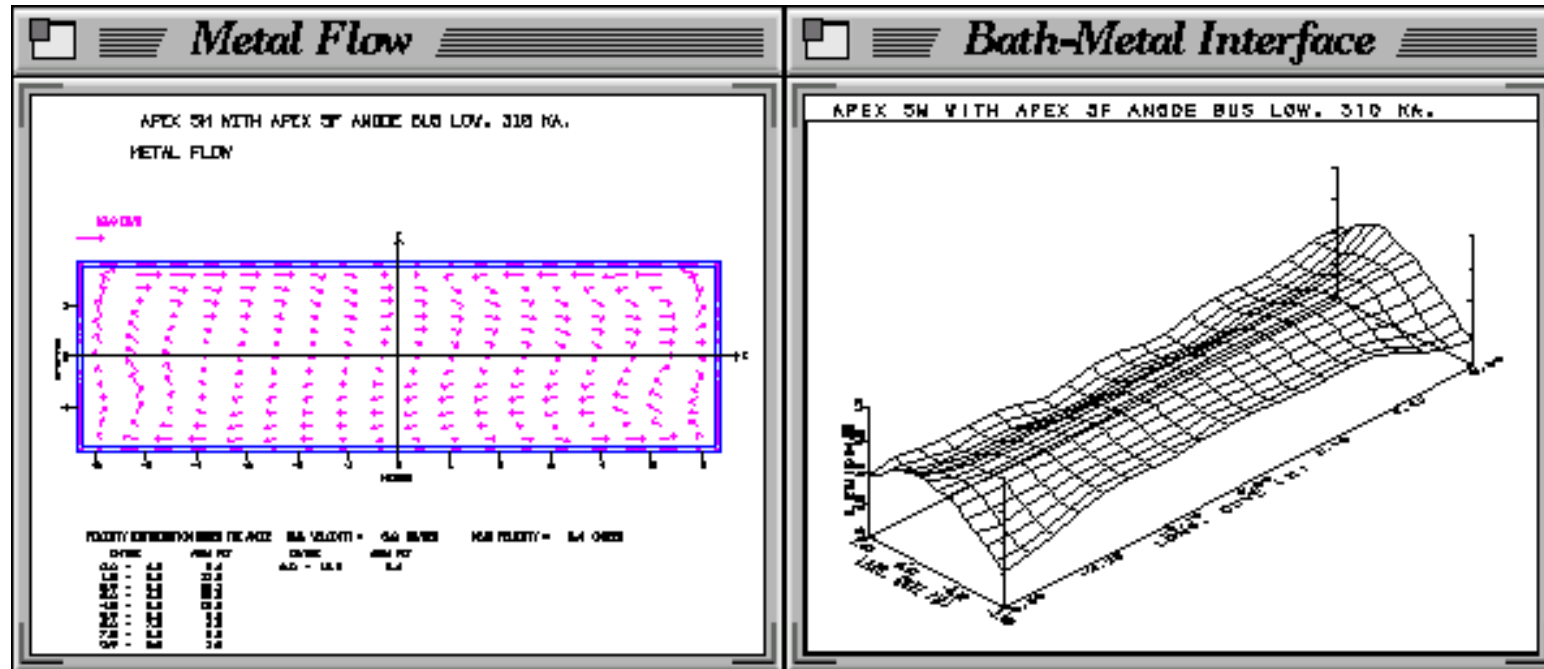
Cell stability MHD Model

- Urata was probably the first to publish MHD flows in 1975. Kaiser publish this flow (left) in TMS 1981. Moreau-Ziegler publish results of the Moreau-Evans MHD model in Trans B 1988 (right) and compared with the existing Kaiser model



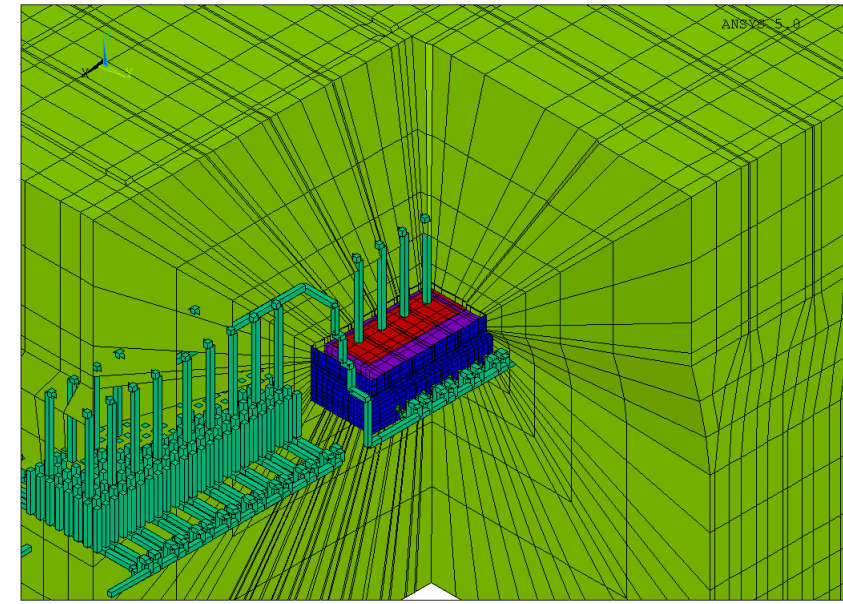
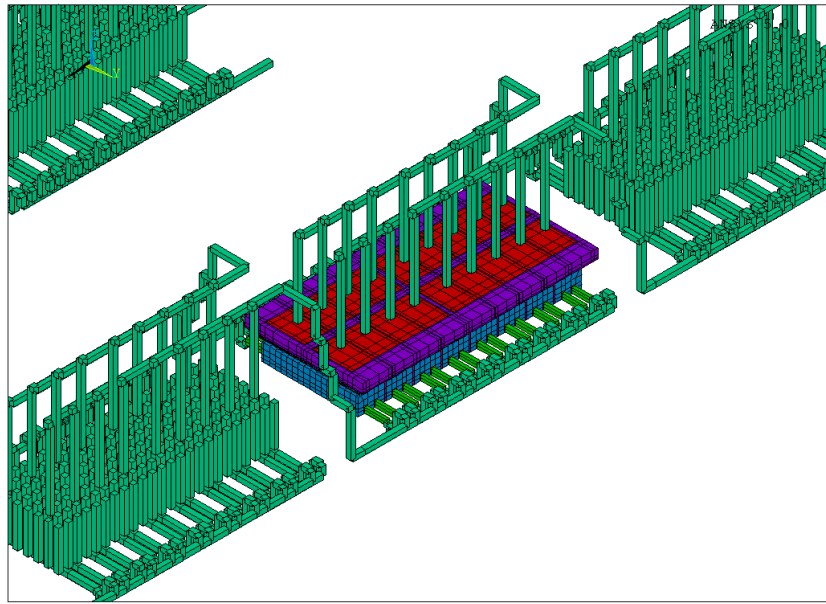
Cell stability MHD Model

- In the 80's Alcan was using TURBU to compute similar MHD flows, also computing the magnetic field with dipole



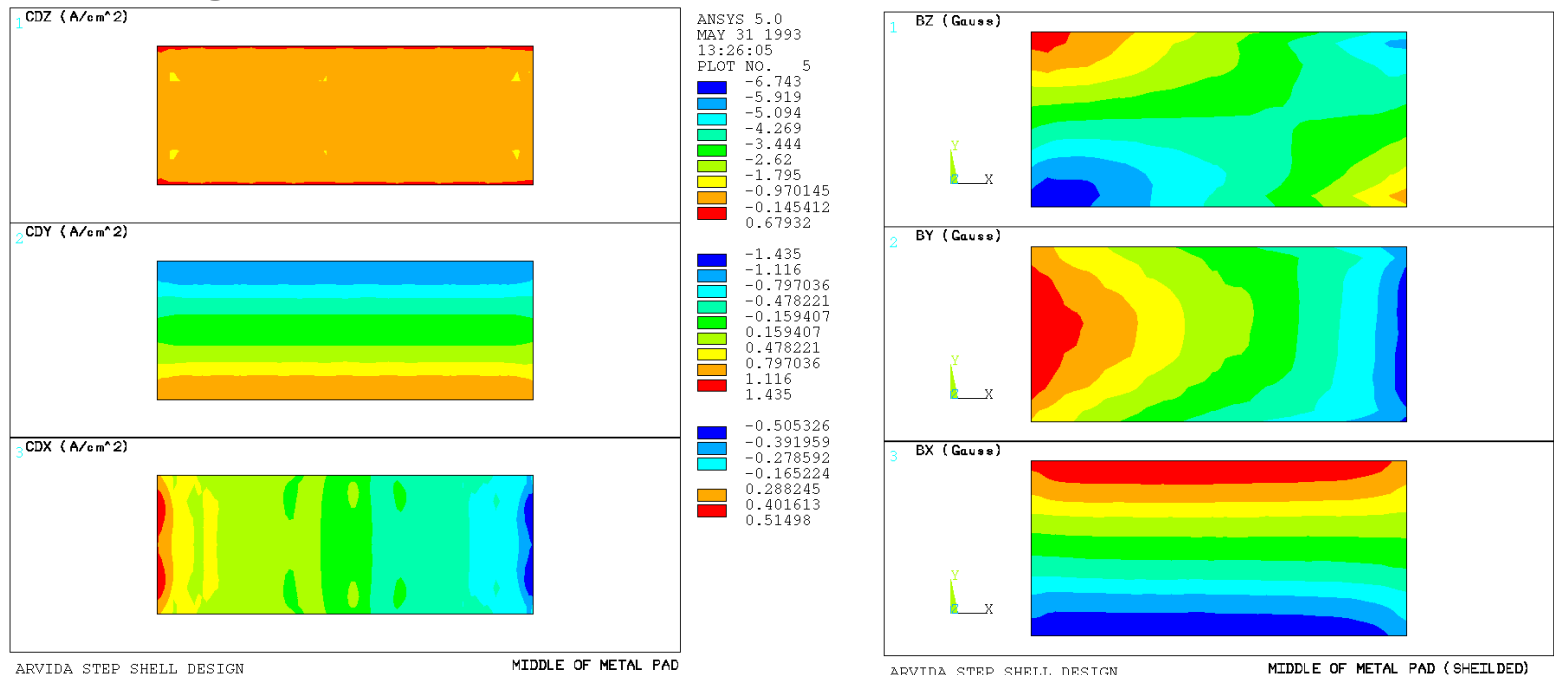
Cell stability MHD Model

- In the early 90's, I experimented using commercial software for the MHD model, ANSYS for the Lorentz force



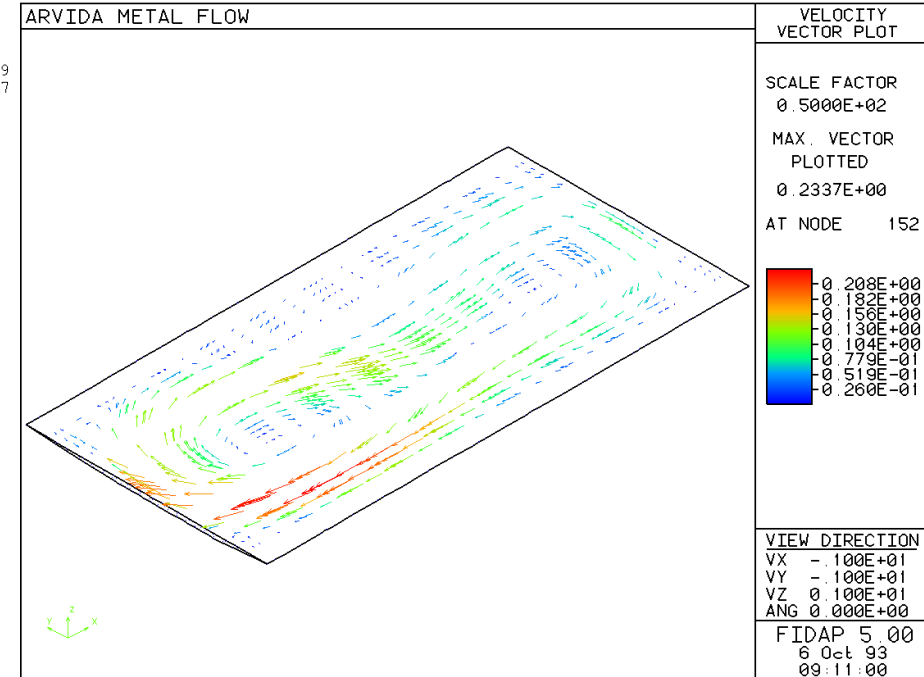
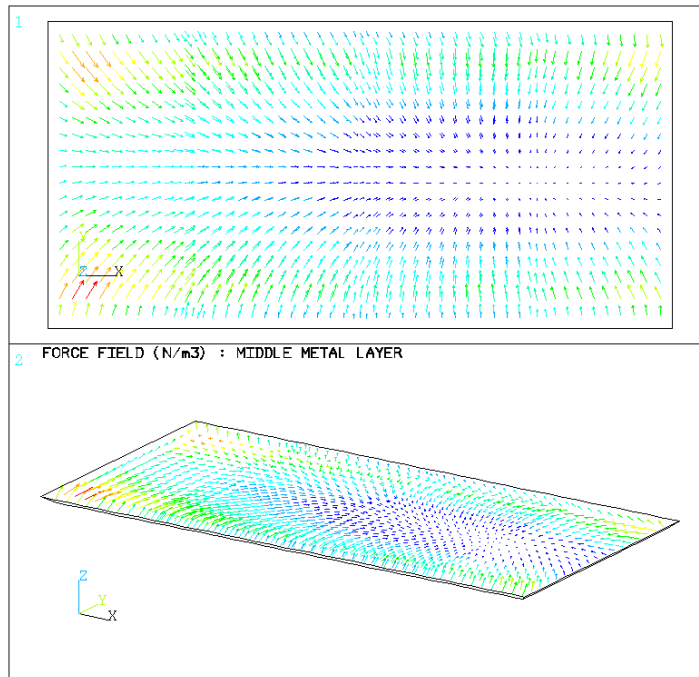
Cell stability MHD Model

- You get both the metal pad 3D current density solution and the magnetic field solution in the same model



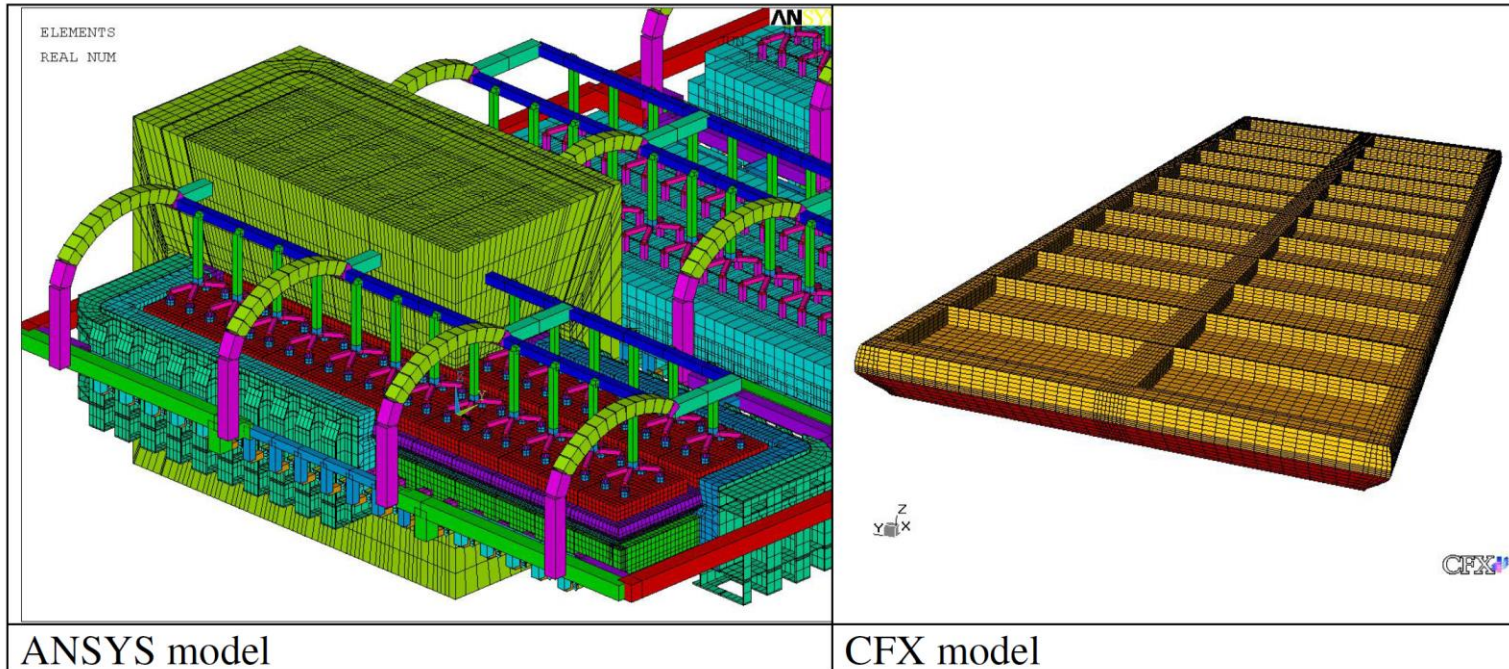
Cell stability MHD Model

- So the Lorentz force can be directly computed on the same mesh, the same mesh is used by Fidap for the metal flow



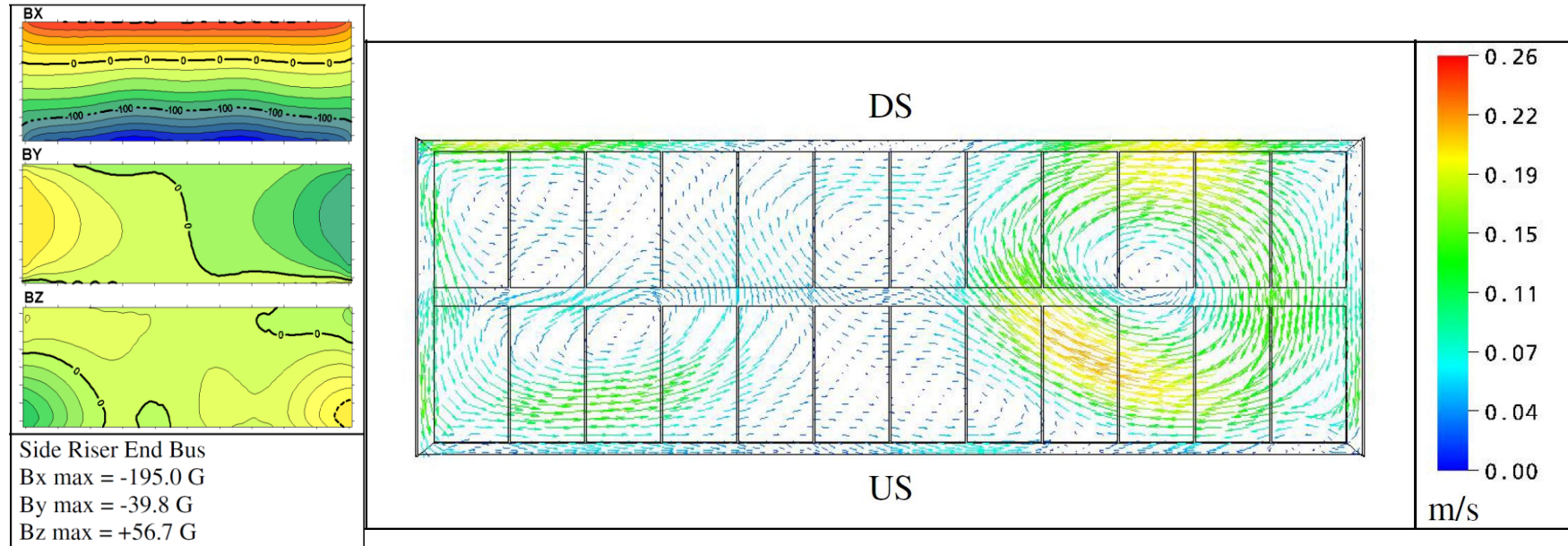
Cell stability MHD Model

- Caete (AASTC 2004) developed a similar full 3D MHD model using ANSYS and CFX using a much finer mesh



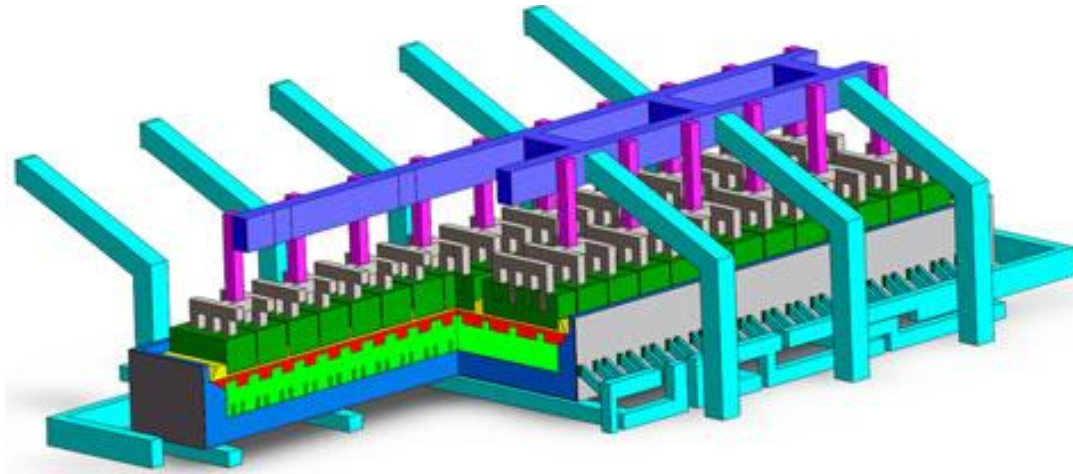
Cell stability MHD Model

- Obtained magnetic field on the left and metal flow on the right



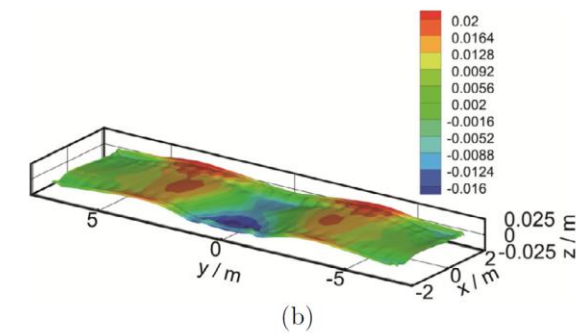
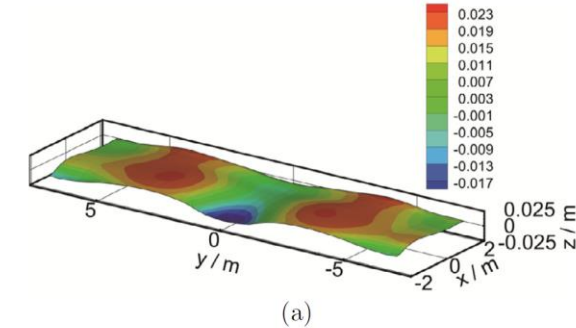
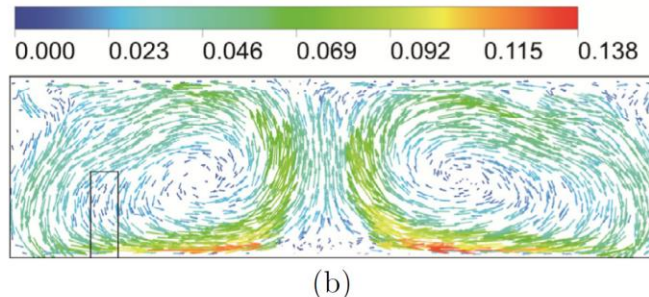
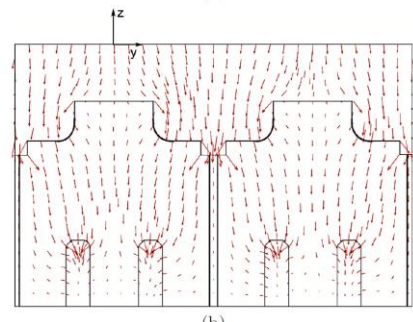
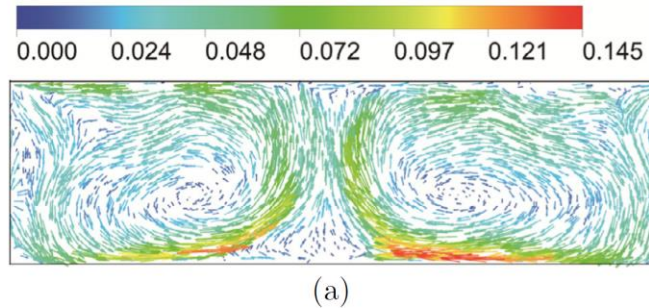
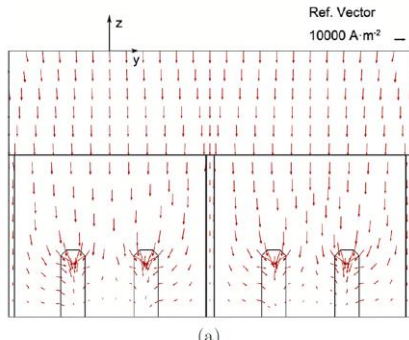
Cell stability MHD Model

- NEU in China used a 3D ANSYS-CFX MHD model to study the impact of irregular cathode technology (Trans B 2014)



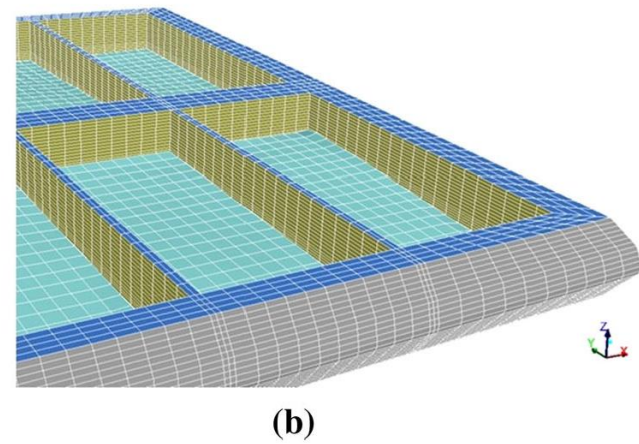
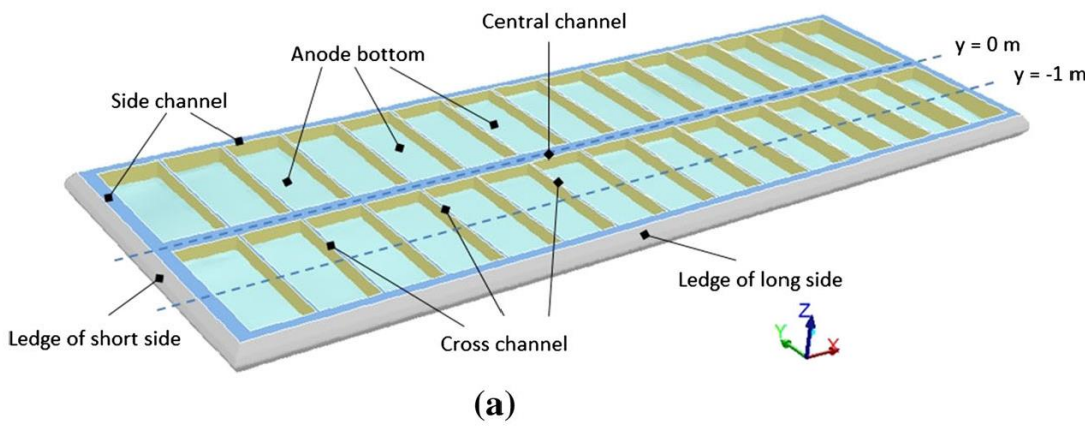
Cell stability MHD Model

- NEU published a second study using their 3D ANSYS-CFX MHD model still on irregular cathode design (Trans B 2016)



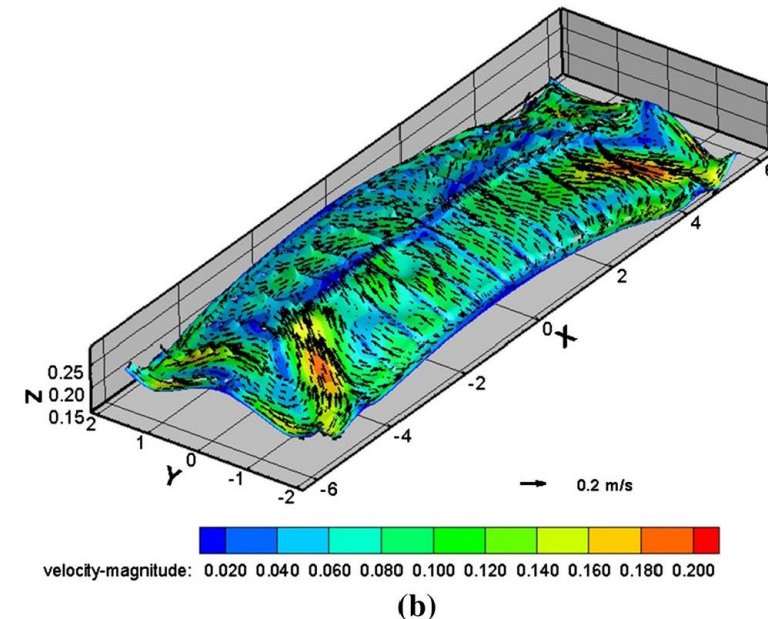
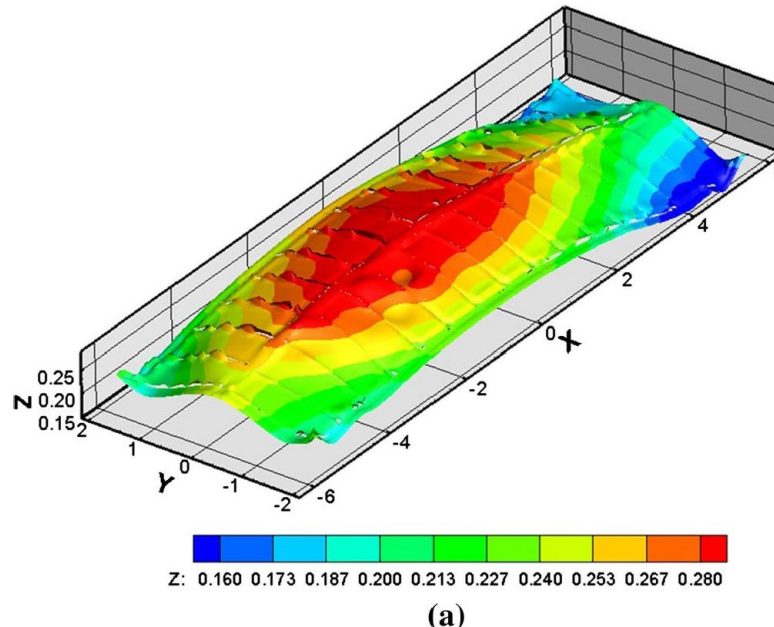
Cell stability MHD Model

- Hydro Aluminium very recently presented a 3D MHD model based on ANSYS and Fluent (Trans B 2018)



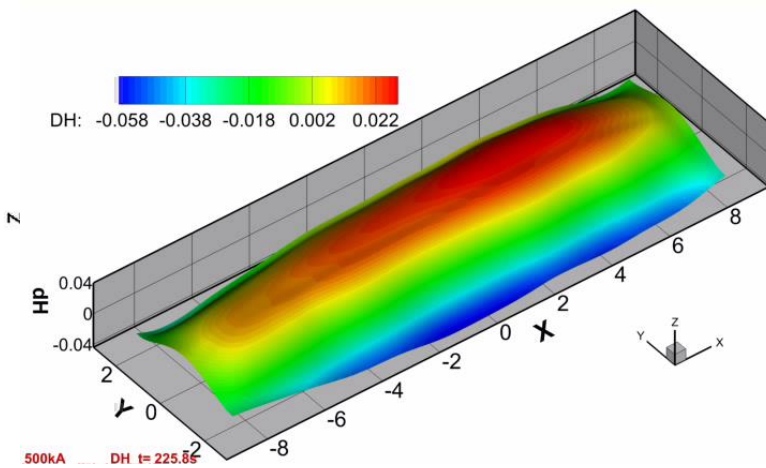
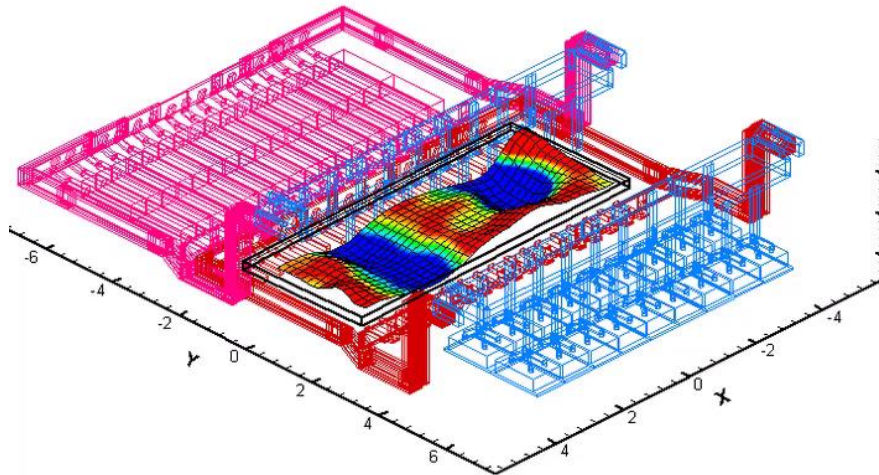
Cell stability MHD Model

- Bath-Metal interface for the open bath boundary condition in the Hydro Aluminium ANSYS/Fluent model



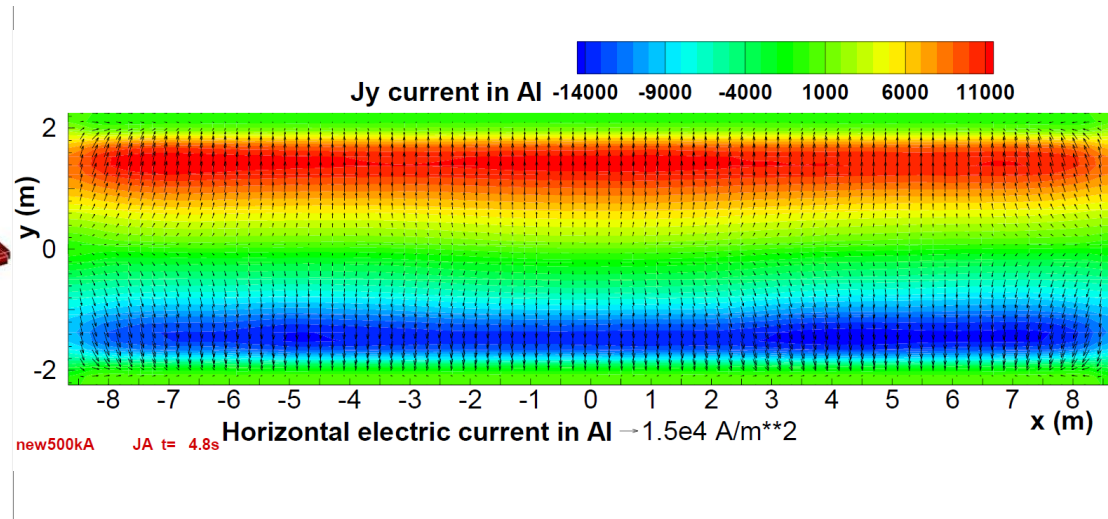
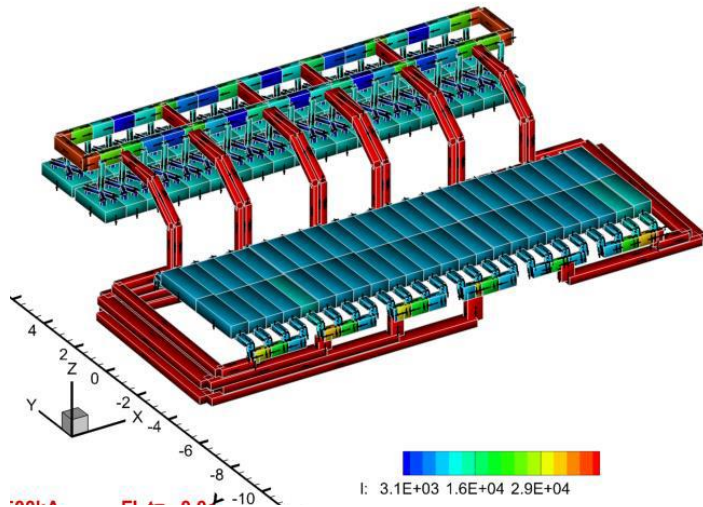
Cell stability MHD Model

- Full 3D MHD model are essentially only used to compute the steady-state solution, yet the cell stability is a dynamic problem, the specialized and optimized code MHD-Valdis is fast enough to solve for the transient evolution of the wave



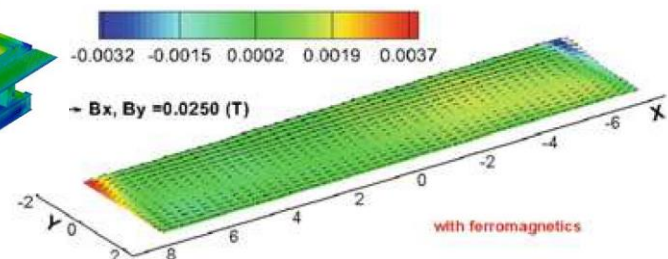
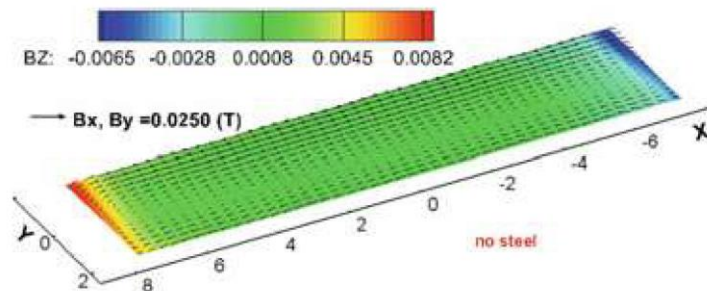
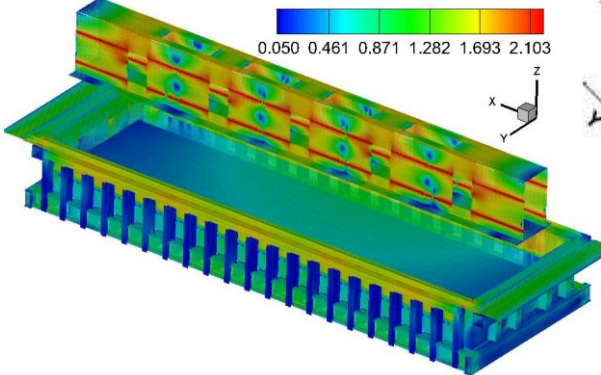
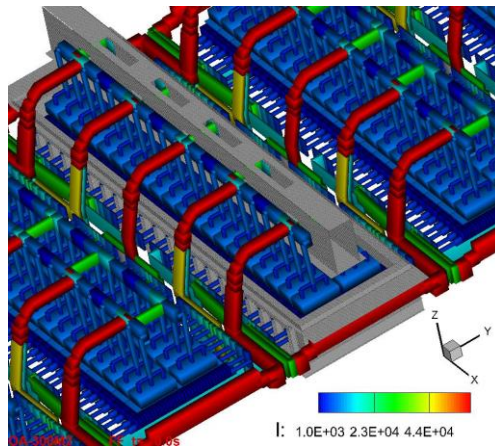
Cell stability MHD Model

- MHD-Valdis solves all the physic required to get to the transient wave evolution. First the current density is solved



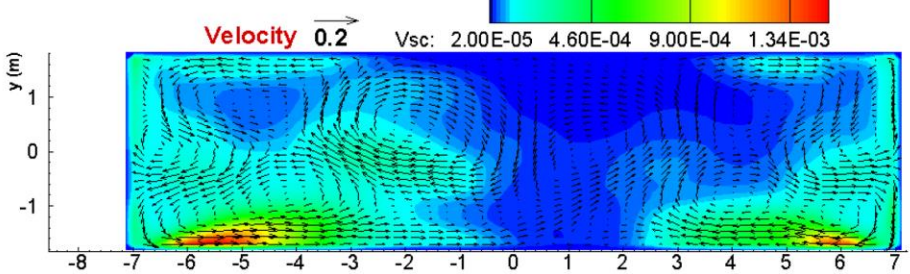
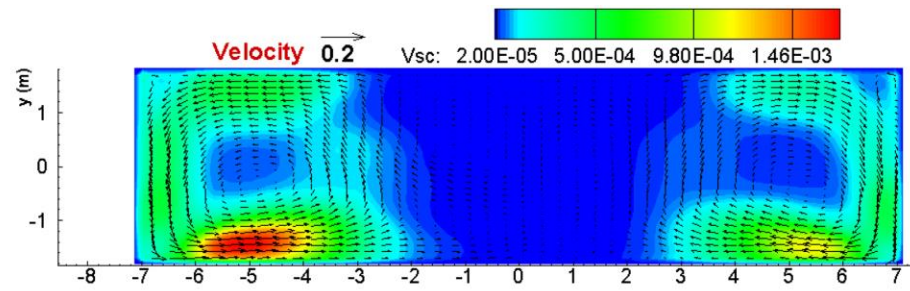
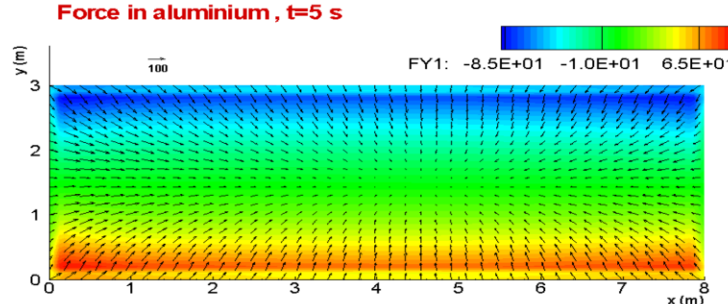
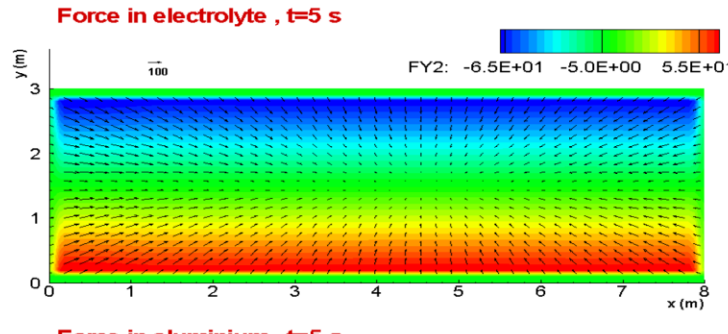
Cell stability MHD Model

- Second the magnetic field is solved using a boundary element formulation that doesn't require air meshing



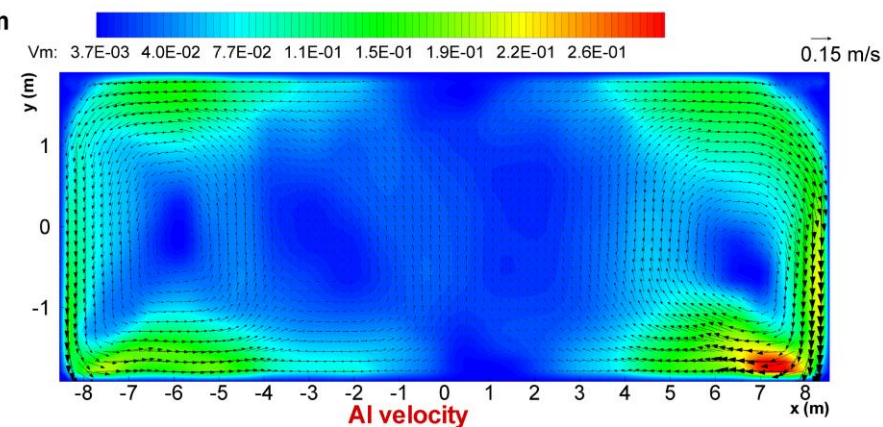
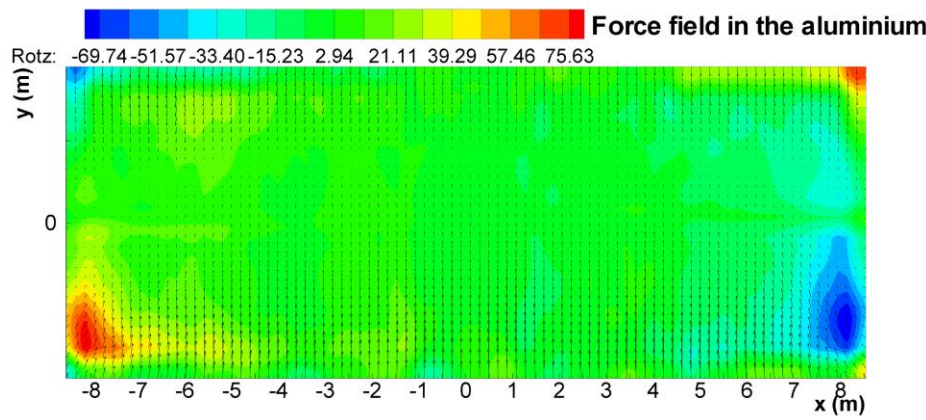
Cell stability MHD Model

- Next the Lorentz force field is calculated and used to solve the 2D shallow water formulated Navier-Stokes equation in order to get the bath and metal flow



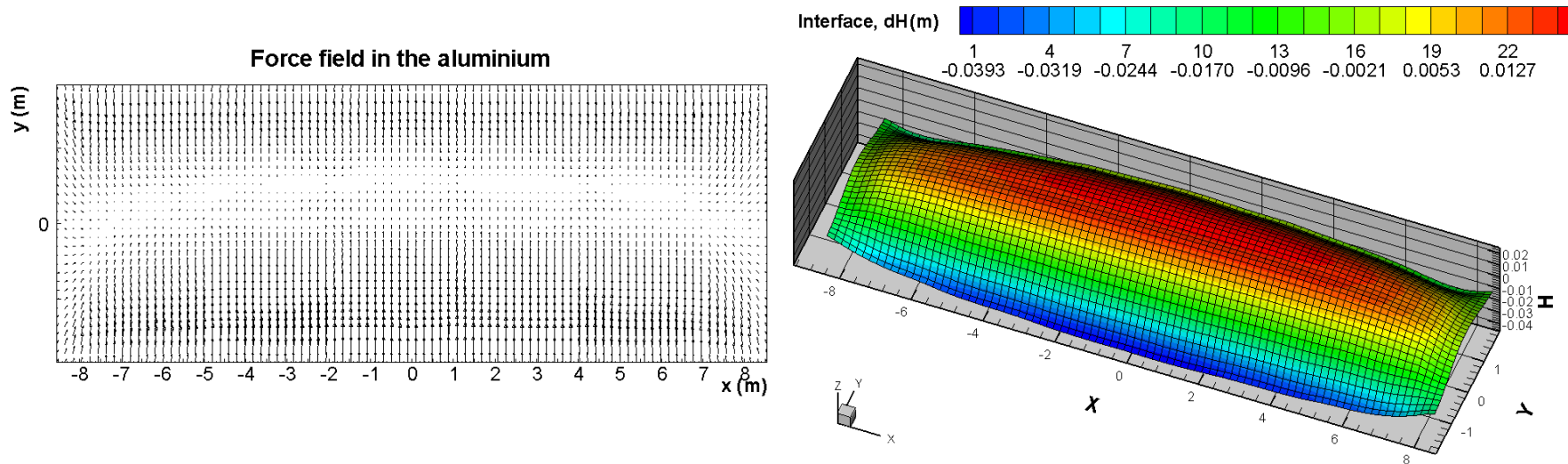
Cell stability MHD Model

- The Lorentz force is very rarely displayed, what really dictates the flow obtained is the rotational of the force field



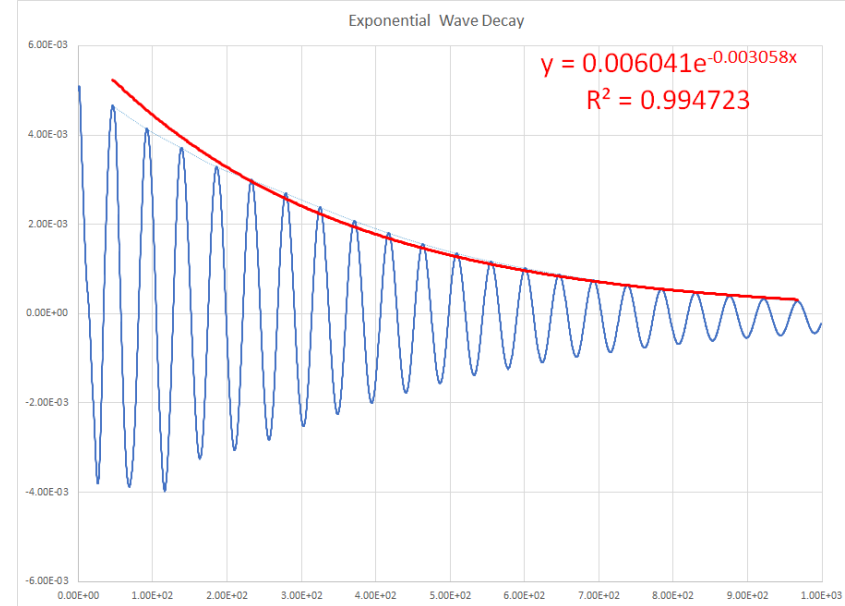
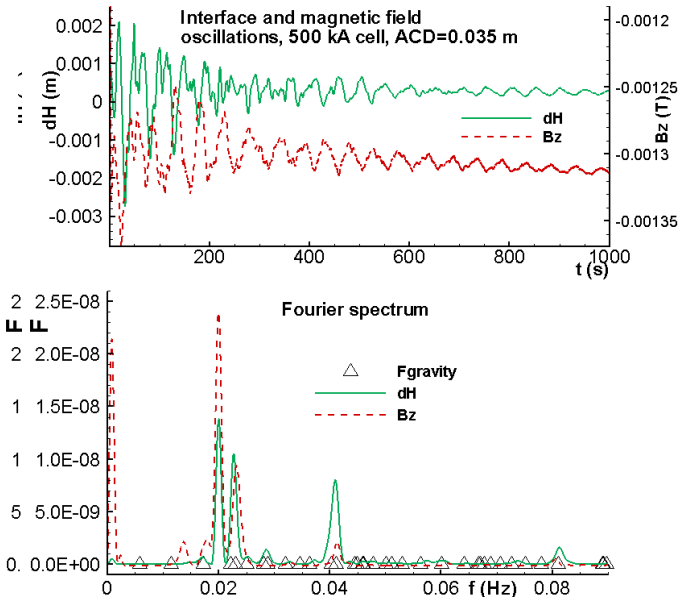
Cell stability MHD Model

- The dominant divergence part of the force field is globally pushing the metal in downstream direction



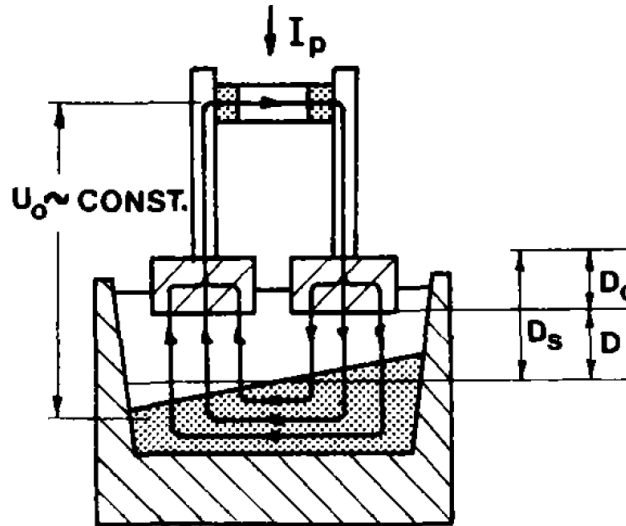
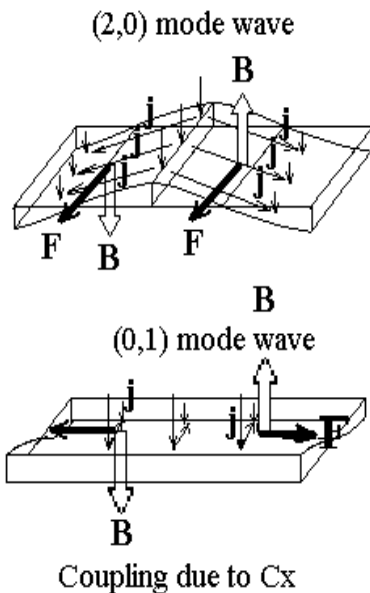
Cell stability MHD Model

- The possibility to run a fully nonlinear transient analysis of the flow after a perturbation on the steady-state solution using a manageable amount of CPU time is the key advantage of using MHD-Valdis MHD model

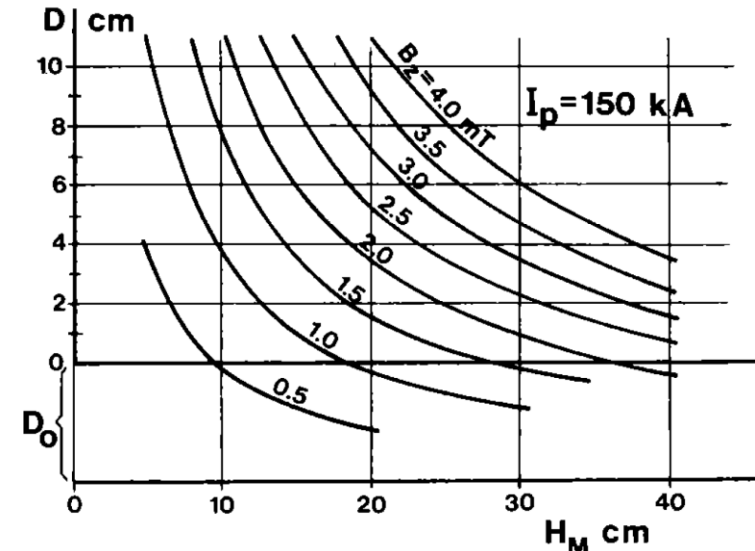


Cell stability MHD Model

- The alternative is to do a perturbation analysis pionner by Urata (1976) and Sele (Trans B 1977)



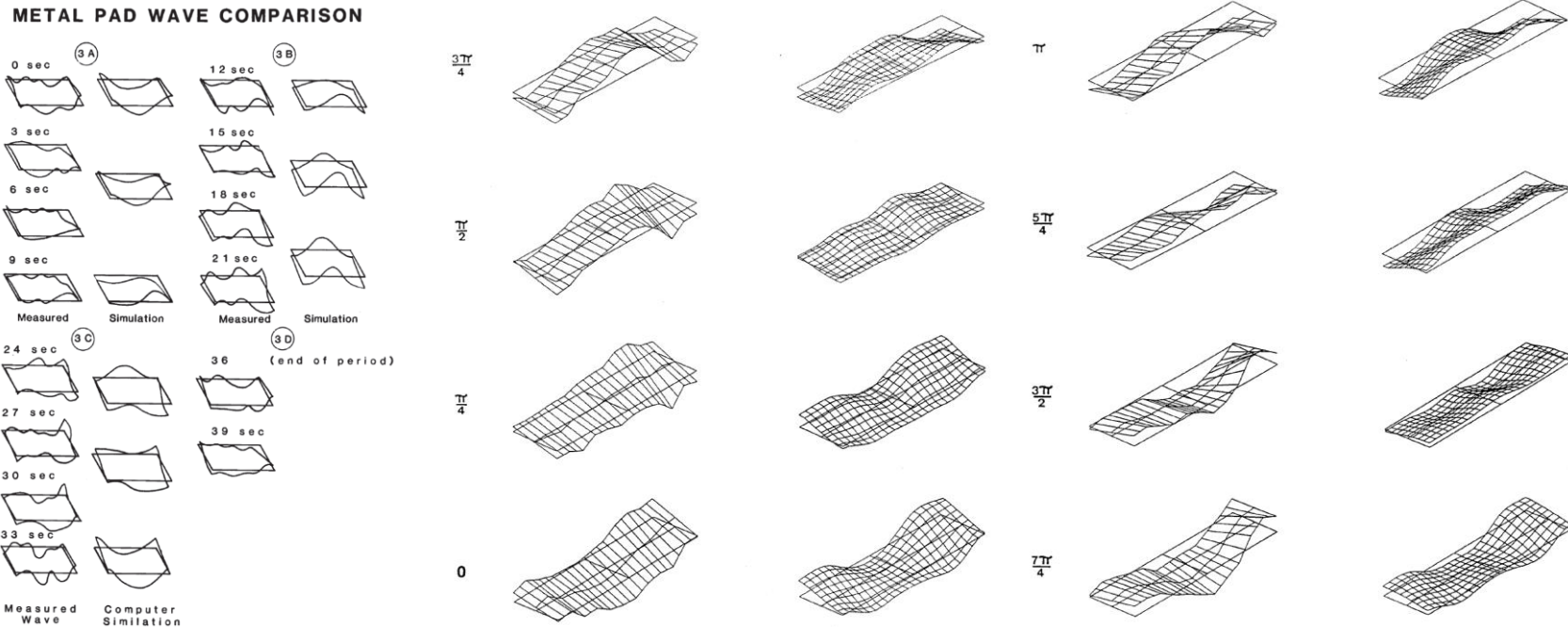
1) INTERNAL CIRCULATING CURRENT



4—Stability limit for 150 kA prebake cells.

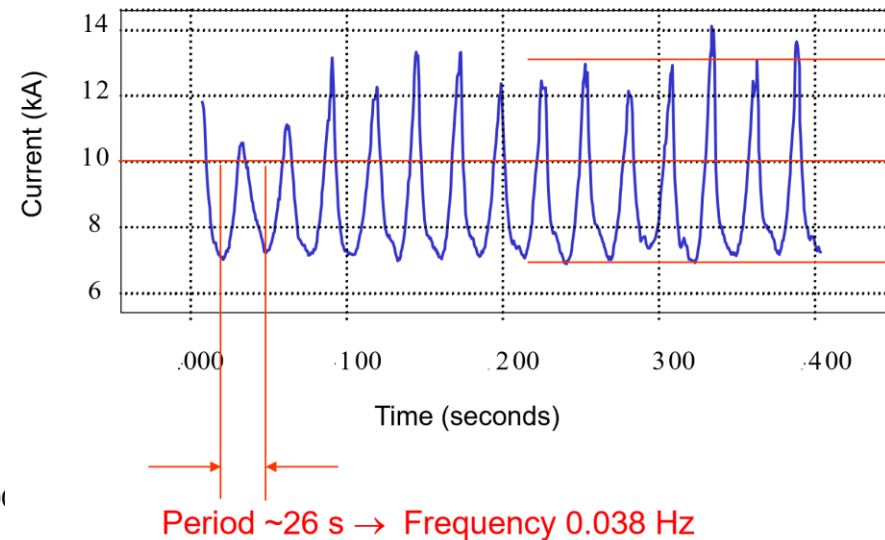
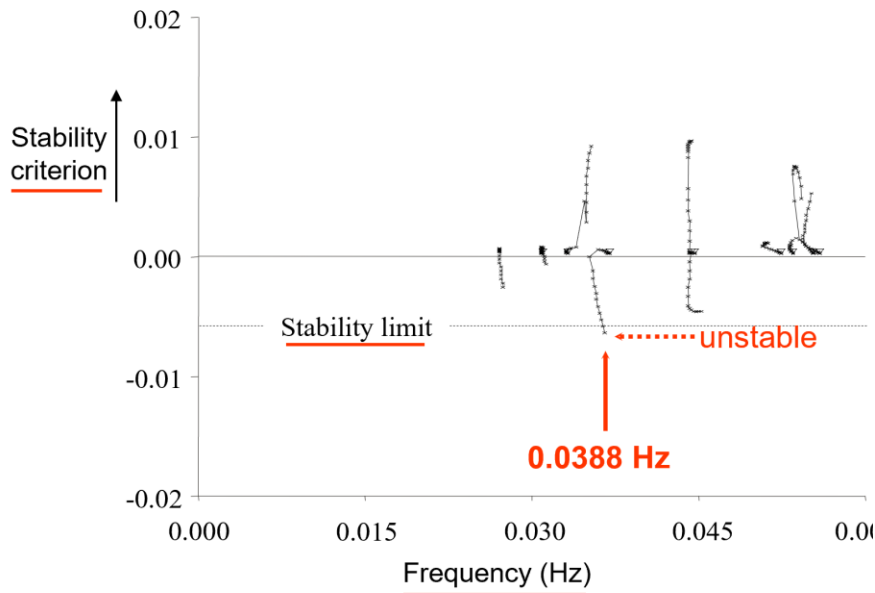
Cell stability MHD Model

- Urata (TMS 1985) presents an improved stability analysis,
Urata works was reproduced by Alcan after its publication



Cell stability MHD Model

- Application of linear stability analysis by Antille (TMS 2002)



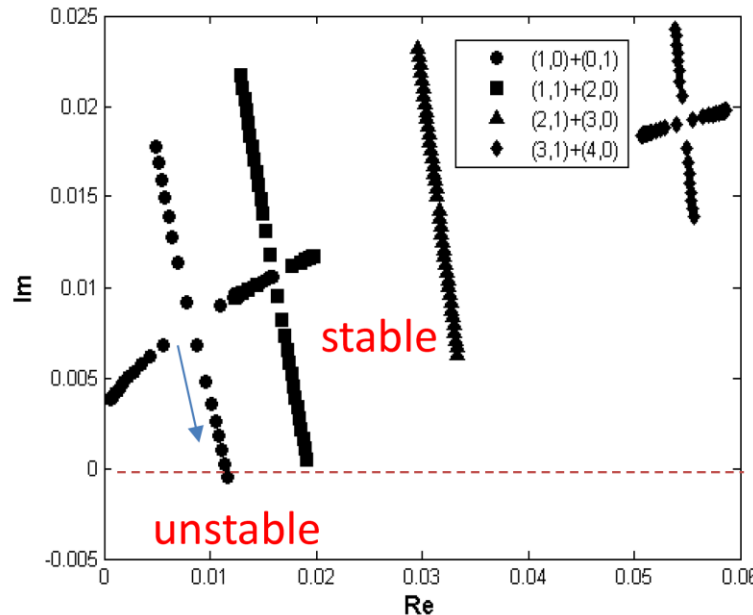
Cell stability MHD Model

- In TMS 2018, Bojarevics presented his second linear cell stability analysis:

Friction coefficient balance against the magnetic interaction

- Urata et al., *Keikinzoku*, 1976
- Sele *Metall. Trans.*, 1977
- Urata *Light Metals*, 1985
- Sneyd & Wang *J. Fluid Mech.*, 1994
- Bojarevics & Romerio *Eur. J. Mech. B*, 1994
- Davidson & Lindsay *J. Fluid Mech.* 1998
- Tucs , Bojarevics & Pericleous *J. Fluid Mech.* 2018

$$H(x, y, t) = H(x, y) \cdot e^{-i\omega t}, \quad \omega = \omega_{\text{Re}} + i\omega_{\text{Im}}$$



Bath Bubble Flow Driven CFD Model

- Dernedde (TMS 1975) was the pioneer with his physical model

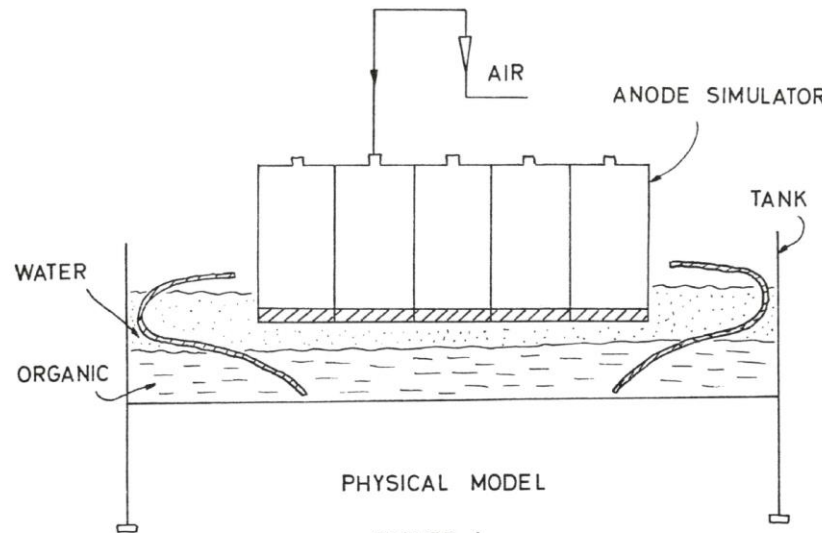


FIGURE 1

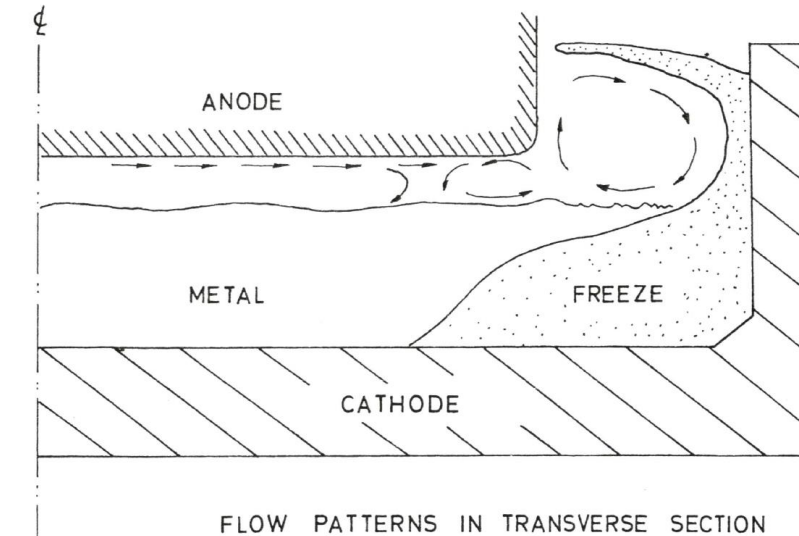


FIGURE 2

Bath Bubble Flow Driven CFD Model

- Chen published pictures of a similar physical model in JOM November 1994 edition

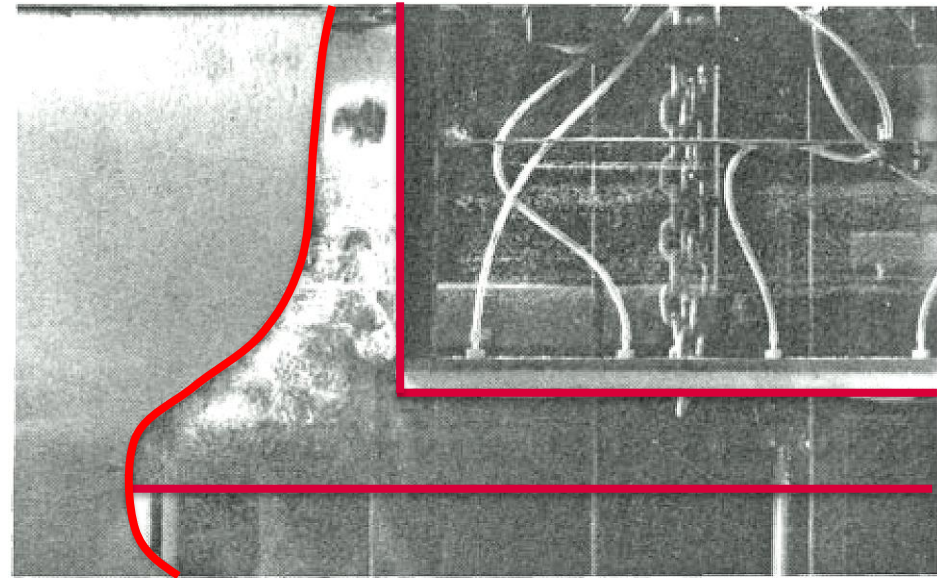
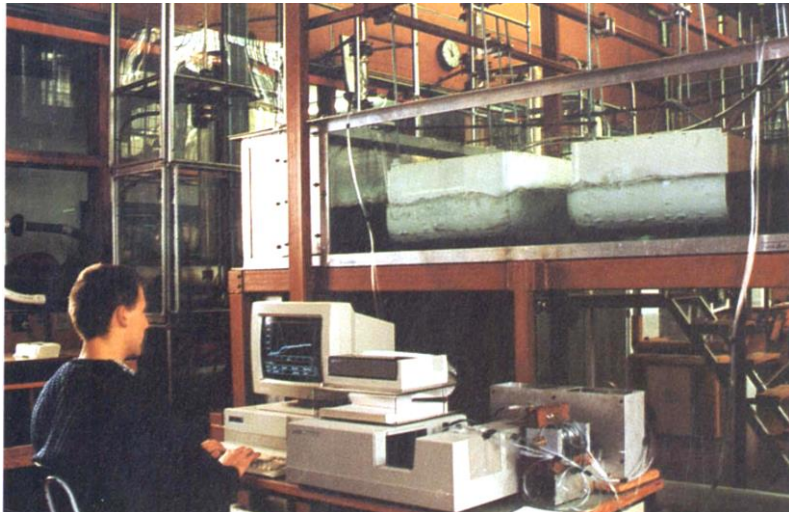


Figure 7. The gas-induced flow pattern in the anode/ledge space as obtained from an air/water model.

Bath Bubble Flow Driven CFD Model

- Shekhar and Evans (Trans B 1994) developed a physical model to study the bubble release of near vertical electrodes

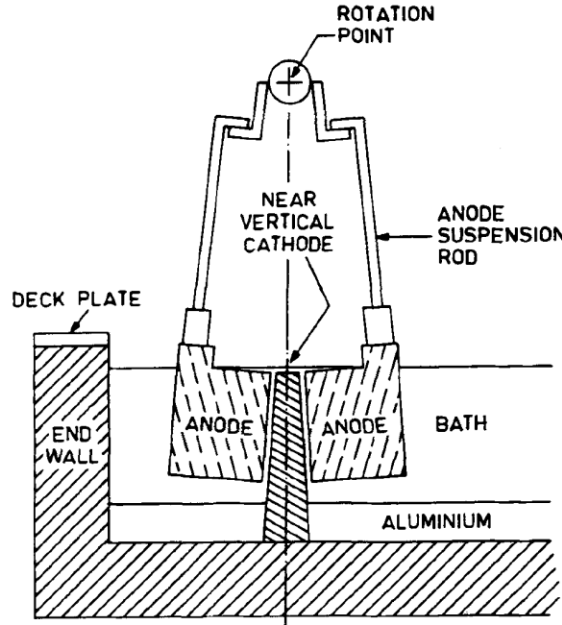


Fig. 3—Schematic representation of a Hall cell with near-vertical electrodes (Ref. 4).

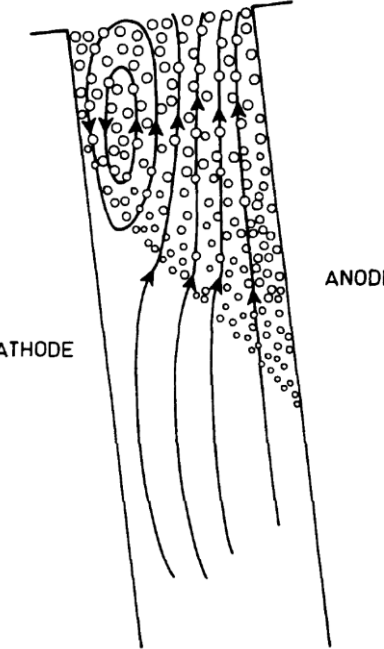


Fig. 15—Schematic diagram of bubble-driven electrolyte flow in the ACG of a near-vertical (simulated) Hall cell.

Bath Bubble Flow Driven CFD Model

- Solheim (1989) published results of a 2D CFD model

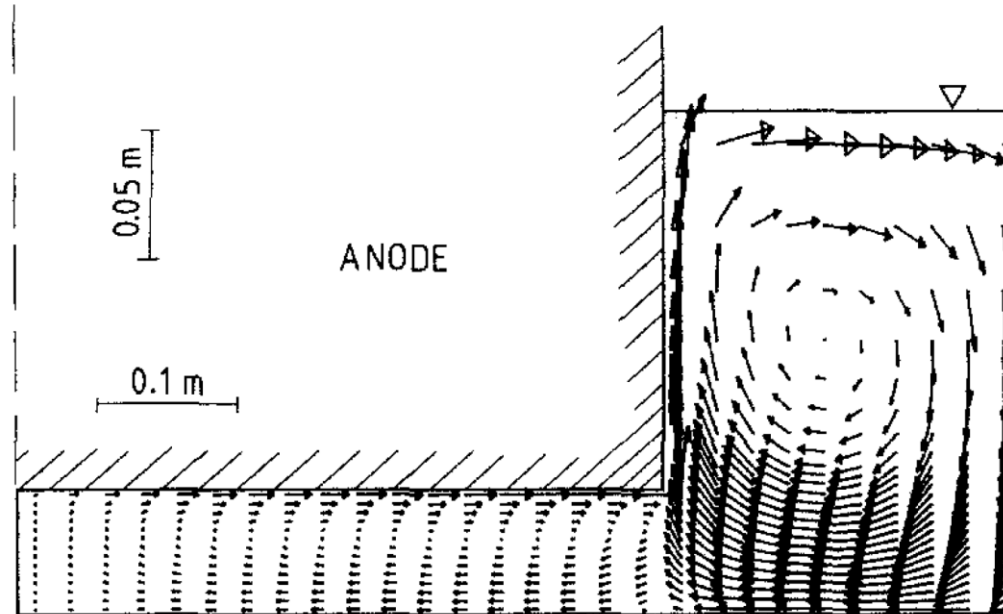


Fig. 1. Flow pattern in the interpolar gap of an aluminium reduction cell.

Bath Bubble Flow Driven CFD Model

- Solheim (TMS 2001) presented a 2D CFD model of vertical ACD

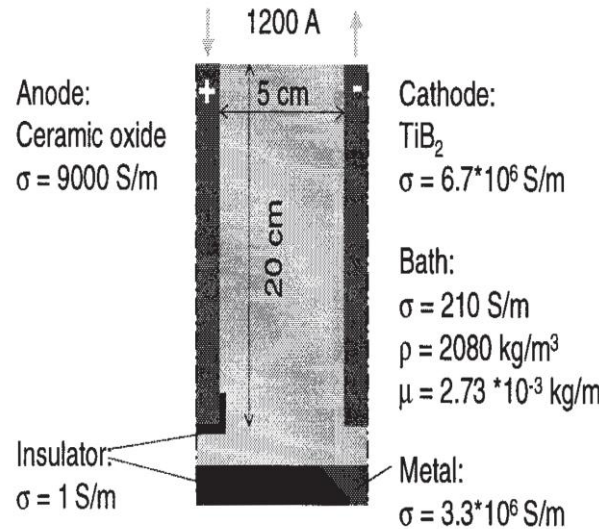


Figure 3: Geometry and parameters. The aspect ratio of the sketch is not correct. The depth of the model is 1 m.

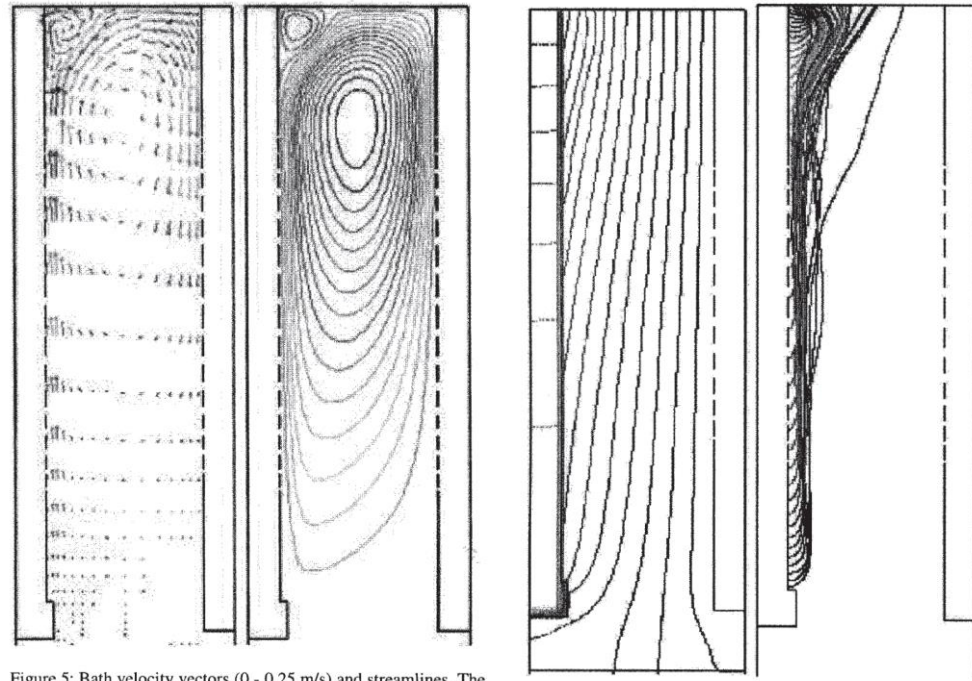
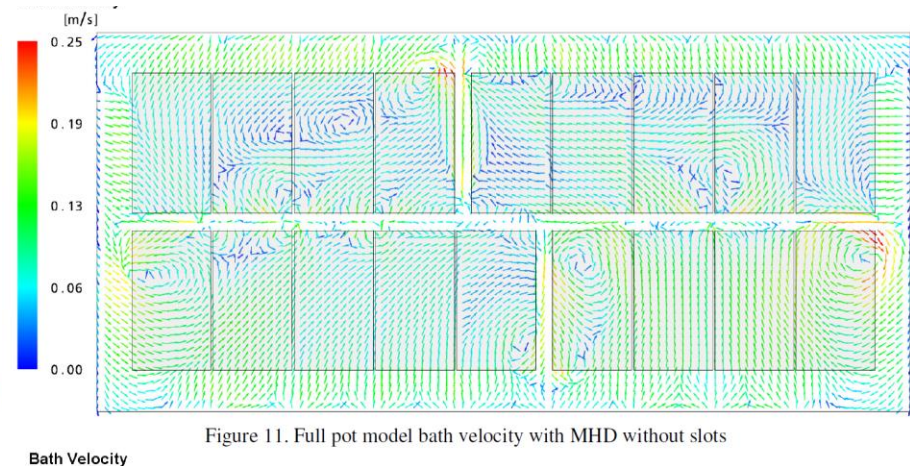
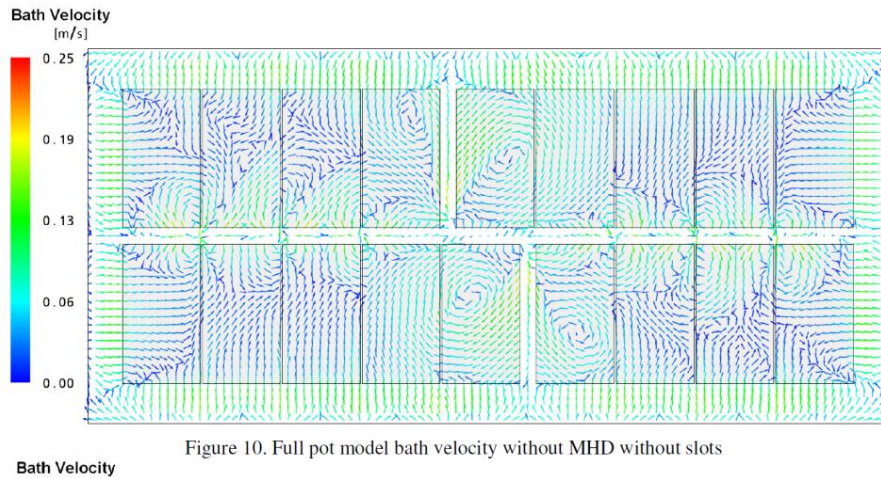


Figure 5: Bath velocity vectors (0 - 0.25 m/s) and streamlines. The bubble diameter is 3mm. The bottom of the cell is not shown.

Figure 4: Electric potential (0-4.5 V) and resulting bubble tracks.

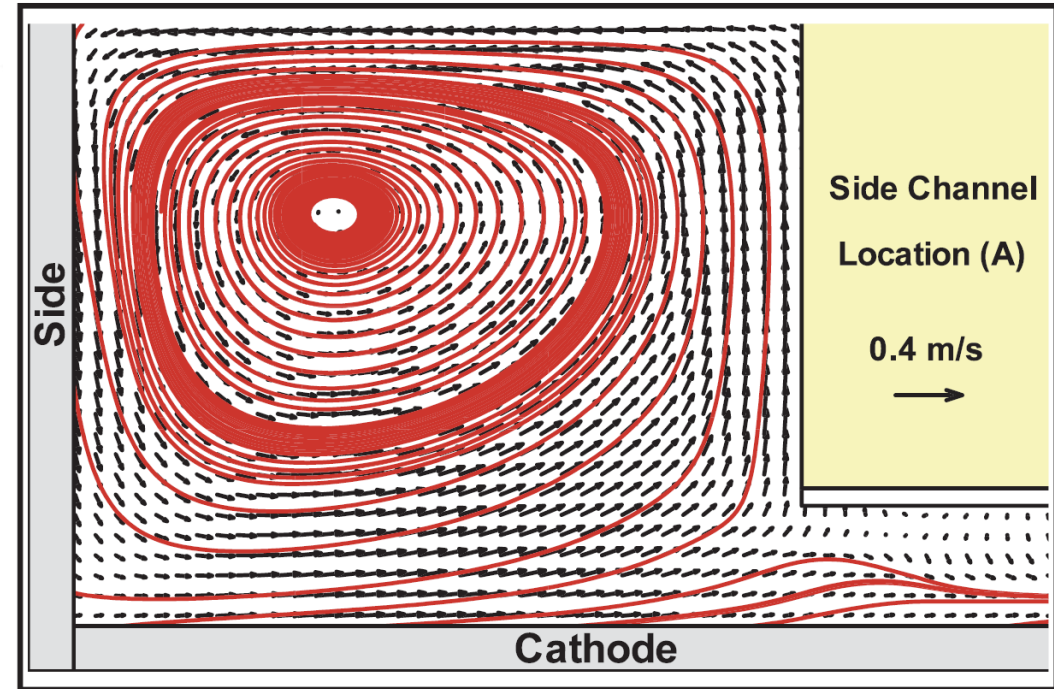
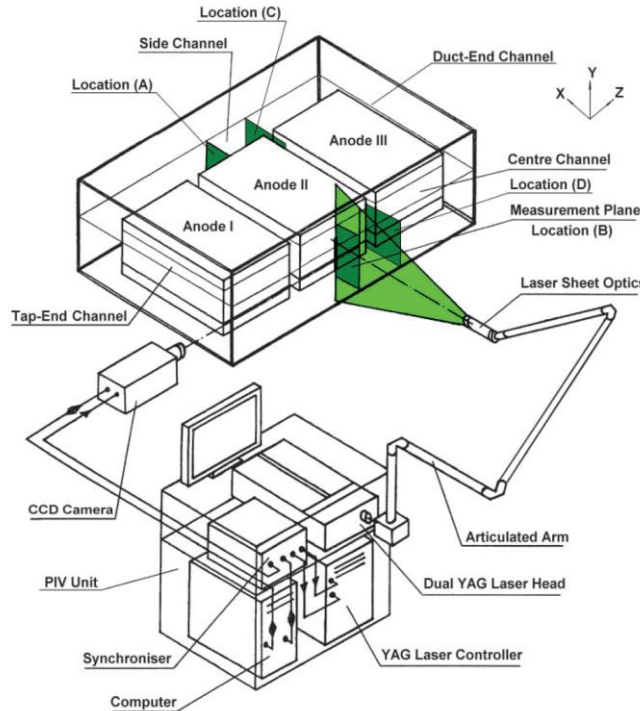
Bath Bubble Flow Driven CFD Model

- **Severo (TMS 2007) published results of a 3D full cell combined bubble driven and MHD driven bath flow**



Bath Bubble Flow Driven CFD Model

- Feng (2010) presented both physical and 3D CFD models



Bath Bubble Flow Driven CFD Model

- Feng (2010) presented both physical and 3D CFD models

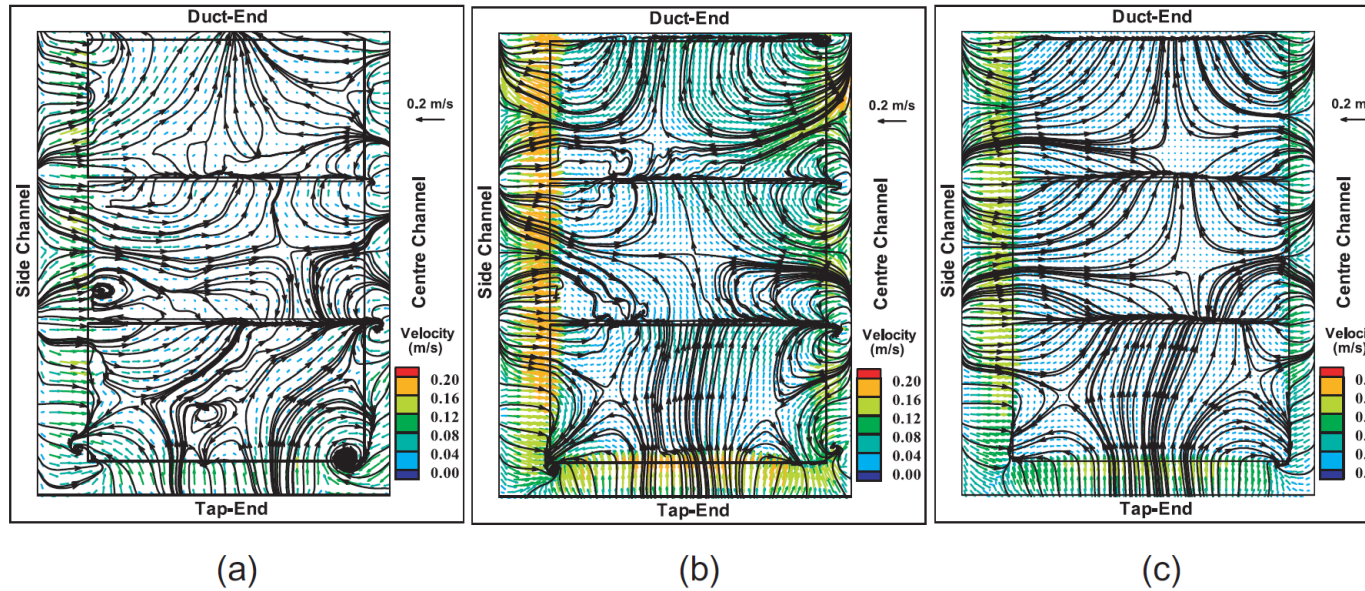
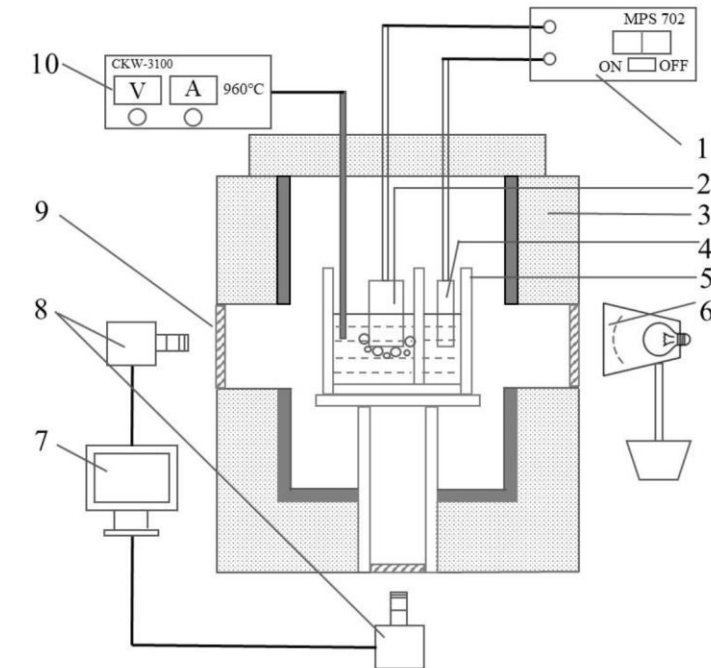
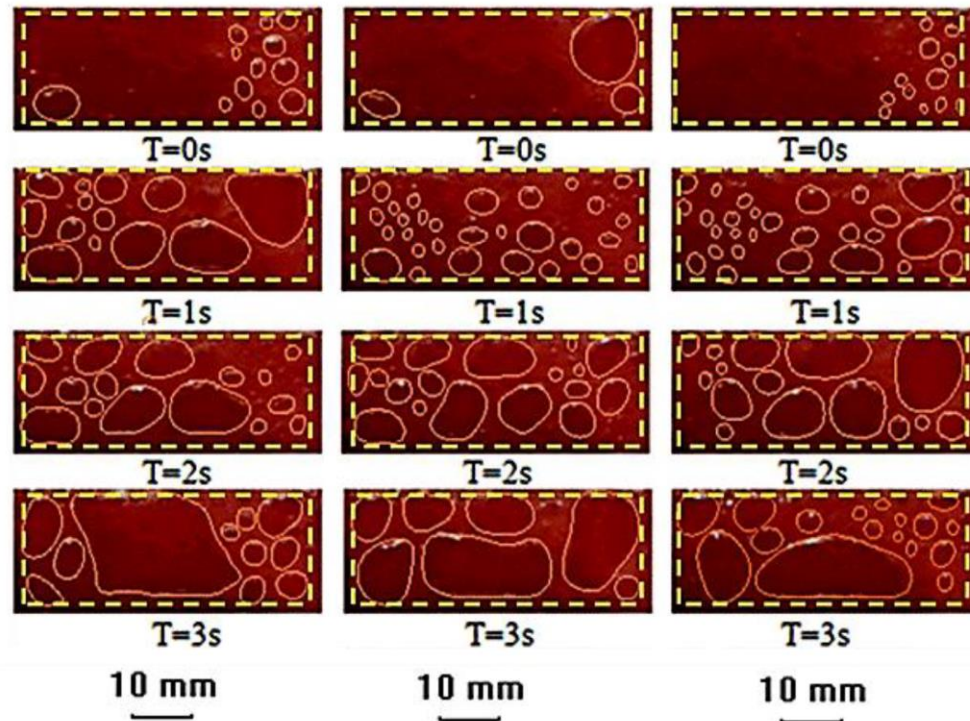


Figure 6. Water velocity distribution and streamlines at a horizontal plane in middle of ACD: (a) PIV measurement; (b) CFD simulation by modifying turbulent eddy viscosity; (c) CFD simulation by modifying turbulence kinetic energy.

Bath Bubble Flow Driven CFD Model

- Prof. Gao (2018) observed bubbles from a lab transparent cell



Bath Bubble Flow Driven CFD Model

- A coupled VOF-DPM CFD model can be used to represent large bubble formation and the frequency of bubbles escape

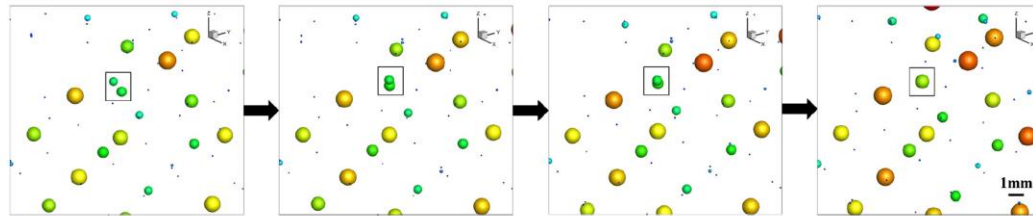


Fig. 9—Discrete bubble coalescence process.

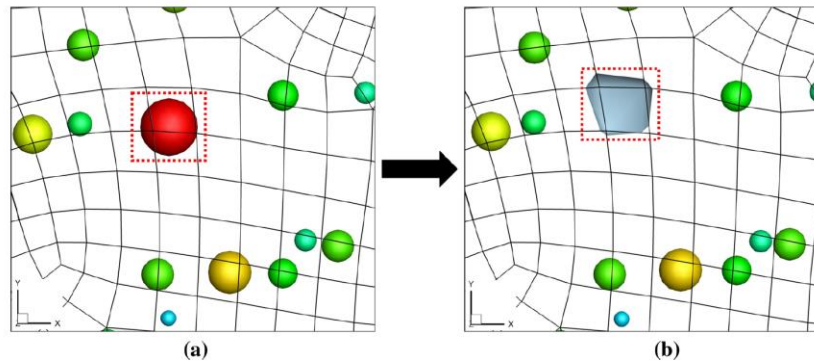


Fig. 10—Discrete-continuum transition if $V_b \geq V_{cell}$: (a) before transforming; (b) after transforming.

Bath Bubble Flow Driven CFD Model

- These figures of a VOF-DPM CFD model behavior are from Sun (Trans B 2018)

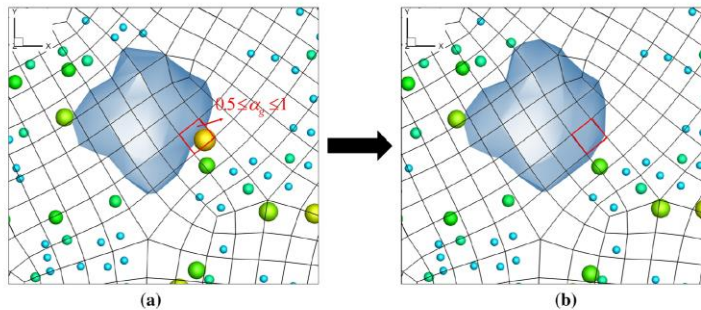
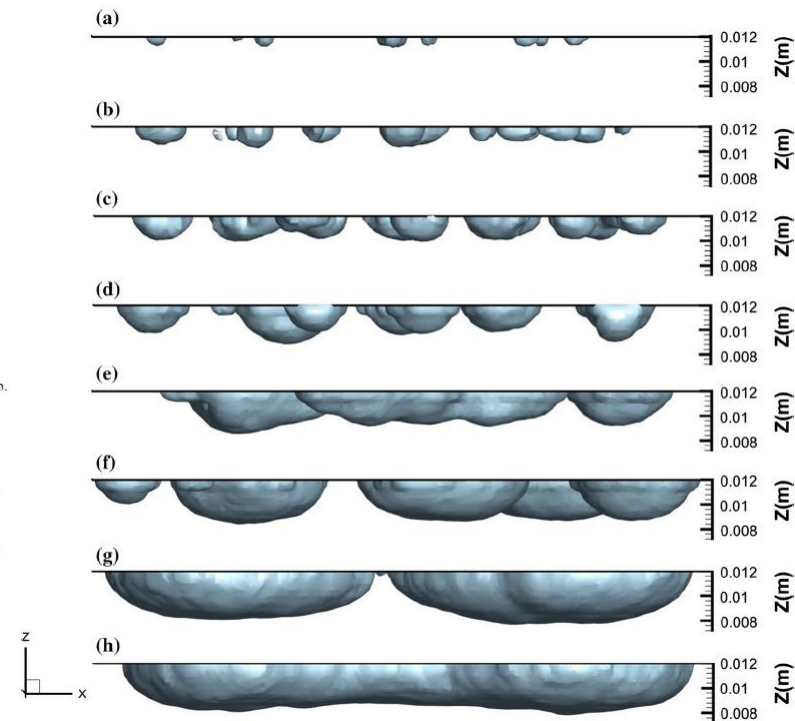
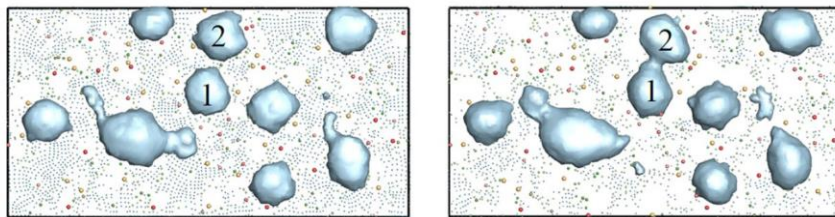


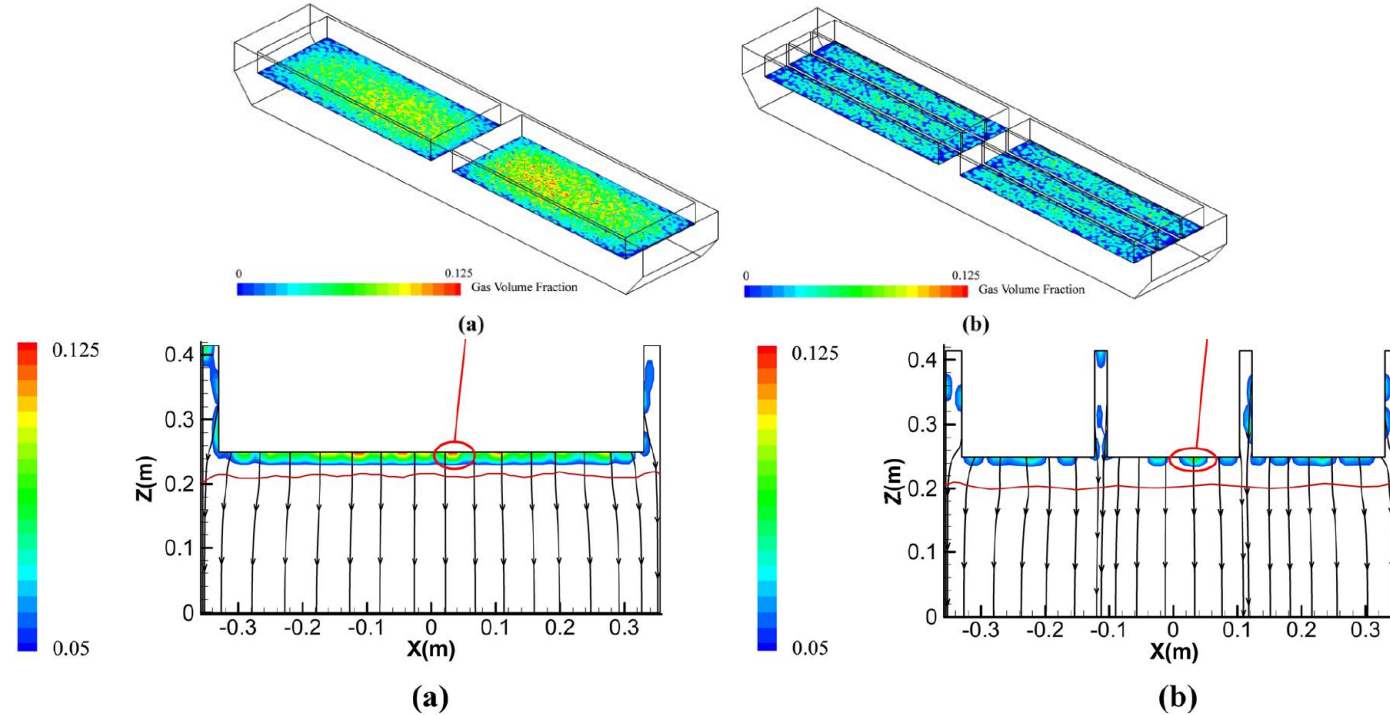
Fig. 11—Large deformed bubble swallowing up the discrete micro-bubble if $0.5 \leq \alpha_g \leq 1$: (a) before swallowing up; (b) after swallowing up.

(a) S-S



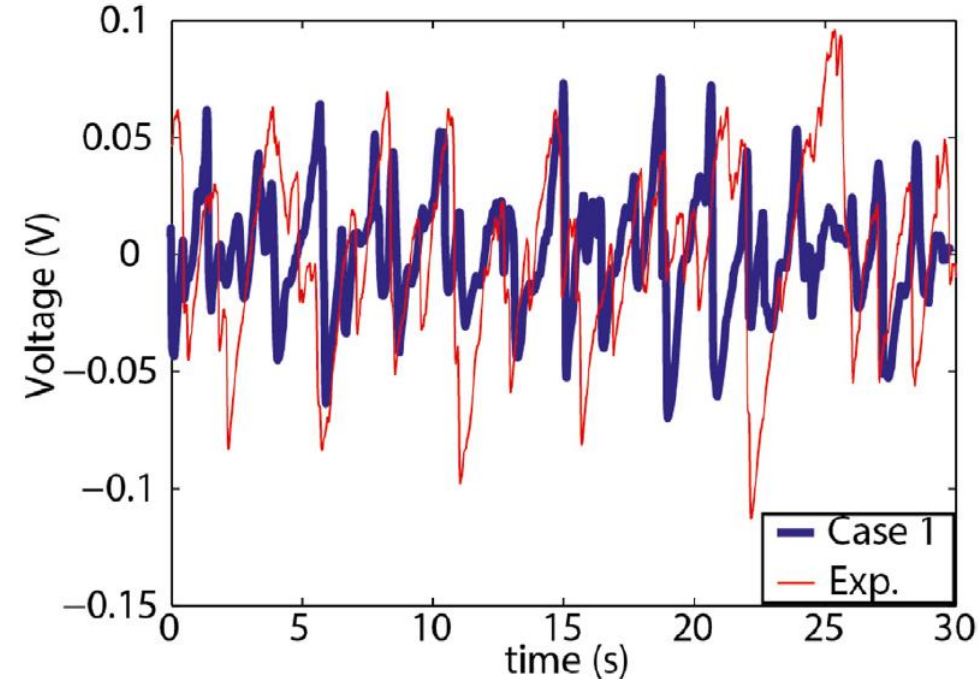
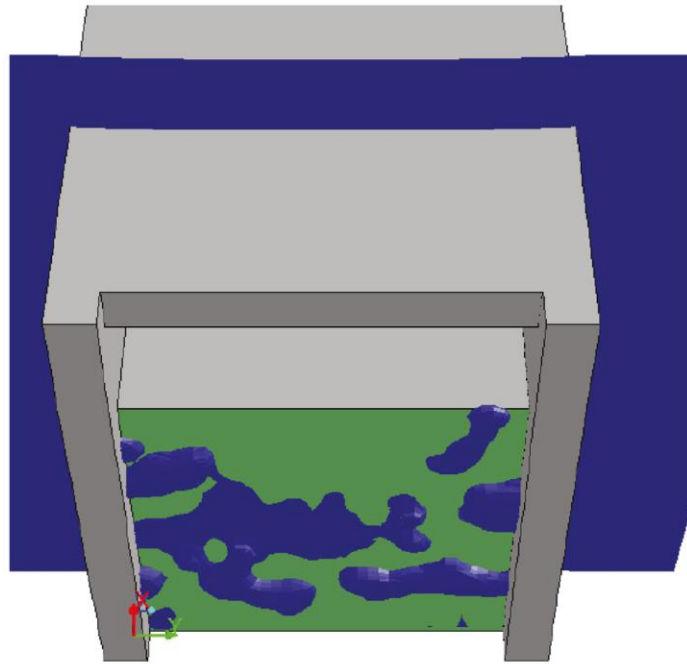
Bath Bubble Flow Driven CFD Model

- The voltage can then be solved to see the impact of bubbles as done in Sun (Trans B 2017)



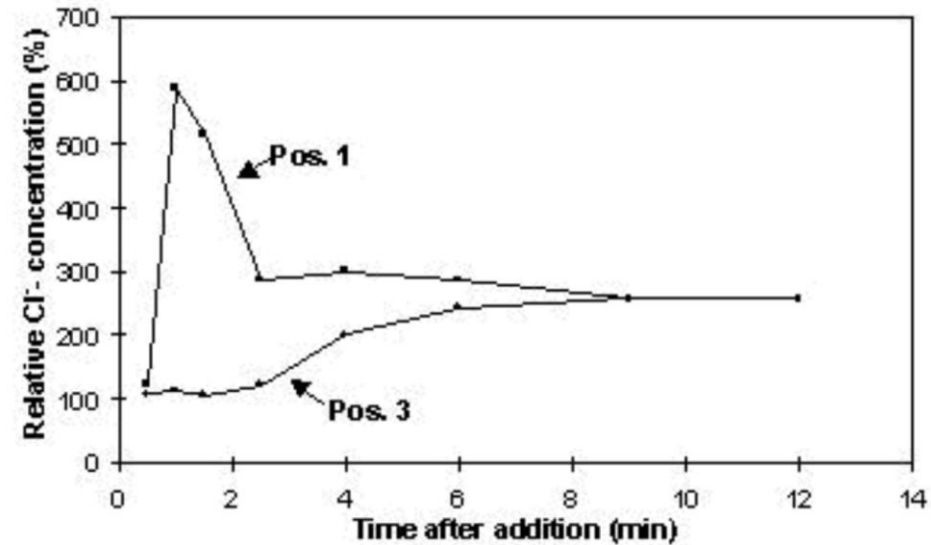
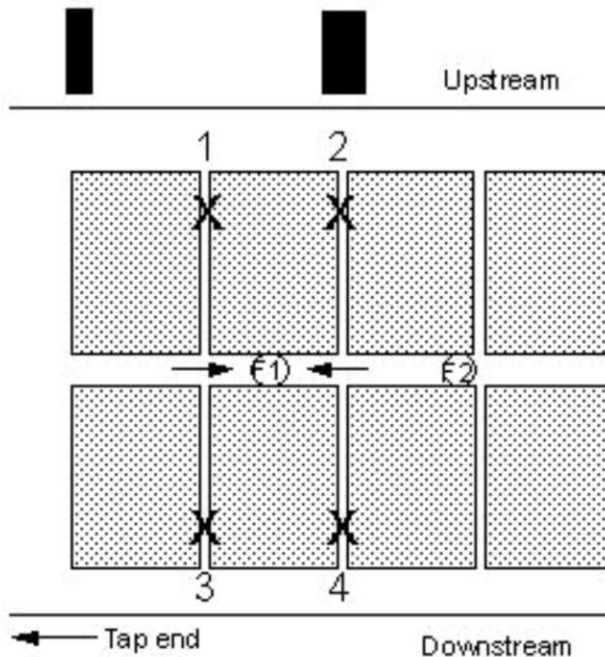
Bath Bubble Flow Driven CFD Model

- Finally that type of model can be used to predict the bubble release noise frequency as in Einarsrud (2016)



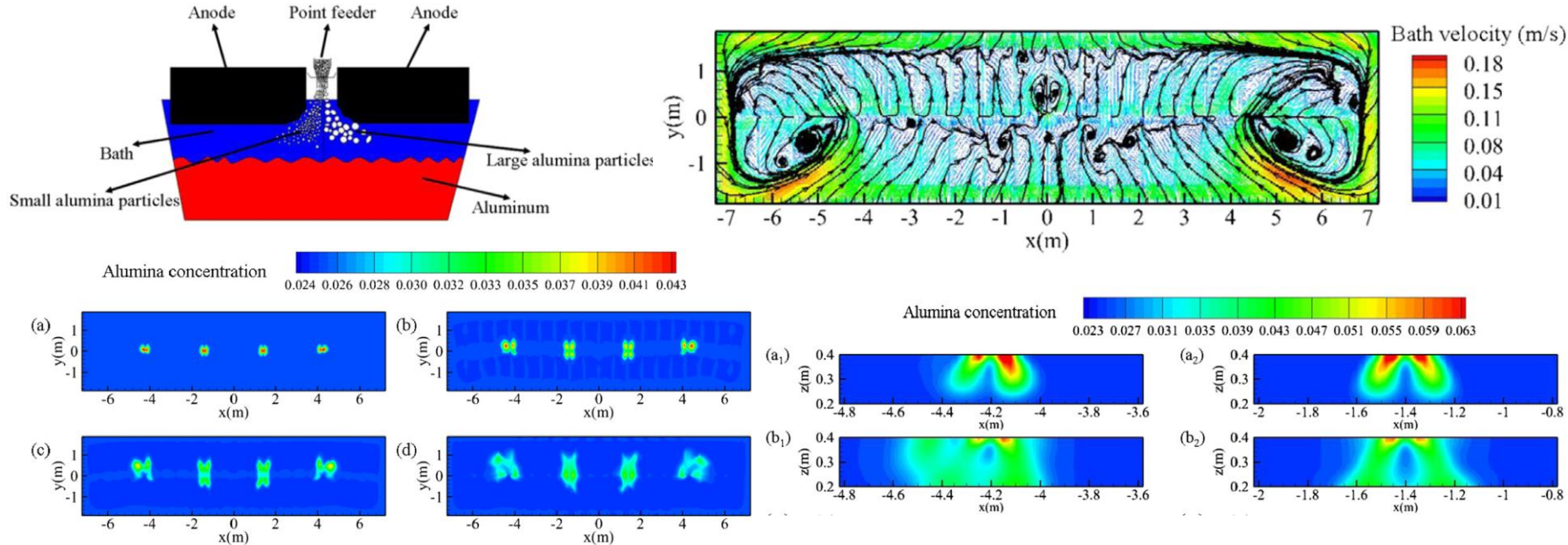
The Alumina Dissolution CFD model

- It is very hard to get experiential results as the only option is to measure in actual cells, SINTEF reported some (TMS 1997)



The Alumina Dissolution CFD model

- Zang (2014) presented a CFD-TPPBM alumina dissolution model using bath flow generated using both MHD and bubble



The Alumina Dissolution CFD model

- Einarsrud (2016) presented a more advanced alumina dissolution model that account for anode burn off shape

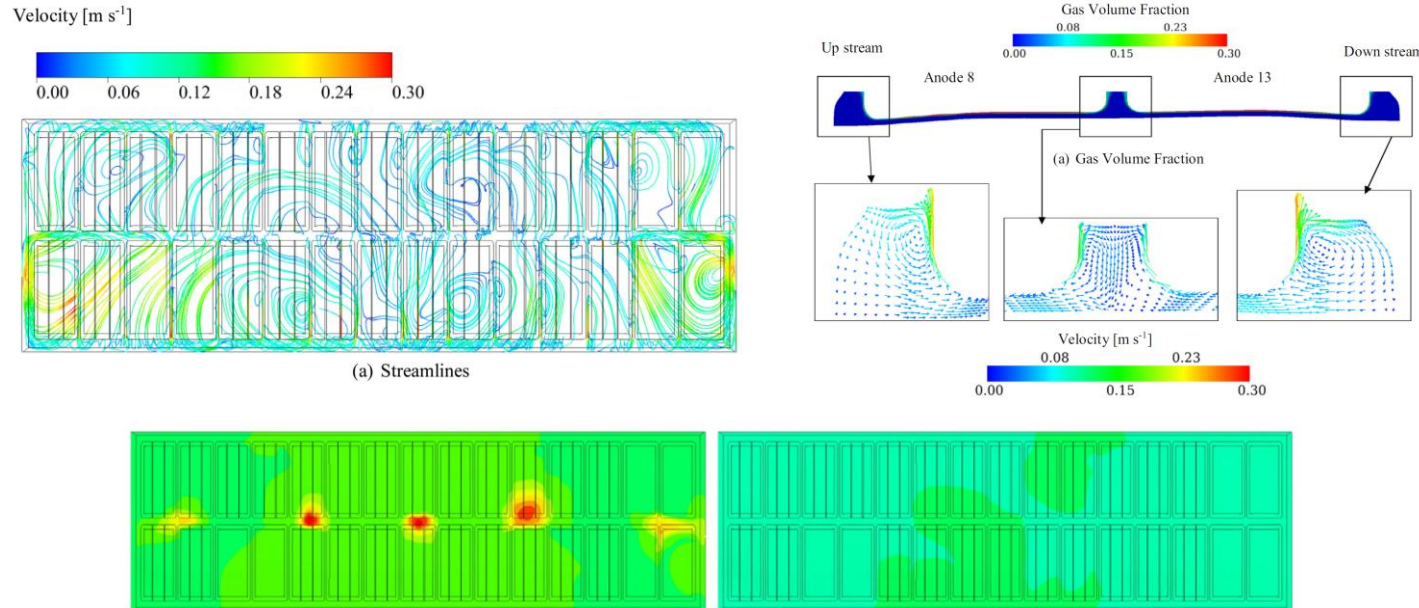


Fig. 17. Undissolved alumina species during the first 12,000 s of the feeding cycle.

The Alumina Dissolution CFD model

- But the physic of above model is incomplete, Gylver (TMS 2019) presented a paper of raft formation observations

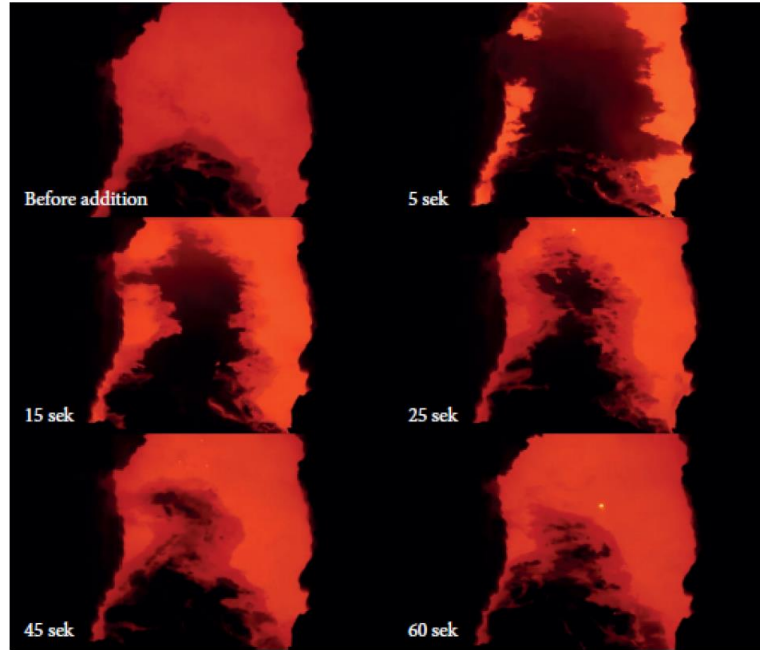
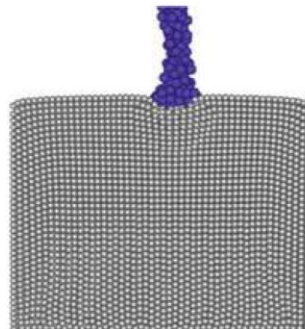


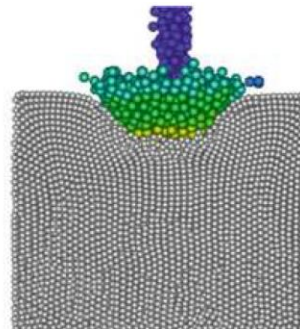
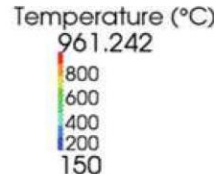
Fig. 2 Sample images from video recording where the crust has been broken between the feeding and tap hole for enhanced visualization. The dark area is floating undissolved alumina - e.g. a raft. The time is set relative to a single feeding event.

The Alumina Dissolution CFD model

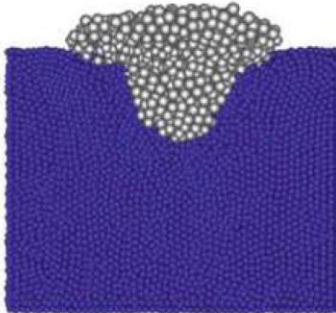
- Roger (TMS 2021) presented a paper of raft formation



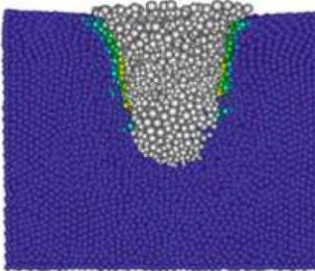
$t = 0 \text{ ms}$



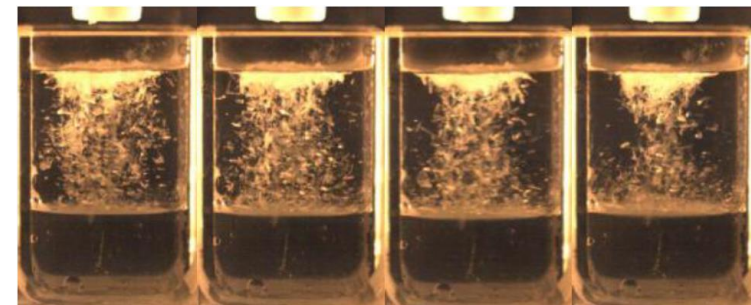
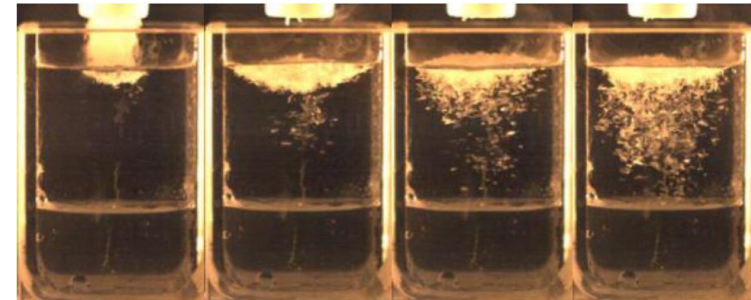
$t = 125 \text{ ms}$



$t = 500 \text{ ms}$



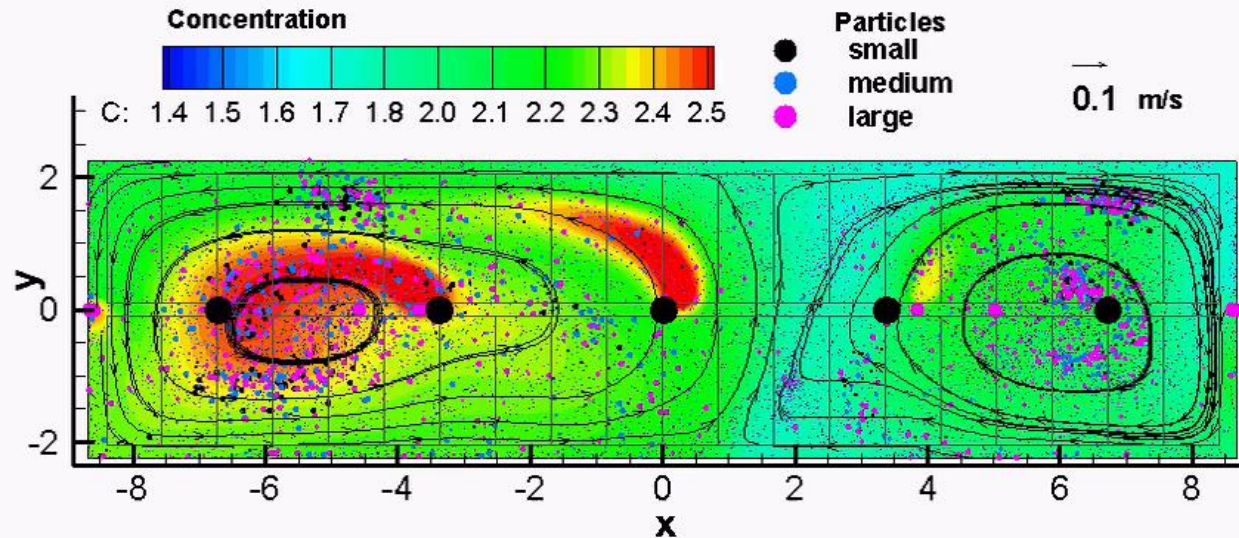
$t = 625 \text{ ms}$



- Kaszas (2020)

The Alumina Dissolution CFD model

- Boyarevics (TMS 2022) will presents this first attempt to represent rafts in a full cell alumina dissolution model



The Multi-Physic Model

- The multi-physic model that is a merge of the above 4 models, Einarsson (2016) presented part of the interactions and the multi-scales problematic

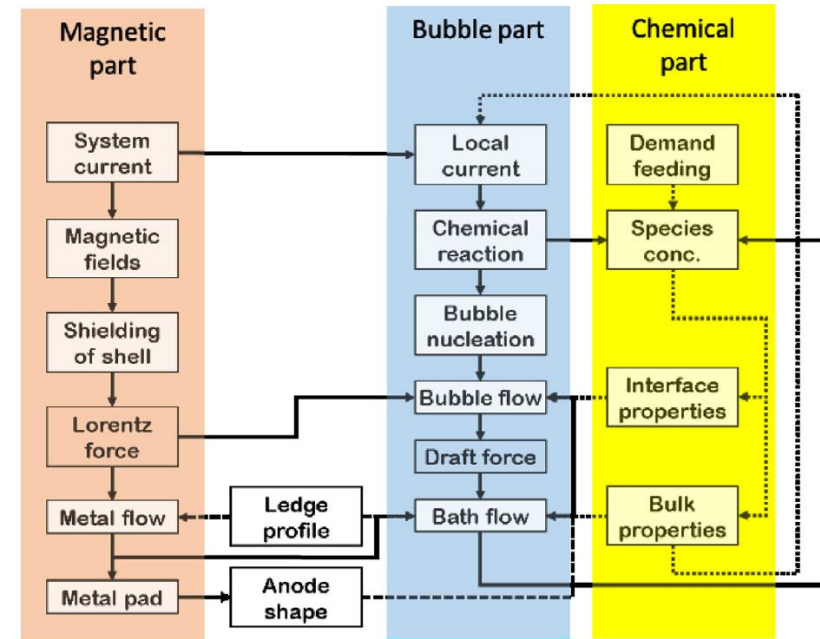
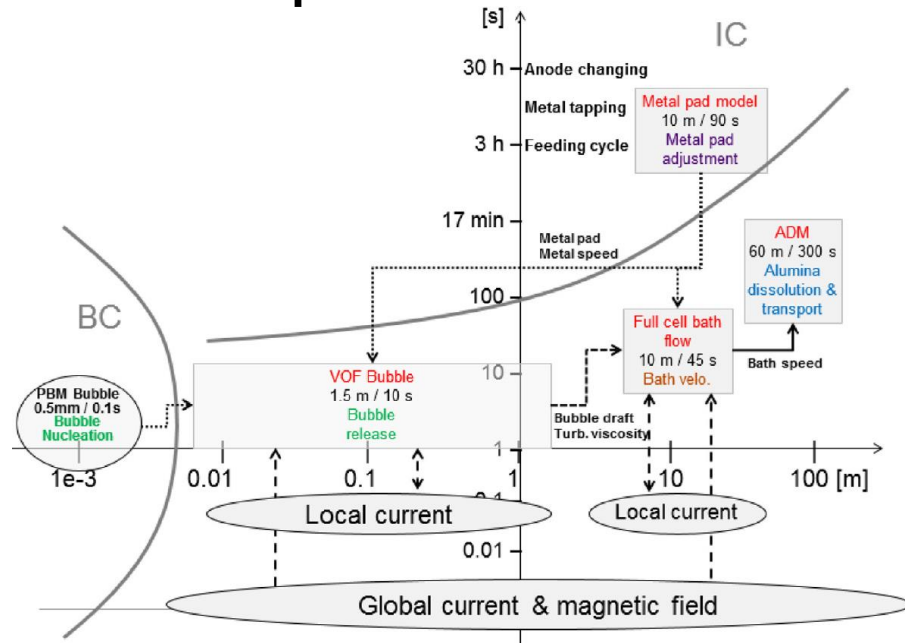


Fig. 8. Primary coupling behaviour of the three process parts.

The Multi-Physic Model

- Renaudier (TMS 2018) presented Rio Tinto's Alucell multi-physic model concept:

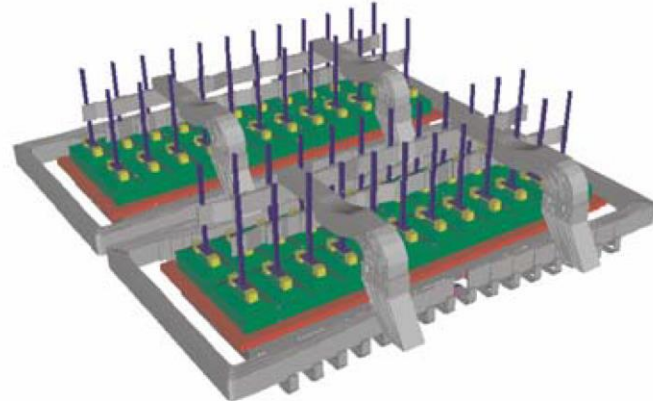
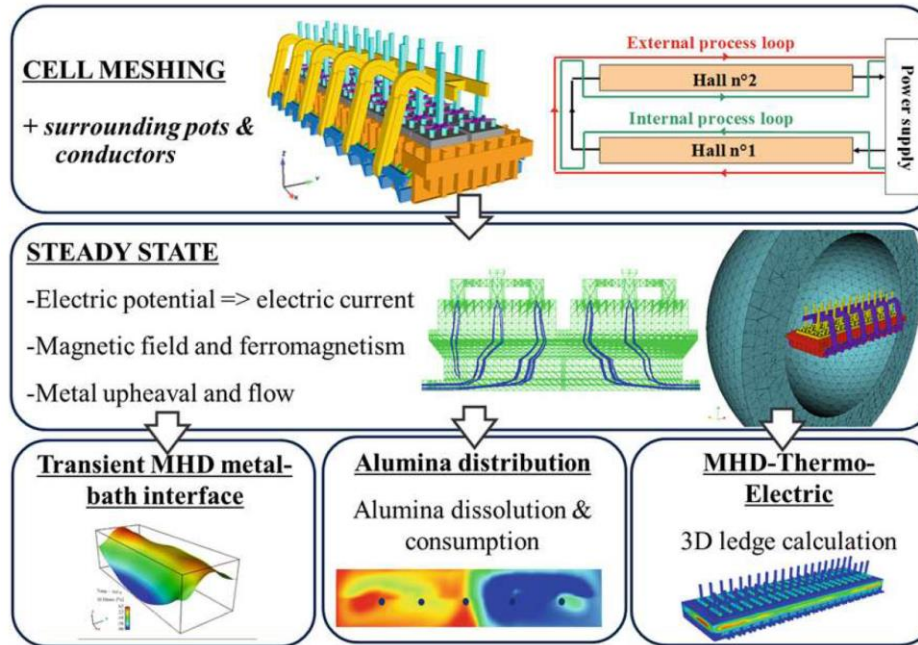


Figure 2: Full MHD cell geometry – P155 technology

- **But Alucell is much older, this is an Alucell model presented by Richard (TMS 2008)**

The Multi-Physic Model

- Langlois (TMS 2015) and Renaudier (TMS 2018) presented some Alucell results:

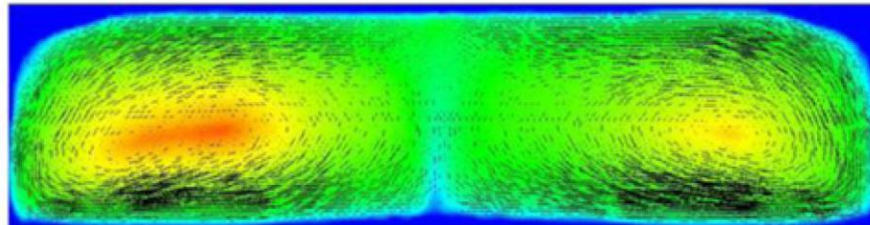
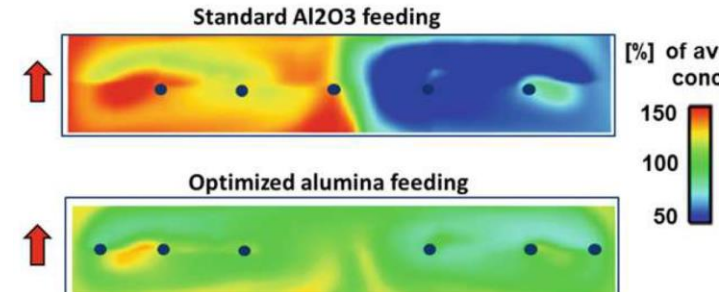
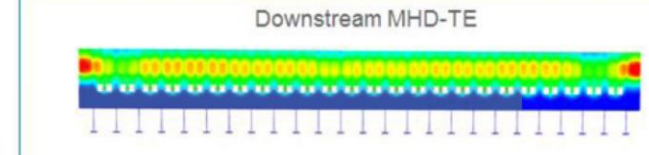
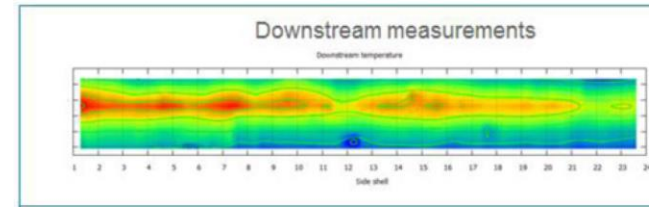
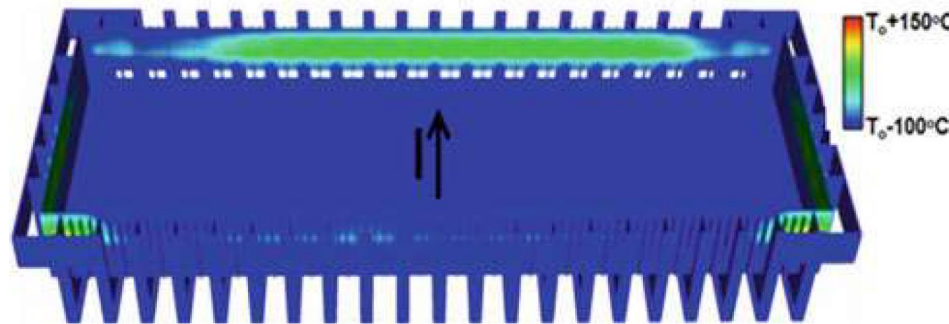
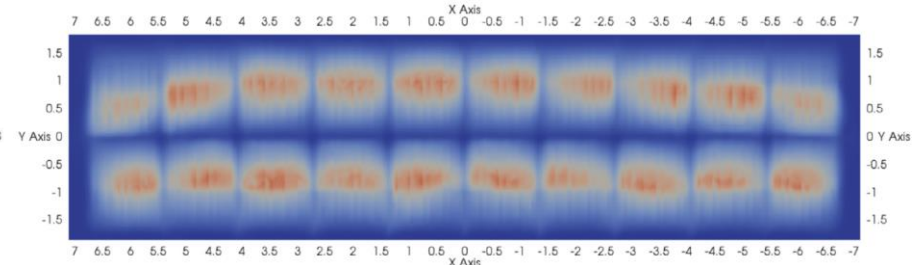
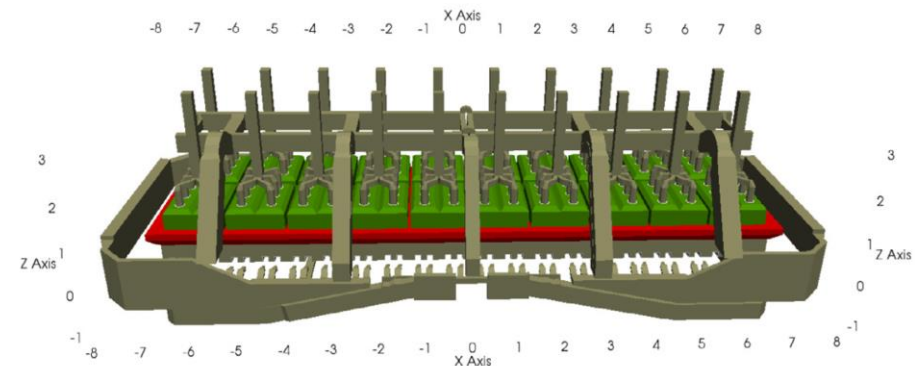
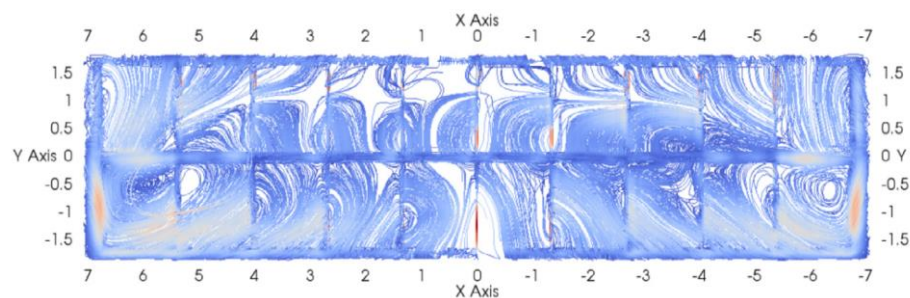
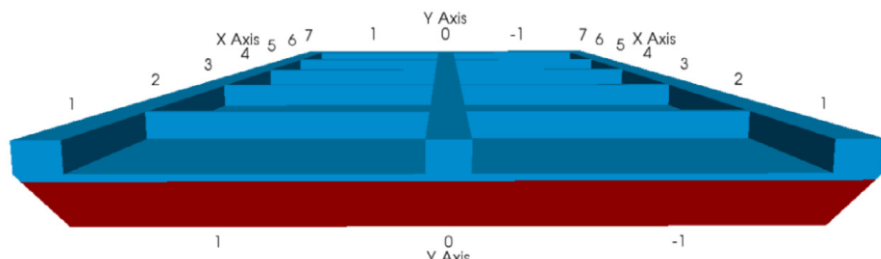


Figure 2: Example of velocity fields at bottom of metal



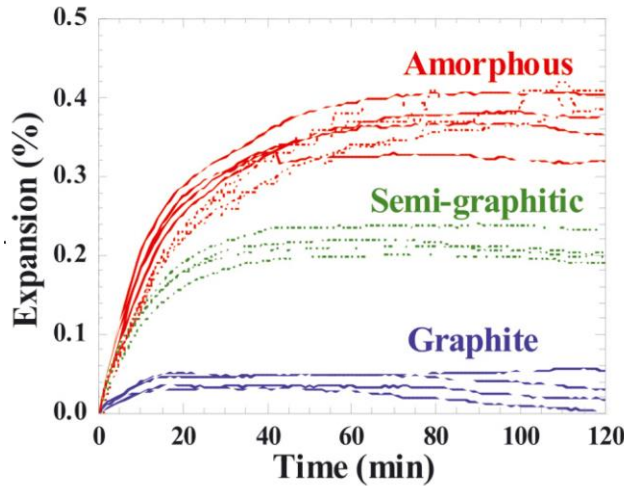
The Multi-Physic Model

- Alucell was developed for Alusuisse/Alcan/Rio Tinto by EPFL, they also publish, per example those bubble flow results (2021) for future addition to Alucell physic

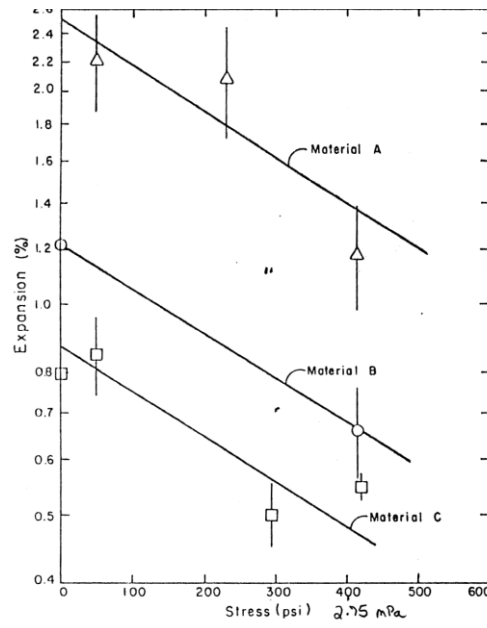


The Thermo-Chemo-Mechanical Potshell Deformation Model

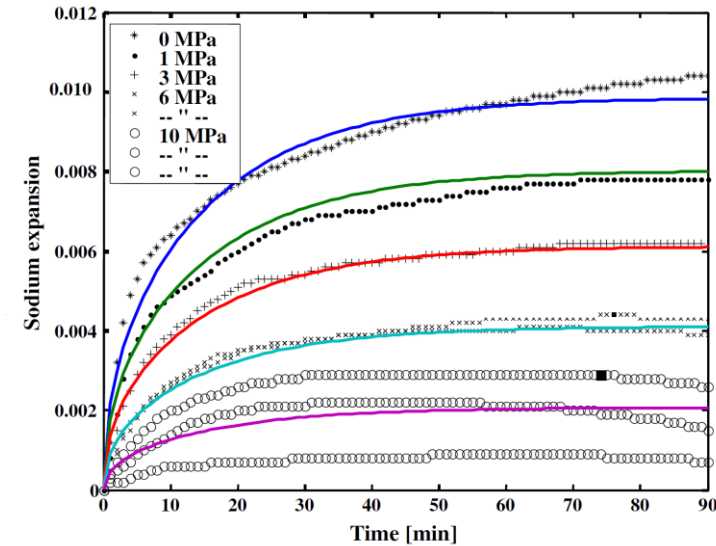
- Dewing (TMS 1975) publish this behavior law, he himself quote
Rapoport (1957)



$$\log (\text{expansion}) = \log (\text{expansion at zero stress}) - 6.4 \times 10^{-4} (\text{stress})$$



- SINTEF NTNU (2005)



- Zolochevsky (2005)

The Thermo-Chemo-Mechanical Potshell Deformation Model

- Waddington (JOM 1969) construct this cell to measure sodium expansion of a full scale cathode block in operation

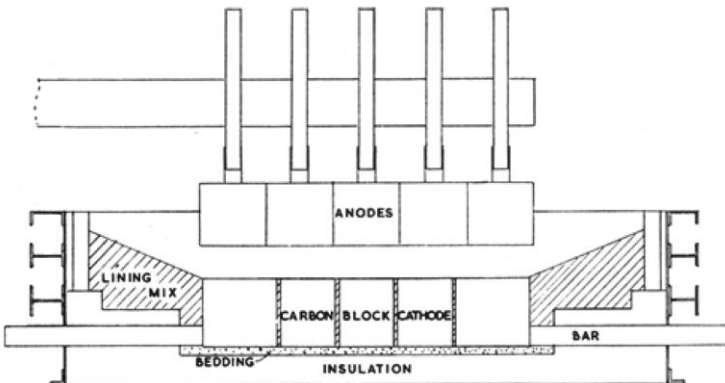


Fig. 1—Sectional elevation of a one-bar furnace.

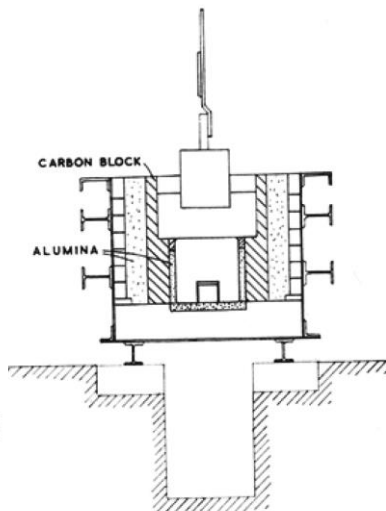


Fig. 2—Cross-section of a one-bar furnace.

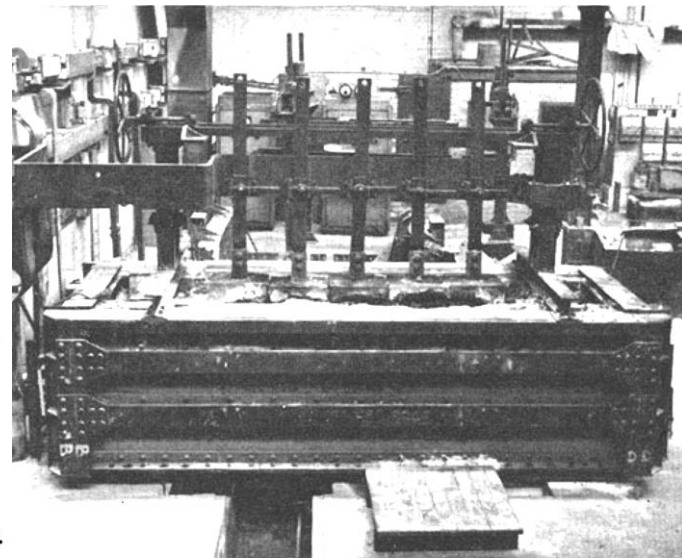


Fig. 3—General view of the one-bar experimental furnace.

The Thermo-Chemo-Mechanical Potshell Deformation Model

- Sun (TMS 2004) published this 3D quarter cathode model

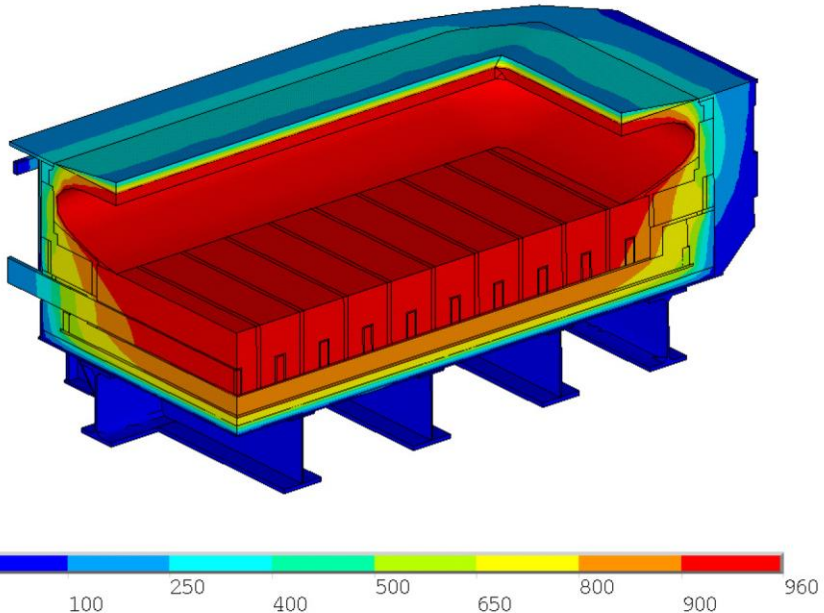


Figure 10: Thermal field distribution, 30 days after start-up (°C)

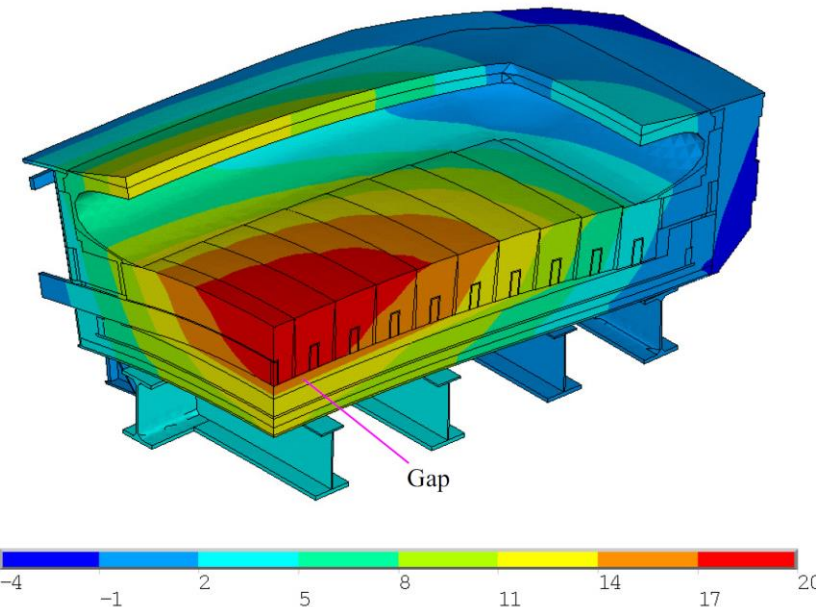
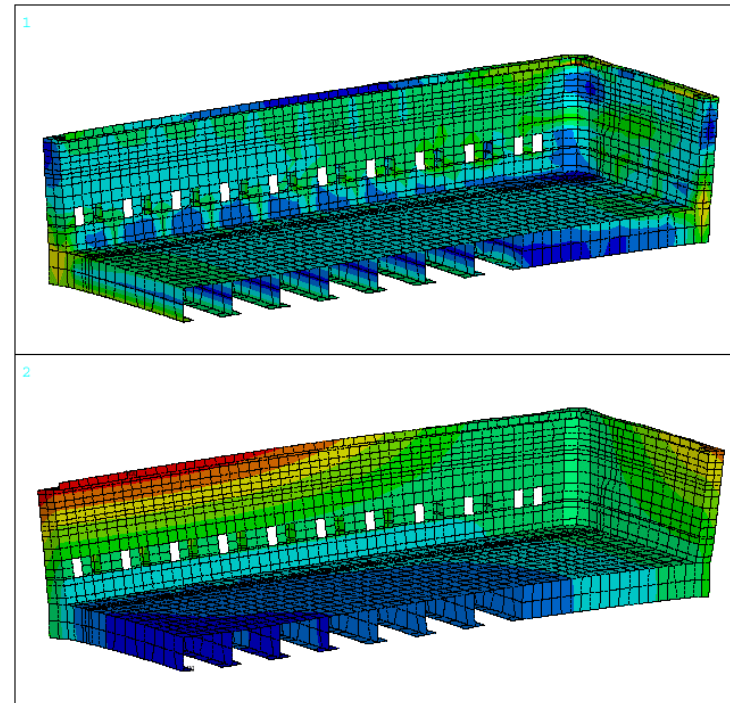
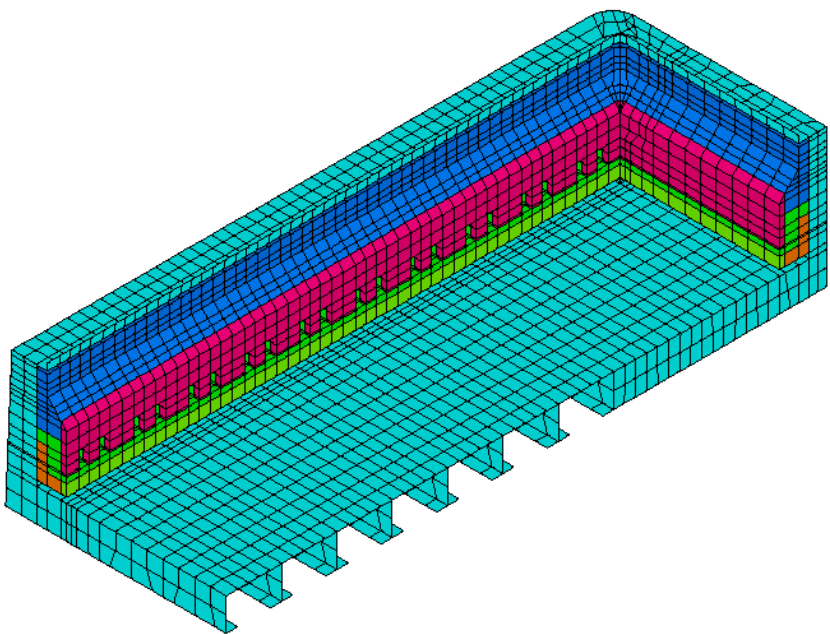


Figure 11: Z-direction displacement with thermal and sodium expansion (deformation enlarged $\times 20$), 30 days after start-up (mm)

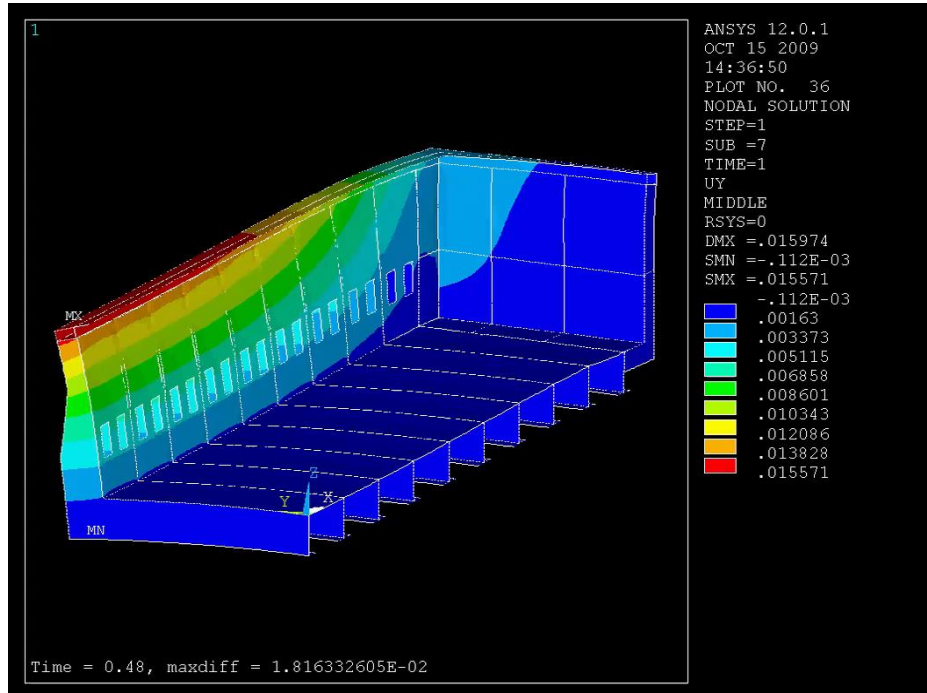
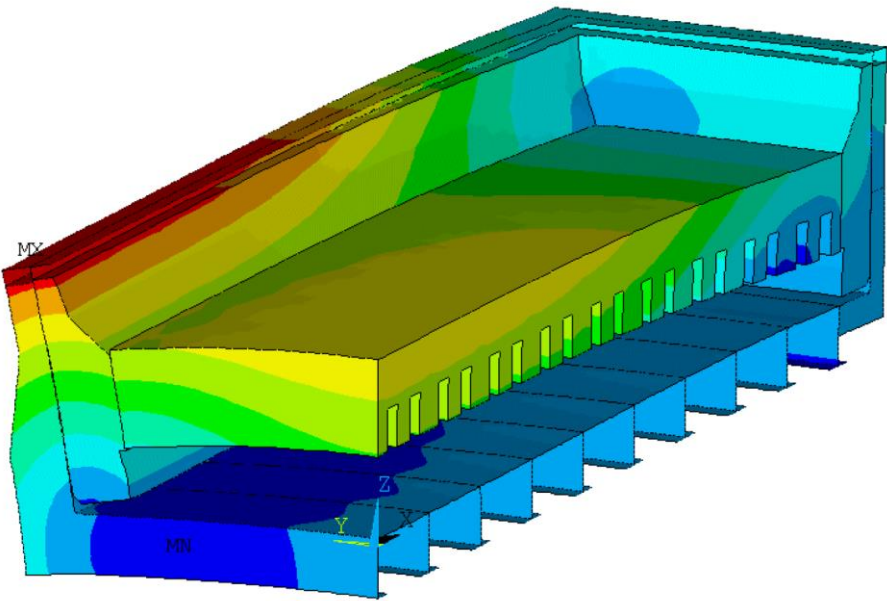
The Thermo-Chemo-Mechanical Potshell Deformation Model

- I developed for Alcan a same type of model (1993)

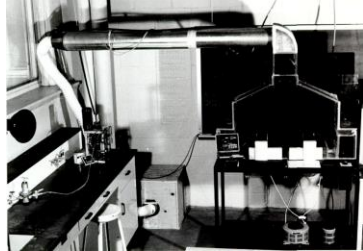


The Thermo-Chemo-Mechanical Potshell Deformation Model

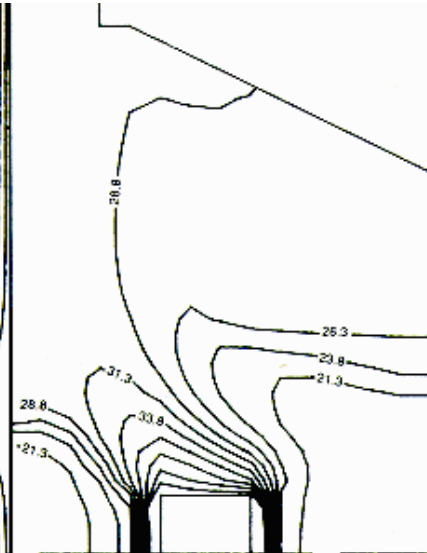
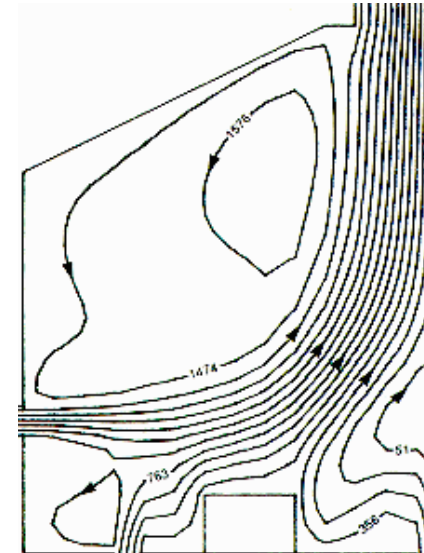
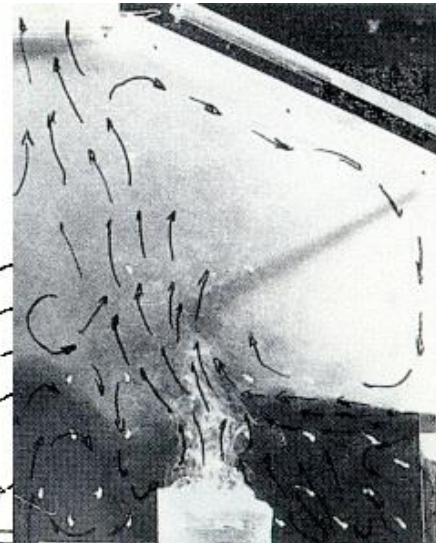
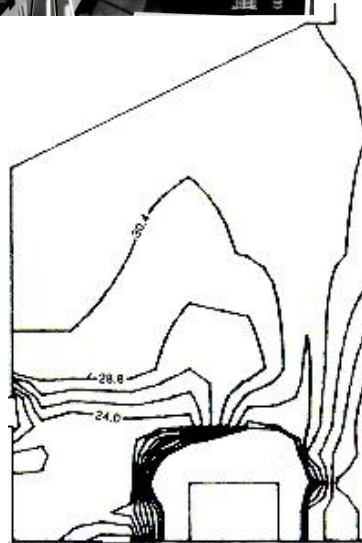
- I republished similar 3D quarter cathode model (TMS 2010)



The Potroom Ventilation CFD model



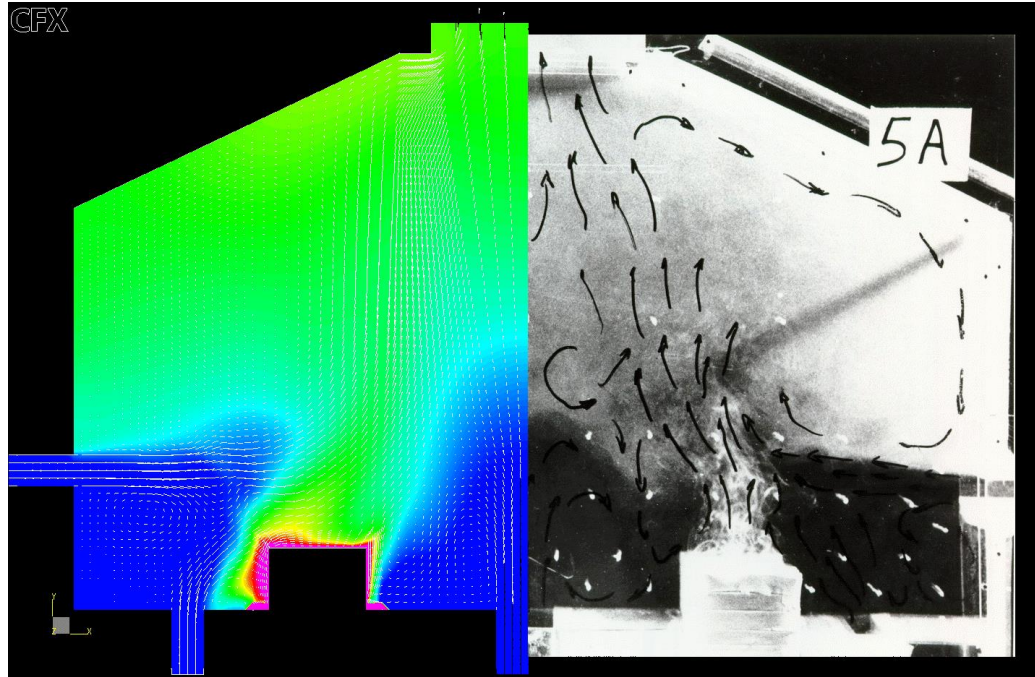
This was the subject of my Ph.D. thesis (1984)



- Left results from physical model, right best results of in house 2D CFD model

The Potroom Ventilation CFD model

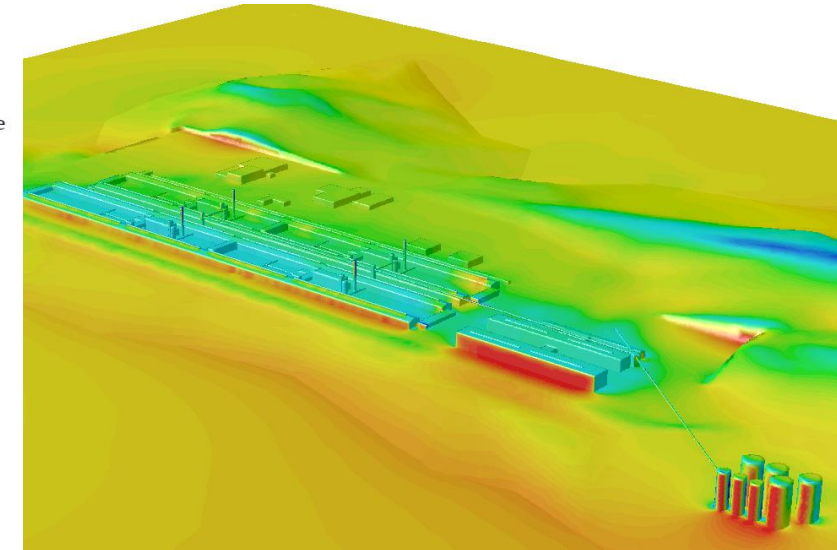
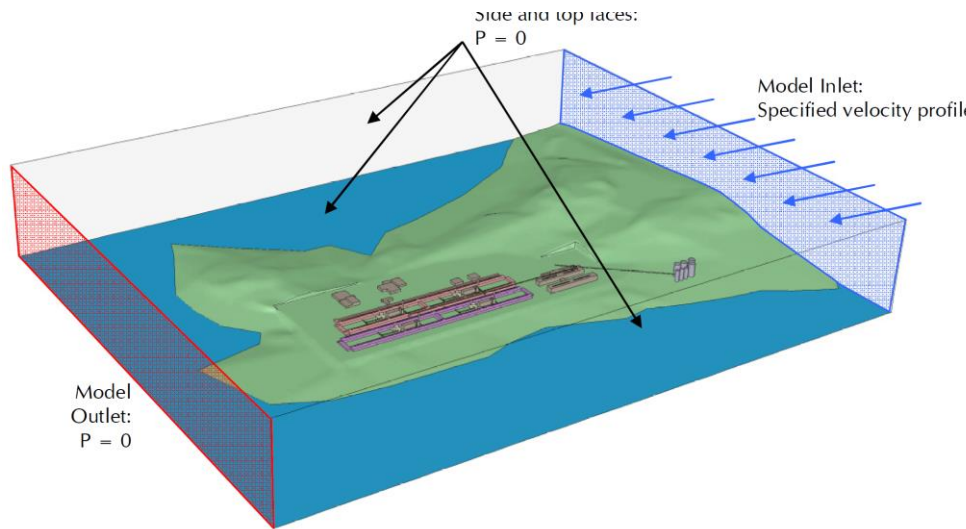
- I obtained a much better match using CFX 4 advanced turbulence model (1993)



- The turbulence model used is an asymmetric RANS Reynolds Stress model that in 2D requires the solution of 6 equations
- This type of turbulence model is not popular anymore, I did not test newer turbulence models since then.

The Potroom Ventilation CFD model

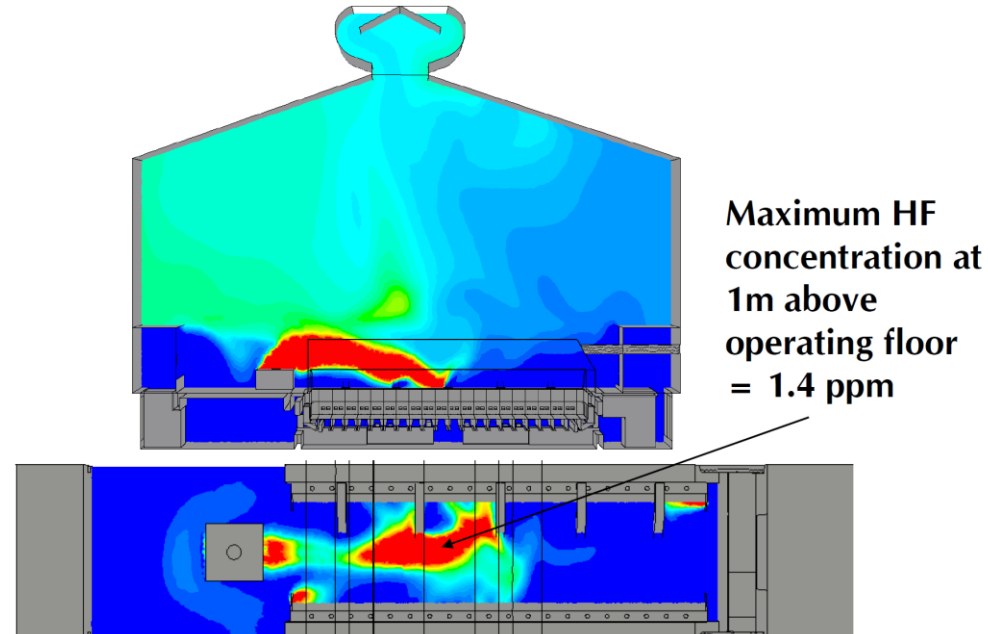
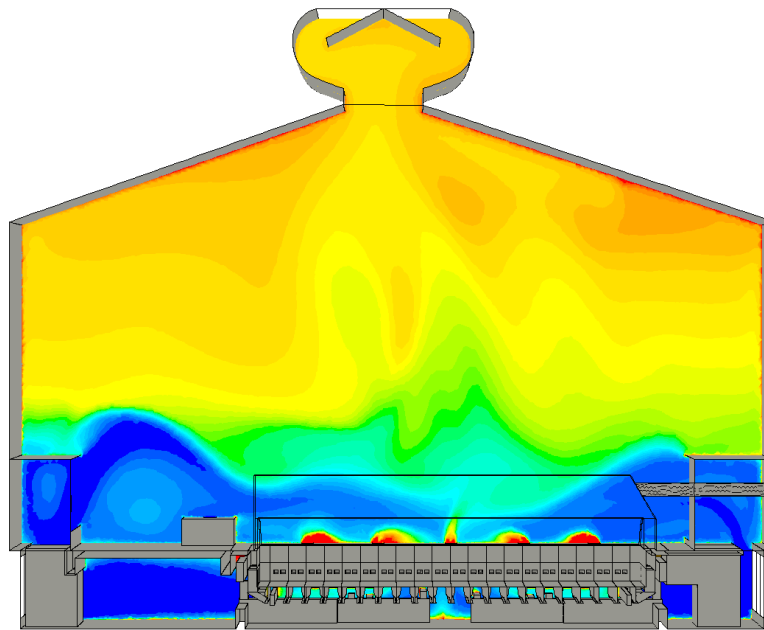
- Now modeling is obviously done in 3D like presented in this Hatch paper: Vershenya (TMS 2011)



- Left boundary conditions for wind from potline end and right pressure solution for wind from potline side

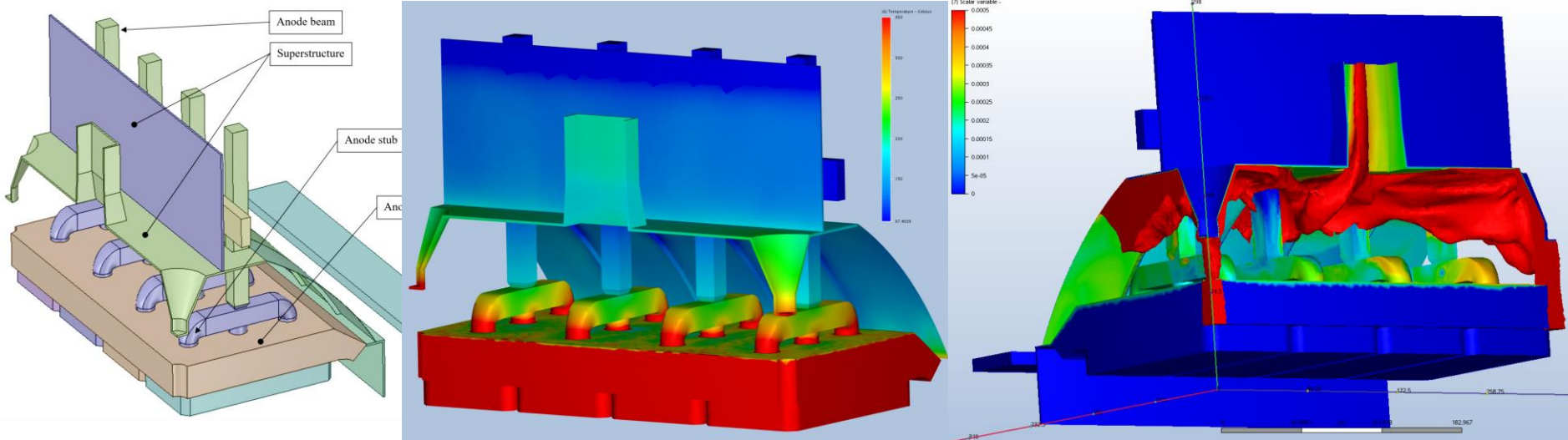
The Potroom Ventilation CFD model

- Now modeling is obviously done in 3D like presented in this Hatch paper: Vershenya (TMS 2011)



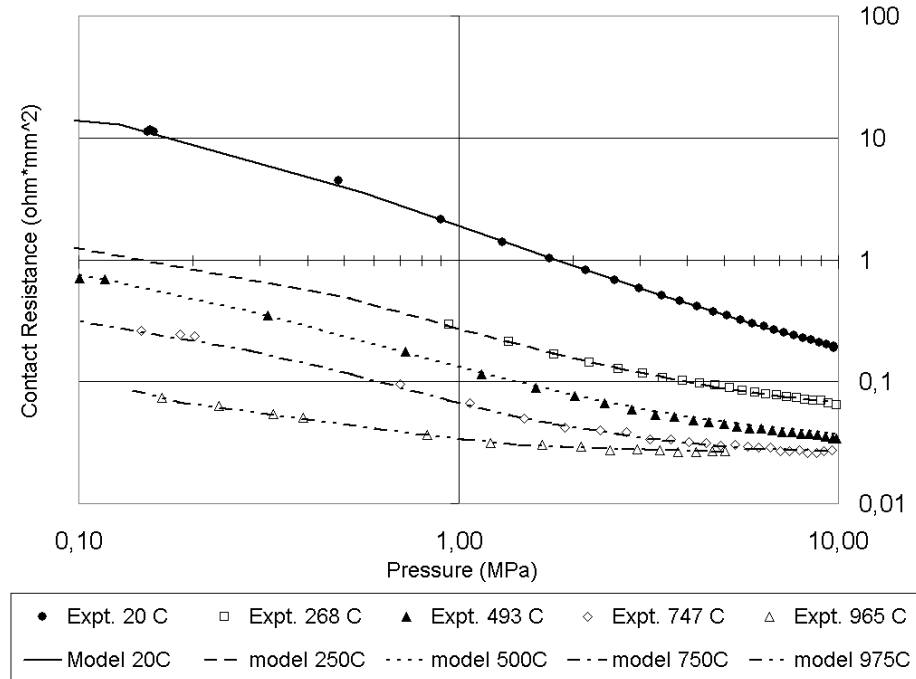
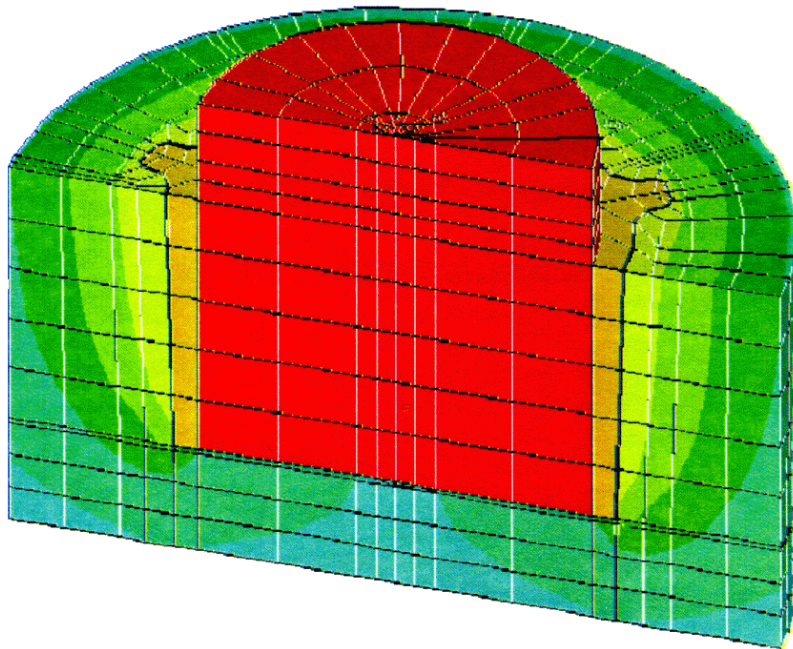
The Potroom Ventilation CFD model

- In 2017, I presented this combined TE-CFD model of the hood HF captation model



The Thermo-Electro-Mechanical Models

- Richard (TMS 2000) is the original developer of that new time of model that predict the contact resistance



The Thermo-Electro-Mechanical Models

- I presented (TMS 2010) my own version of TEM model

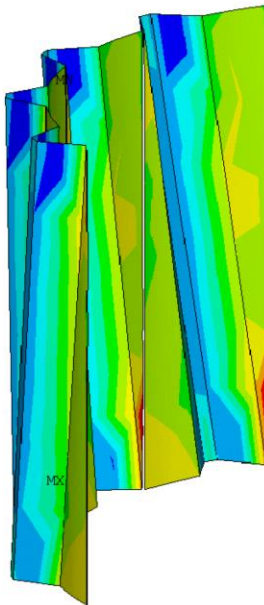


Figure 11 Cast iron/anode carbon interface
(MPa)

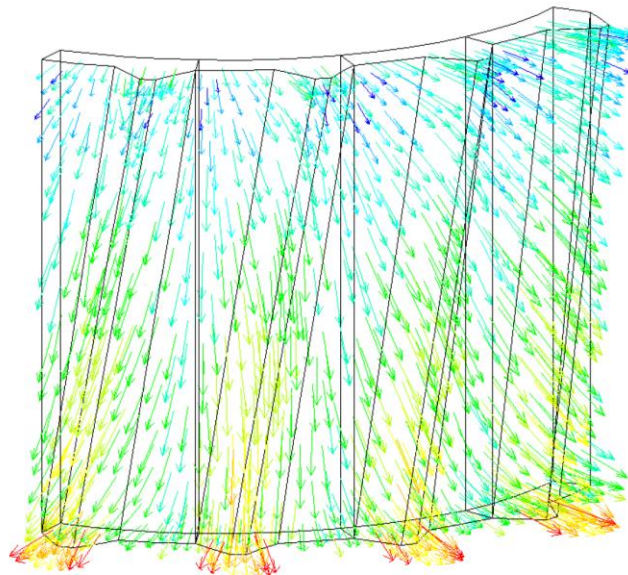


Figure 12: Current density distribution in the

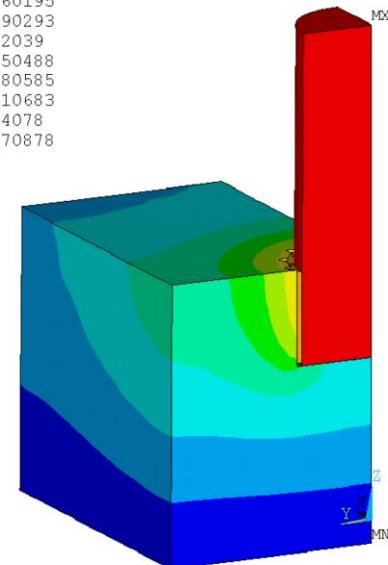
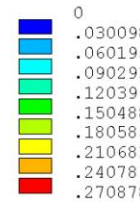
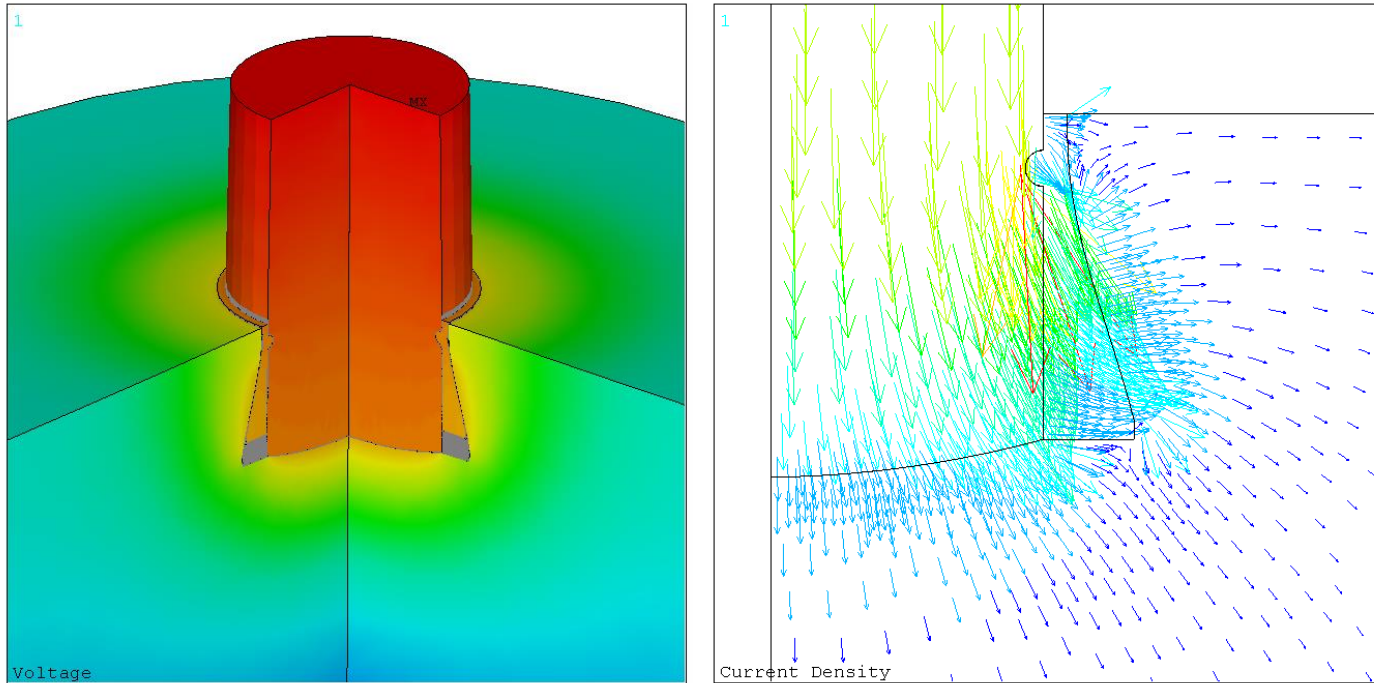


Figure 10: Model predicted voltage drop for the pressure and temperature dependent contact resistance setup (V)

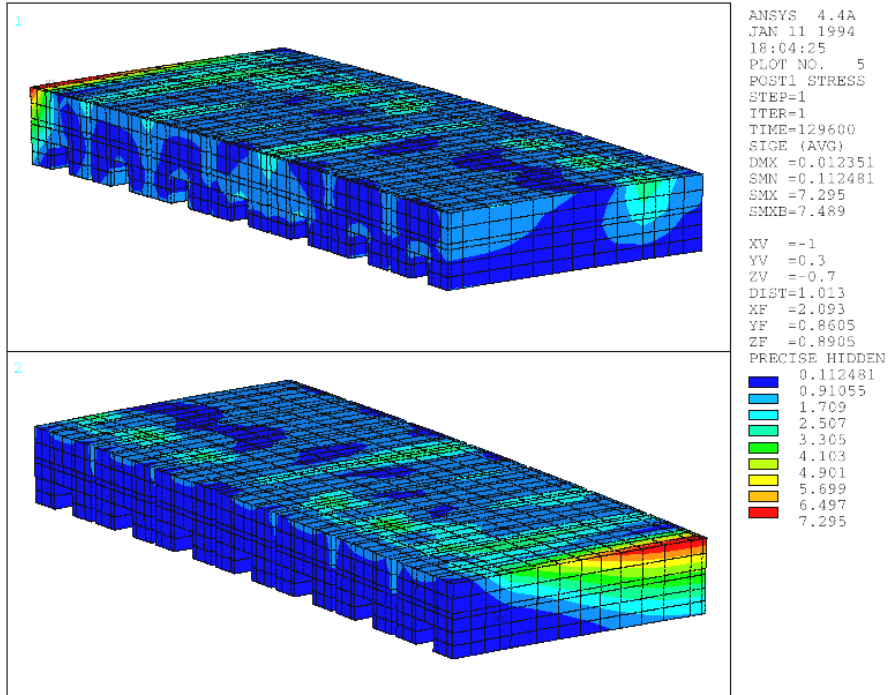
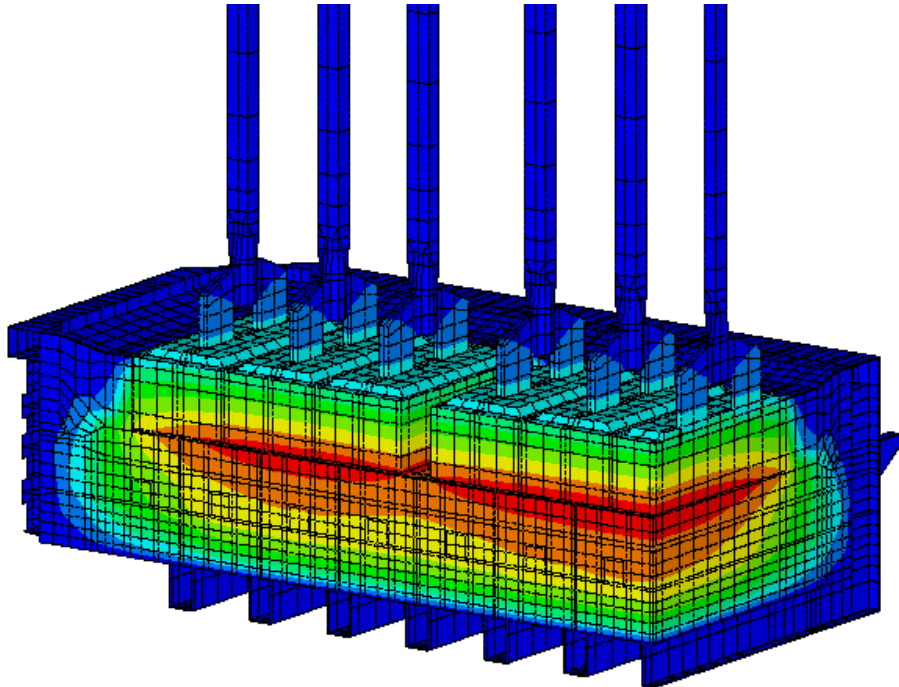
The Thermo-Electro-Mechanical Models

- I presented with Richard (2016) this new anode stub/carbon connection design patented by Hatch



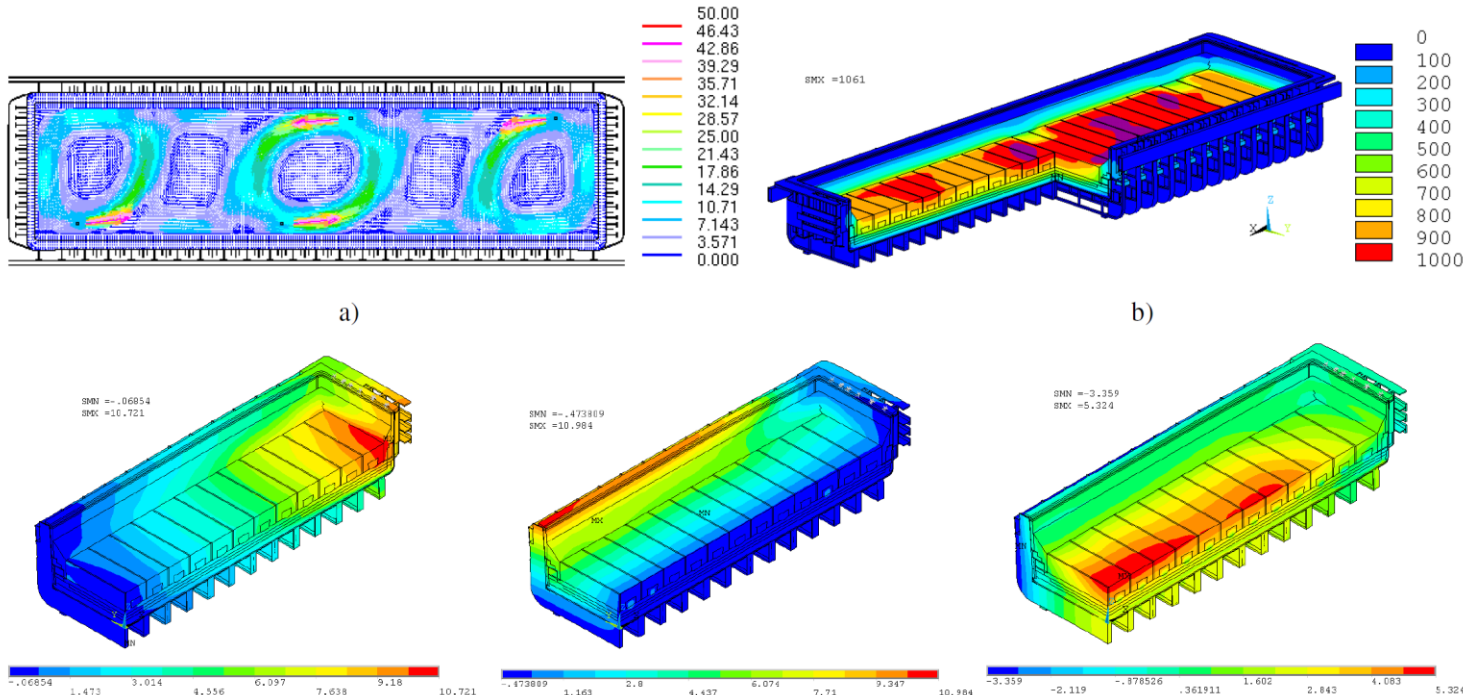
The Transient Thermo-Electro-Mechanical Cathode Preheating Model

- I developed for Alcan (1992) this type of preheat model



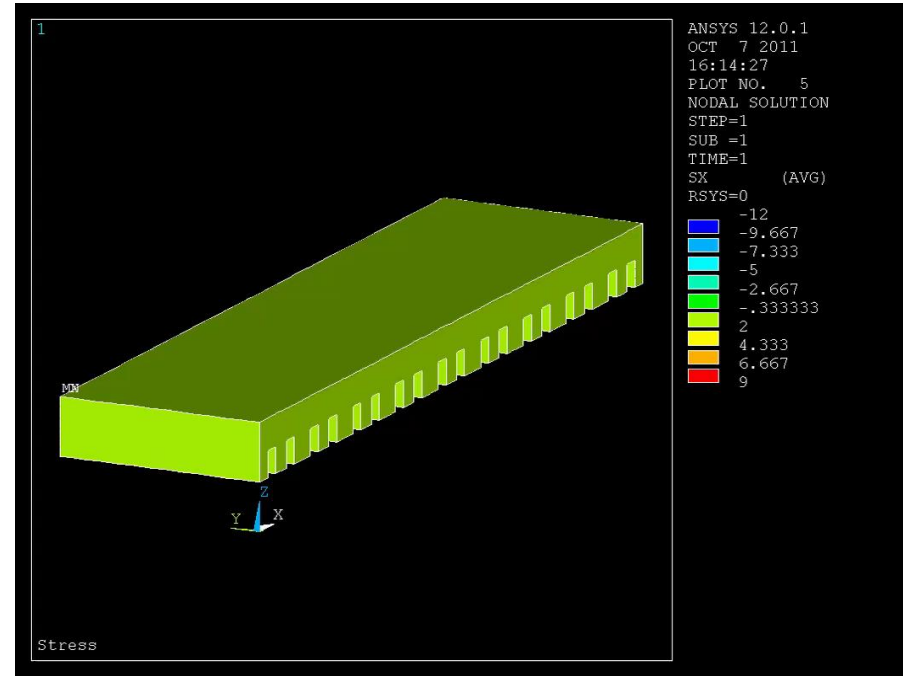
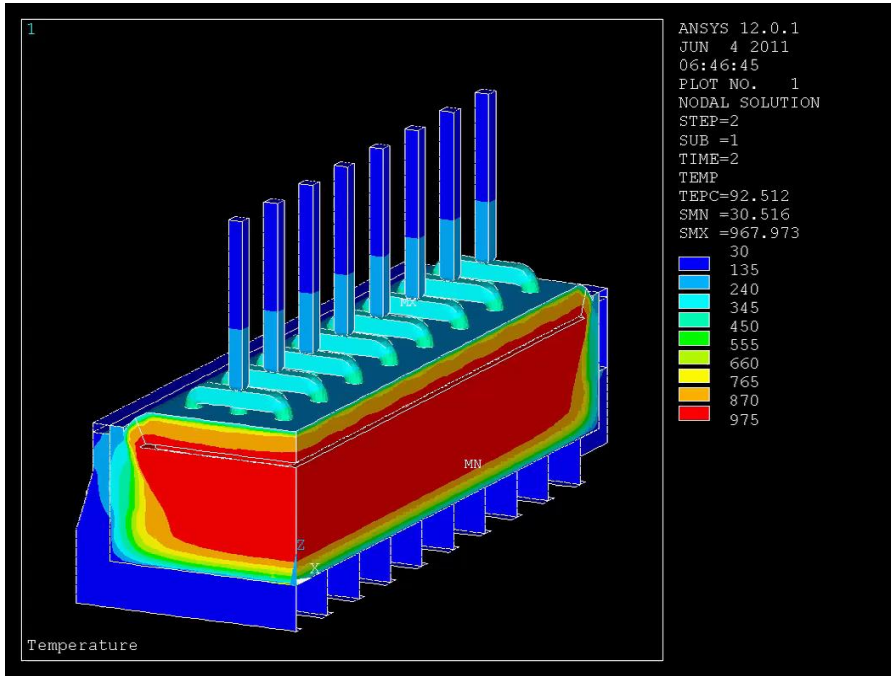
The Transient Thermo-Electro-Mechanical Cathode Preheating Model

- Arkhipov (TMS 2011) presented a gas preheat model



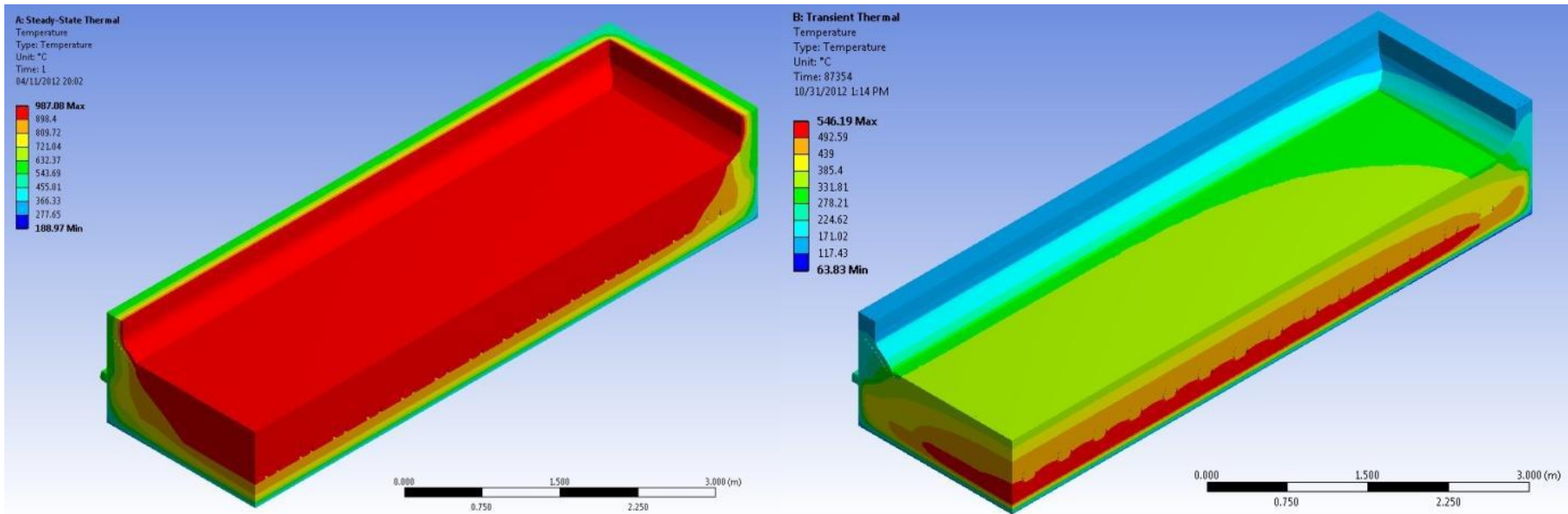
The Transient Thermo-Mechanical Cathode Cooling Model

- I developed that for Alton Tabereaux (TMS 2012)



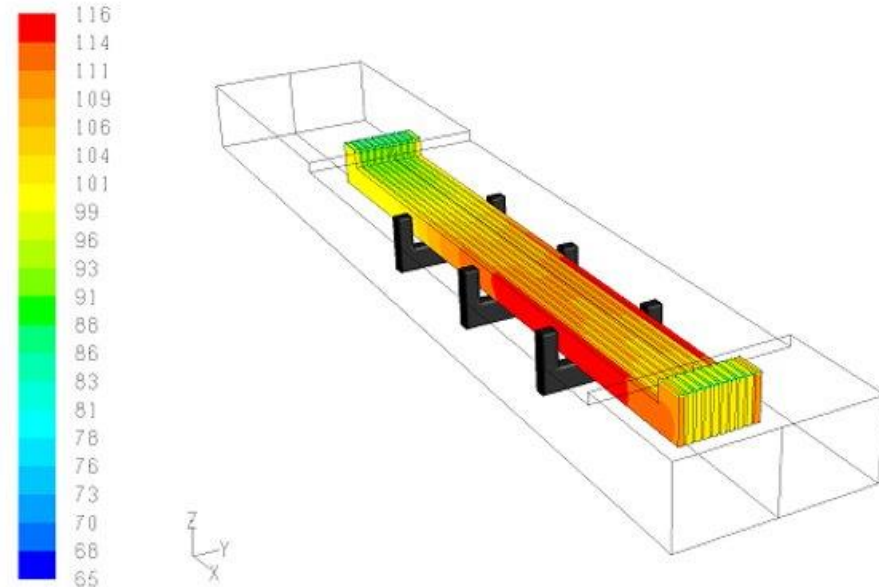
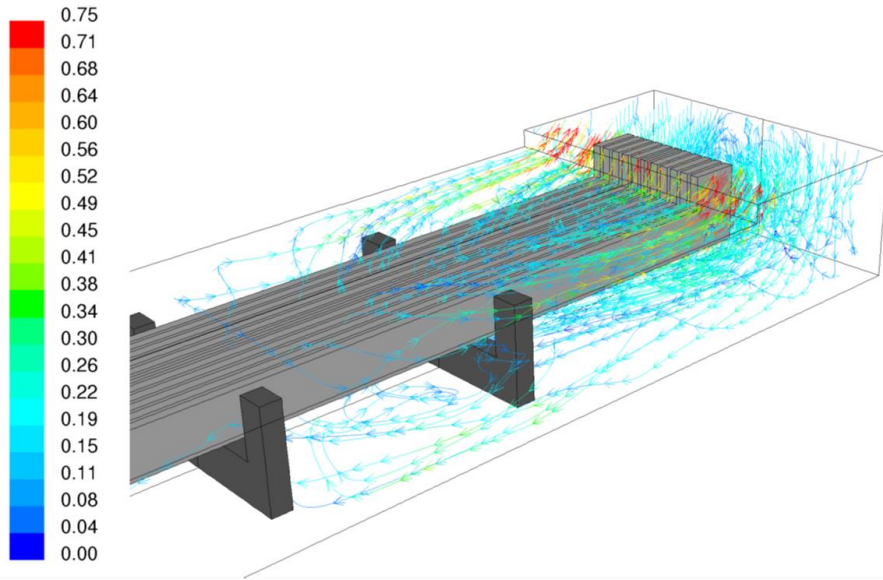
The Transient Thermo-Mechanical Cathode Cooling Model

- Hassan (TMS 2013) presented a similar cooling model



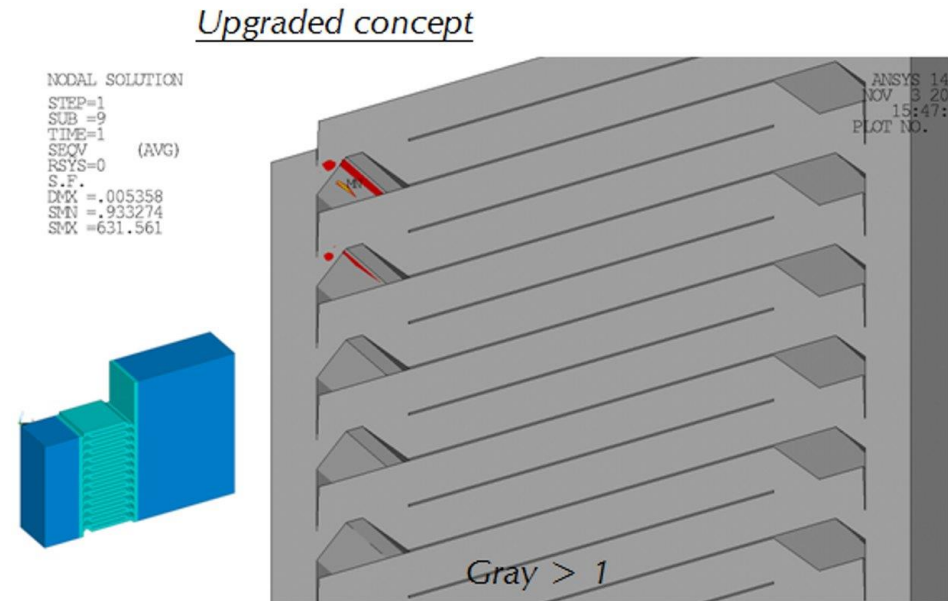
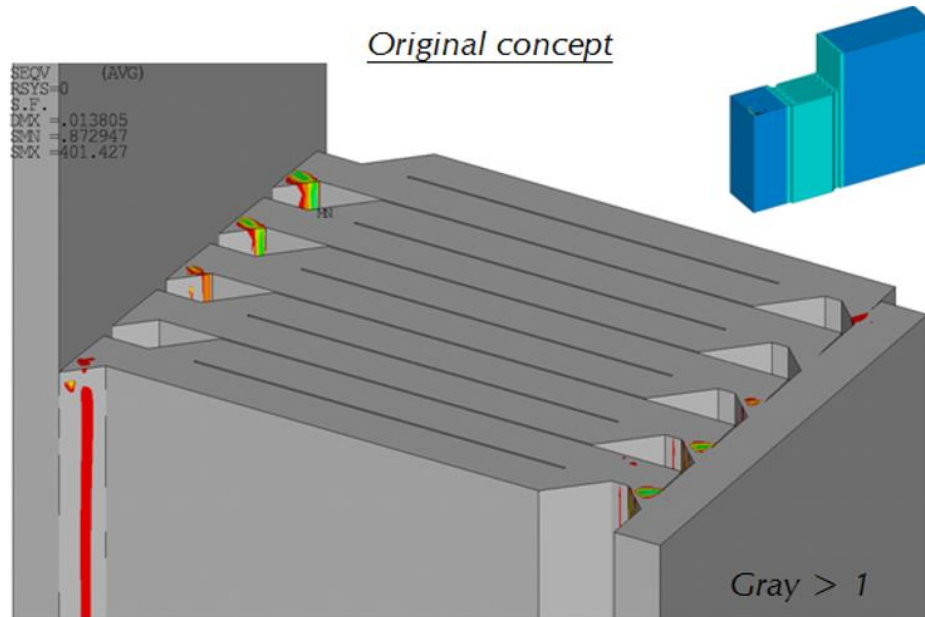
The Busbar and Flexes Thermo-Electro-Mechanical Models

- Schneider (TMS 2009) presented for Hatch a thermo-electro-CFD model of a busbar in a tunnel



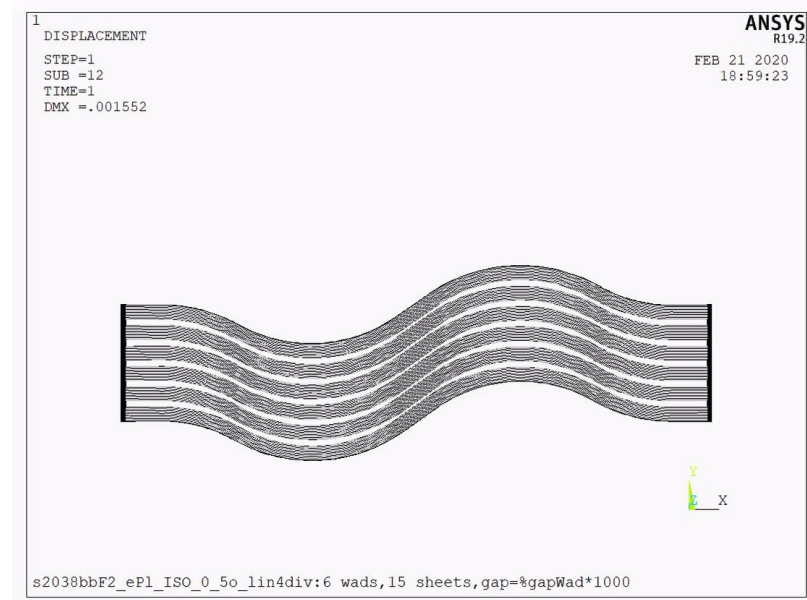
The Busbar and Flexes Thermo-Electro-Mechanical Models

- Schneider (TMS 2010) presented the stress analysis of welds. Safety factor results are presented here.



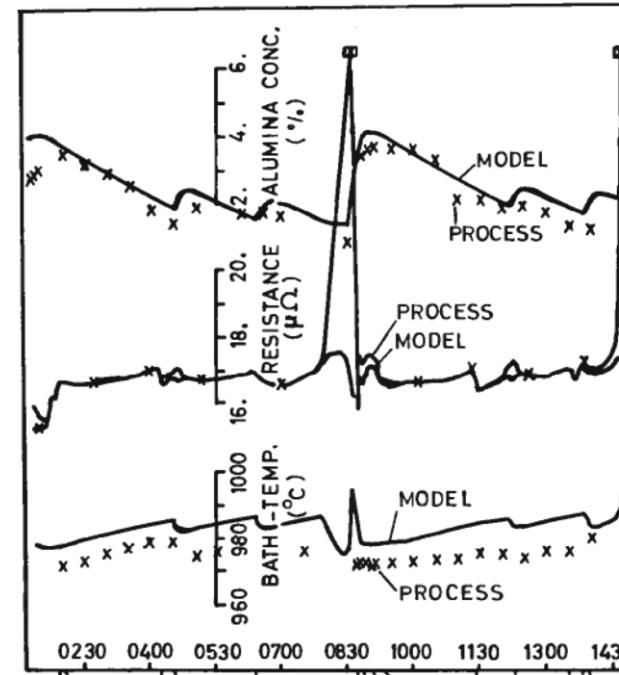
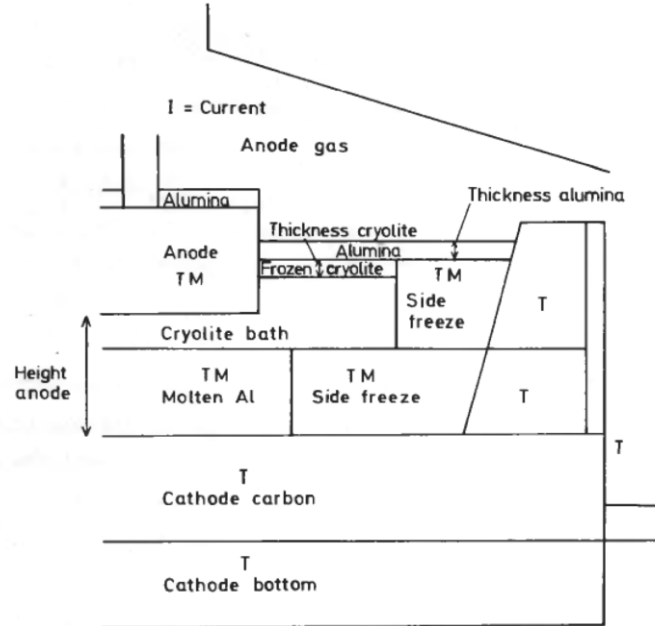
The Busbar and Flexes Thermo-Electro-Mechanical Models

- Schneider (TMS 2020) presented a mechanical analysis of flexibles involving large deflection and many contacts



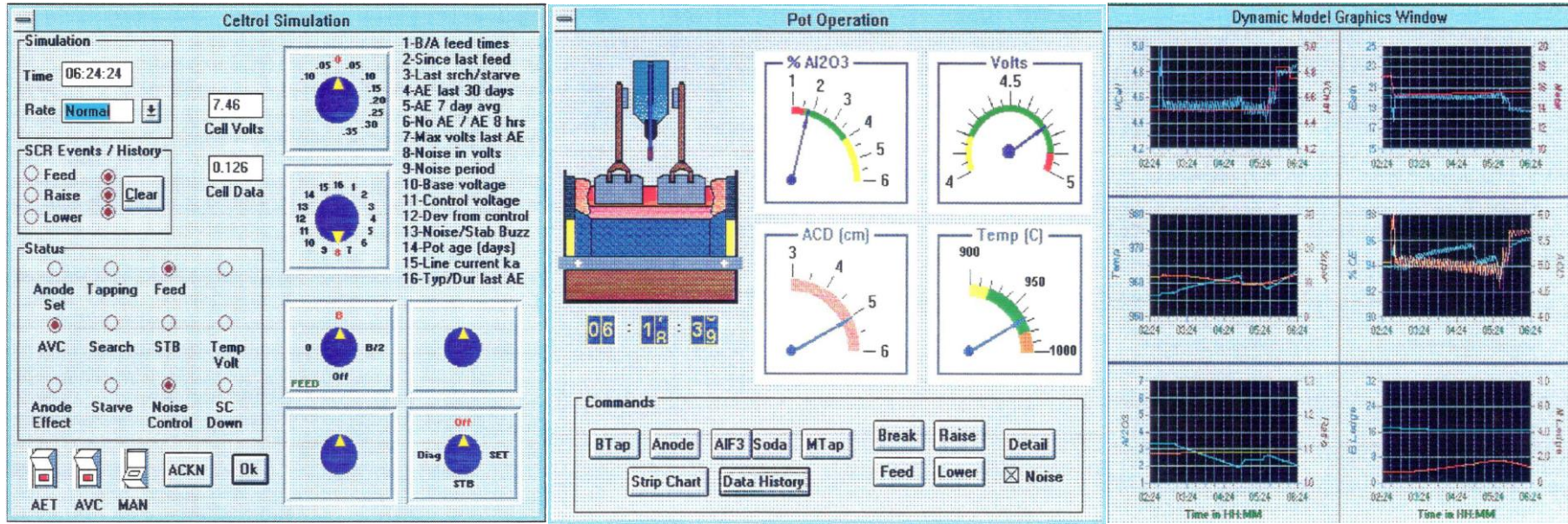
The Lump Parameters Dynamic Cell Simulator Model

- Gran (1980) presented the dynamic model developed by ASV (now Hydro Aluminium) to be used it as a digital twi



The Lump Parameters Dynamic Cell Simulator Model

- TANG (TMS 1998) presented the dynamic model developed for Kaiser by Wright (Ph.D. thesis 1993)



The Lump Parameters Dynamic Cell Simulator Model

- Gusberti (Ph.D. thesis 2014) presented the dynamic model he developed for Caete

Cell Balance Inputs

Methods

- Heat Balance Method
 - General Mass/Enthalpy Balance
 - Voltage Equations (Haupin, 1998)
- Pot Voltage Method
 - Voltage Output
 - Voltage Input

Operational Data

Current Efficiency [%]	92.09	Short Circuit CE Loss Fraction [0-1]	0.5
Bath Temperature [°C]	962.1045	Scrubber Eff. [%]	99.75
Delta T (Tbath-T Metal) [°C]	0	Hood Eff. [%]	99.8
Potroom Temperature [°C]	50.5	Duct Gas Temperature [°C]	147.5
Potroom Relative Humidity [%]	31	Duct Gas Flow Rate [Nm ³ /h] per cell	5900
Pot-to-Pot Voltage Drop [V]	4.354	Dust Escaped from Potroom [kg/ton Al]	0.46
Bath Height [mm]	170	Gross Carbon [kg/ton Al]	591
Metal Height [mm]	200	Anode Change Frequency [h]	32
Anode Cover [mm]	80	Anode Hole Expansion Time [s]	600
R cathode [μΩ]	1.2519	Cover/Crust Removed per Anode Butt [kg]	158.3
Bath Chemistry Targets			
Al2O3 [%]	2.45	Propotion of Crushed Bath [%]	50
CaF ₂ [%]	5	Pacman Material Mass [kg]	200
MgF ₂ [%]	0	Device Mass [kg]	300
Excess AlF ₃ [%]	11	Device Temperature [°C] Before	150

Primary Alumina

Alpha Alumina [%]	2	Na ₂ O [%]	0.782
Na ₂ O [%]	0.42	CaO [%]	0.006
CaO [%]	0.006	F [%]	1.91
LOI (sum) [%]	1.4		

Secondary Alumina

Na ₂ O [%]	0.782
CaO [%]	0.006
F [%]	1.91

Bath Resistivity Formula [Ωm.mm]

- Wang
- Choudhary
- Hives
- Grotheim and Welch
- User Defined Value

Bubble Layer dV Calculation [V]

- Smooth Anode
- Slotted Anode Reduction Factor
- User Defined Value [V]

Liquidus Temperature Formula [°C]

- Solheim et al. 1996
- Kolas, 2007
- Rostum et al. 1990
- Lee et al.
- User Defined Value

Done!

View Thermal Balance Results

View Mass Balance Results

View Cell Top Heat Outputs

Back to Main Menu

Mass Balance Data

MASSFLOW ENTERING CONTROL VOLUME [kg / ton Al]

Primary alumina from Feeders (plus impurities)	1898.75	AlF ₃ Additions	17.12
Cover Spillage	21.74	Neutralize Na ₂ O	14.57
		Neutralize CaO	0.12
		Maintain Bath Ratio	2.25
		Compensate Recycle Losses	0.19
Al ₂ O ₃ Required	1884.97		
Na ₂ O	8.06		
CaO	0.12		
LOI Total	26.88		
Extra Input to Compensate Dust	0.46		
Air Drawn into the Cell	135222.55		
N ₂	97096.97		
O ₂	29766.84		
H ₂ O (Humidity)	6629.06		
Na ₂ O	6.95		
Recycled Materials	0.00		
CaO	0.00		
AlF ₃	54.03		
Gross Carbon Consumption	591.00		
Net Carbon Consumption	416.00		
Yoke+Pins +Cast Iron (Fe)	177.40		
Cover Added (Alumina)	122.00		
Boudouard Reaction	16.90		
Air Burn	36.62		
Sulfur Content	9.65		
Carbon in COS emission	1.81		
TOTAL	138440.70		
Extra Input to Compensate Dust	2.82		
View Mass Balance Picture			

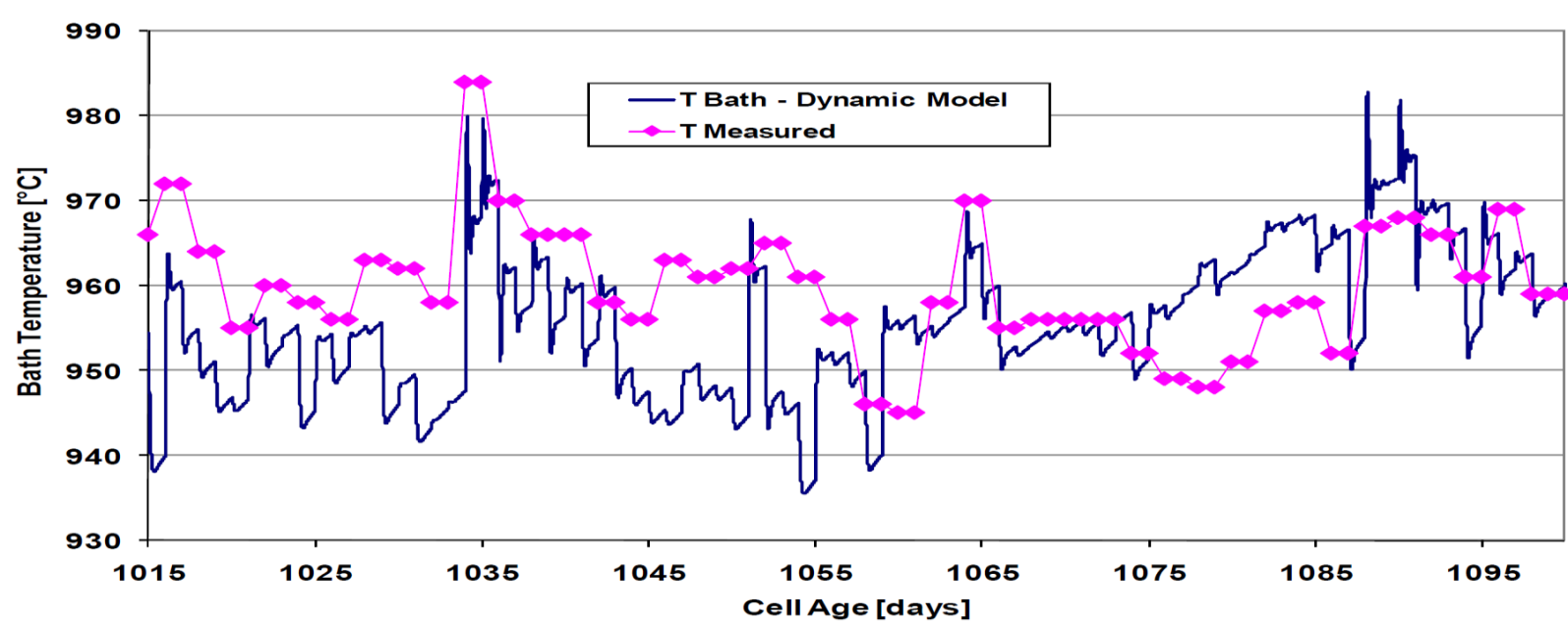
MASSFLOW LEAVING CONTROL VOLUME [kg / ton Al]

Total Duct Emissions	136566.16	Aluminum Produced	1000.00
Total CO ₂	1552.98	Dusts - Carbon	2.82
Total O ₂	29571.59	Dusts - Alumina	0.46
Total Bath Produced	75.63		
Cryolite	18.21	Al2O3 prim. (AlF ₃)	4.49
CaF ₂	0.16	Al2O3 sec. (AlF ₃)	3.77
N ₂	97096.97	2.25 Al2O3 Fluoride Ev.	25.01
Argon and Others	1656.43	Bath Generated from Cover Spillage	21.74
Total AlF ₄	0.00	Anode Butt (C)	175.00
Total SO ₂	19.28	Anode Rod (Al)	65.48
Total CO ₅	0.00	Yoke+Pins +Cast Iron (Fe)	177.40
Vaporized Cryolite	15.52	Butt Cover (Alumina)	44.29
Vaporized CaF ₂	0.00	Butt Cover (Crushed Bath)	44.29
More Emissions Details		Pacman Material (Alumina)	55.96
Back to Cell Input Data		Pacman Material (Crushed Bath)	55.96
Back to Main Menu		Cleaning Device (Iron)	167.89
TOTAL	138440.70		



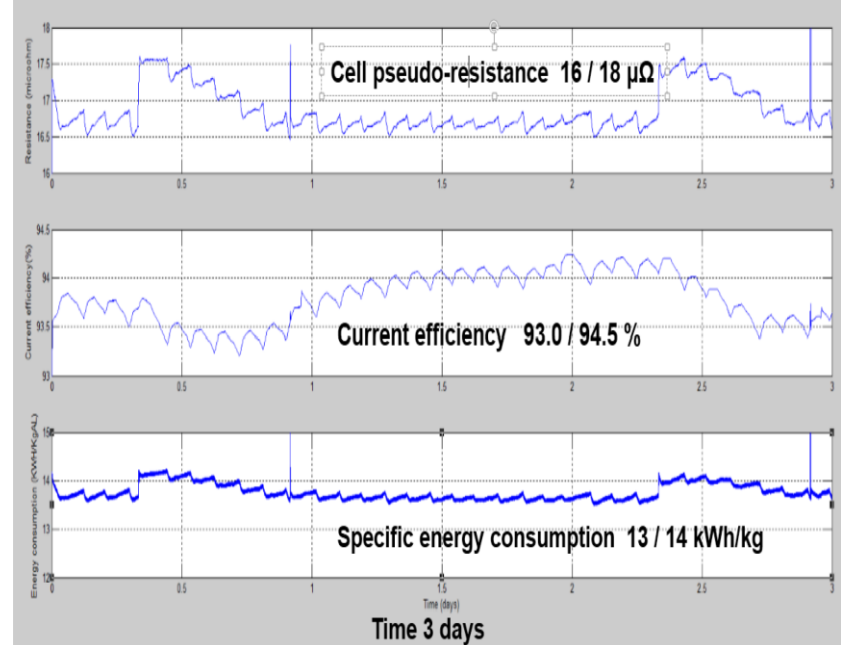
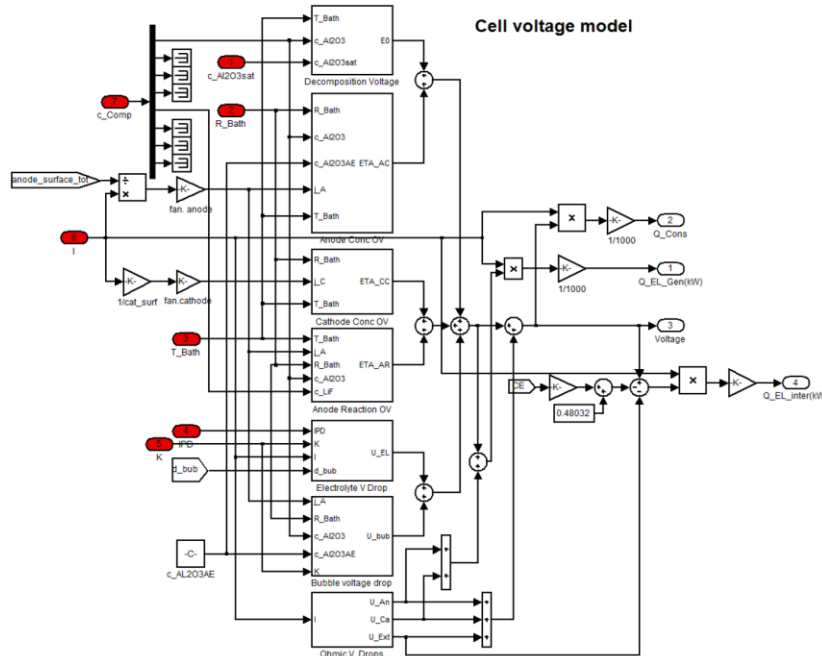
The Lump Parameters Dynamic Cell Simulator Model

- Gusberti (Ph.D. thesis 2014) presented the dynamic model he developed for Caete



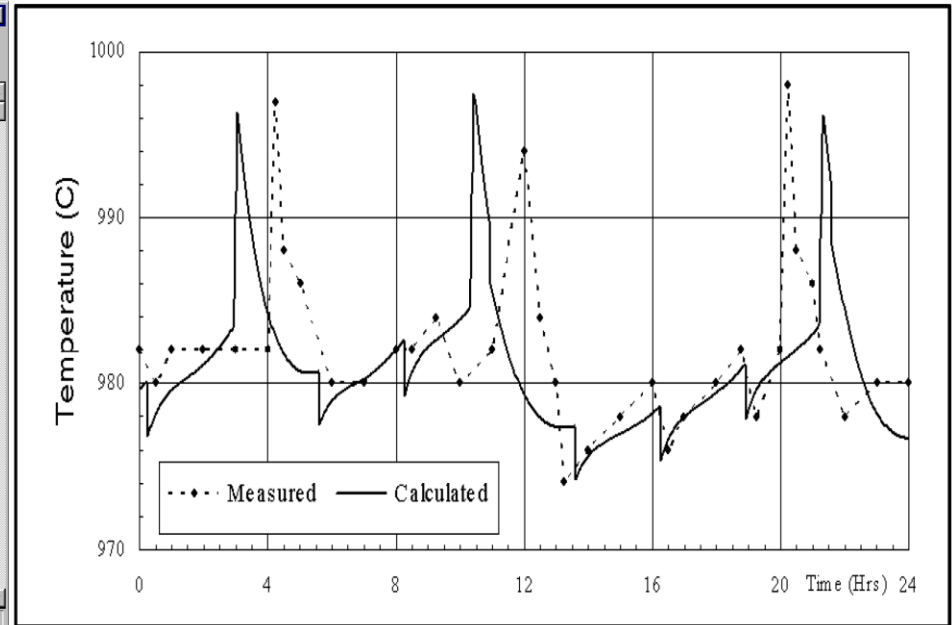
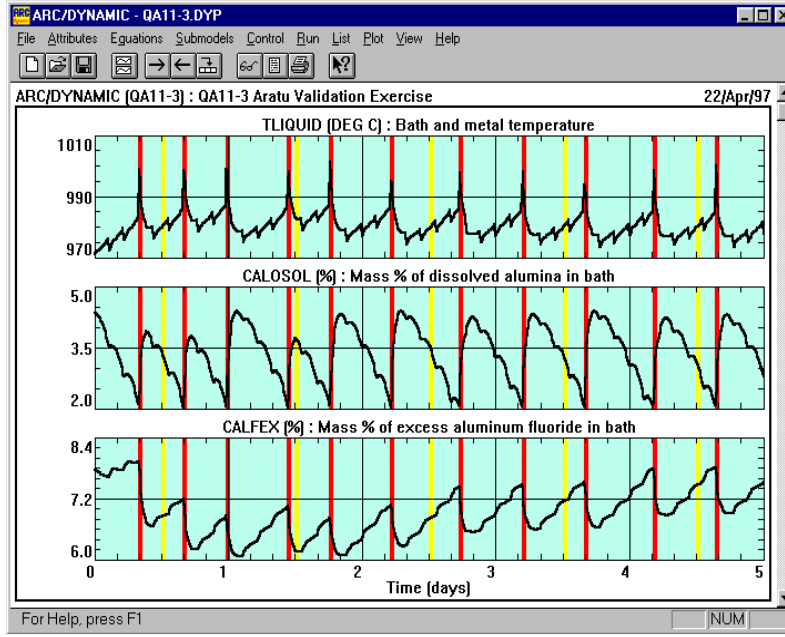
The Lump Parameters Dynamic Cell Simulator Model

- Antille (2015) presented the dynamic model he developed for Kannak using MATLAB-SIMULINK



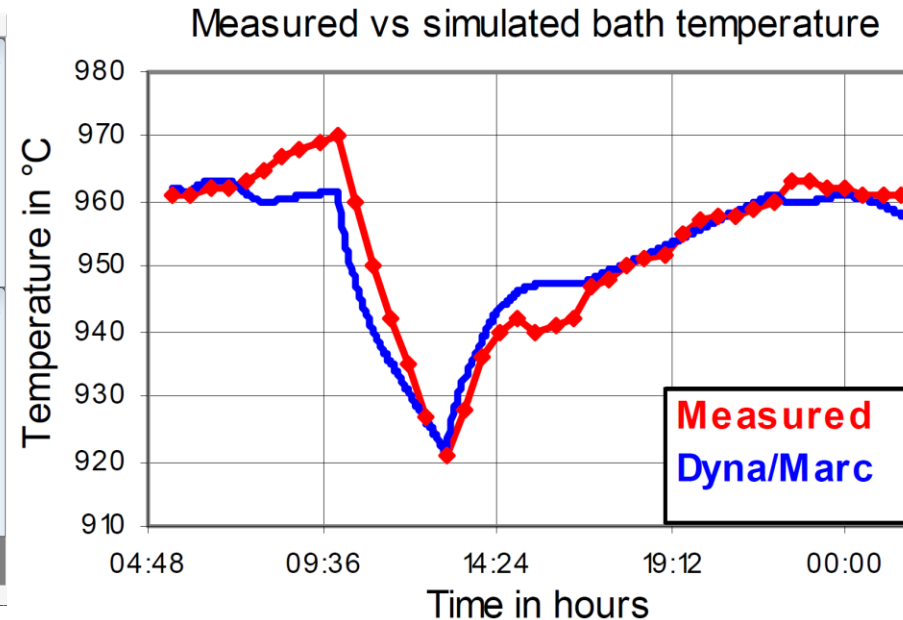
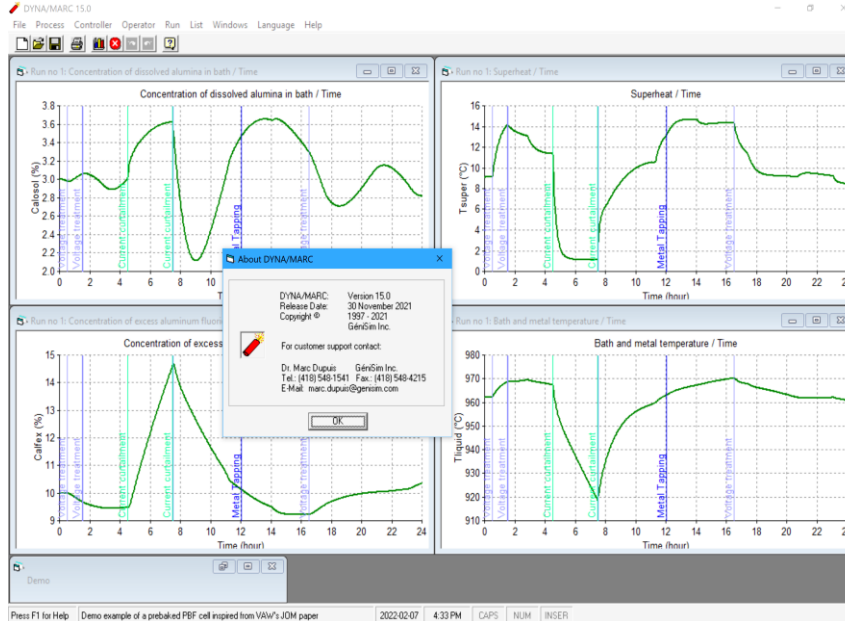
The Lump Parameters Dynamic Cell Simulator Model

- I presented my own dynamic cell simulator Dyna/Marc at TMS 1996, initially commercialized under another name



The Lump Parameters Dynamic Cell Simulator Model

- Eick (2007) presented a Dyna/Marc validation exercise using a recorded data from a 3 hours shutdown event



The Multi-Zones Dynamic Cell Simulator Model

- This is a new type of lump parameters model having multiples liquid zones. From Wong (2021).

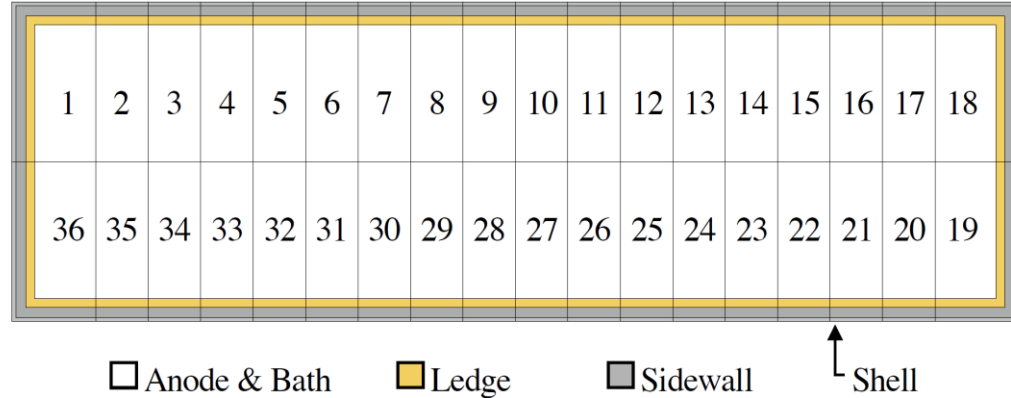
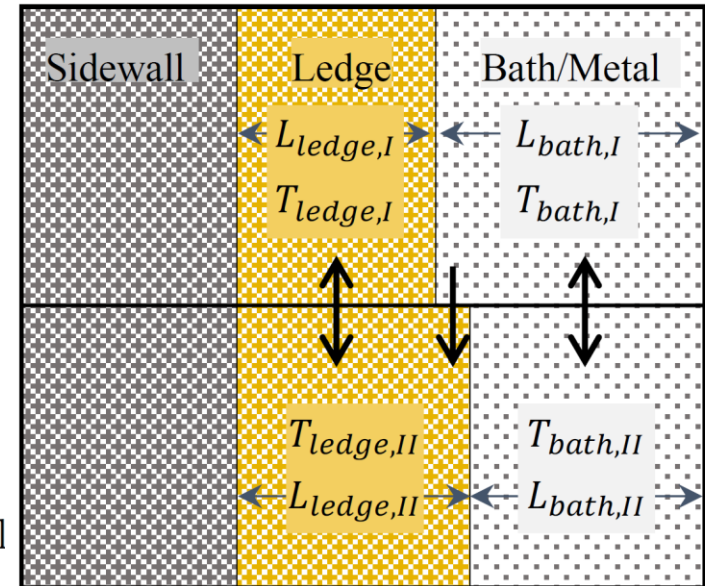
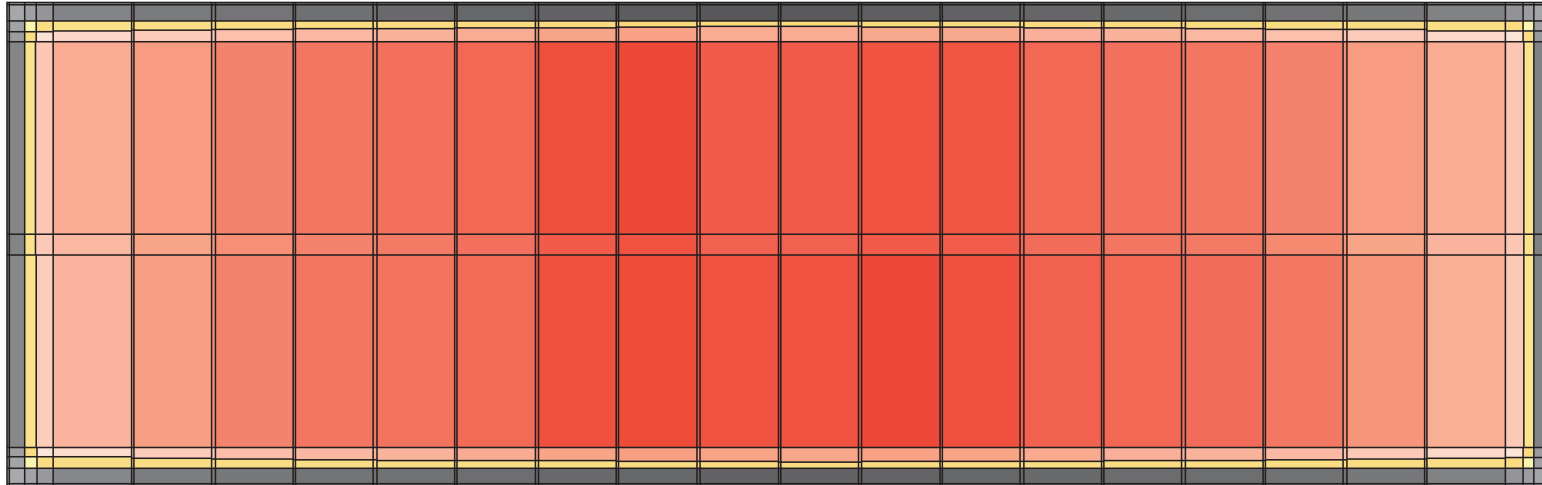


Fig. 2. Proposed model discretization for a 36-anodes cell



The Multi-Zones Dynamic Cell Simulator Model

- This is a new type of lump parameters model having multiples liquid zones. From Wong (2021).



(b)

967

Bath

982

The Multi-Zones Dynamic Cell Simulator Model

- The same can be done to predict alumina concentration.
Wong (2019).

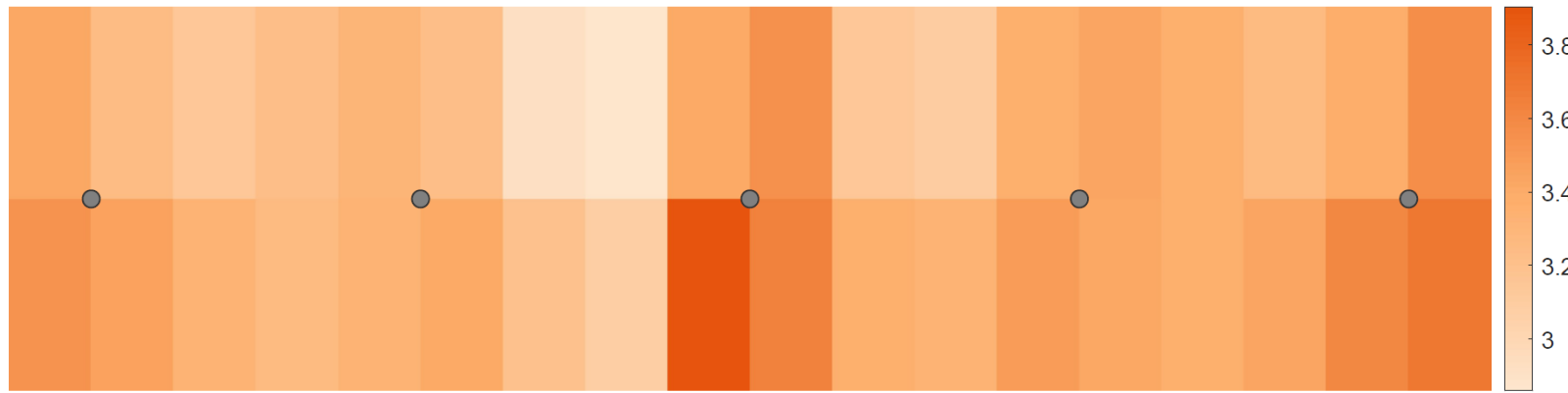
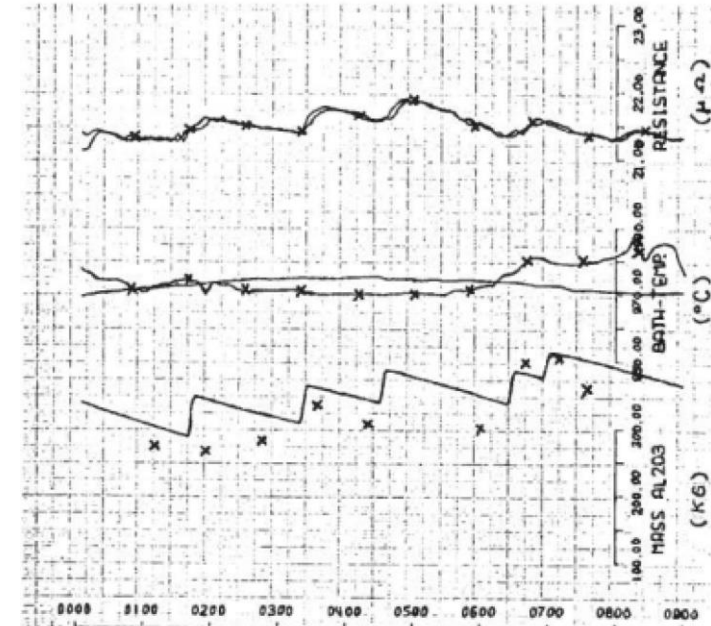
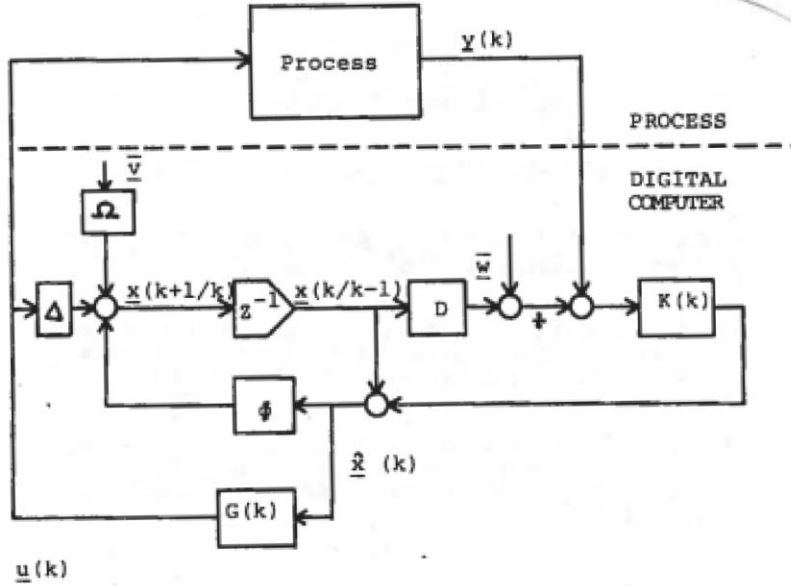


Figure 8 Spatial variations in dissolved alumina concentration (wt%)

The Cell Digital Twin

- Hydro Aluminium (ASV) is by far the leader in that type of model and cell control development (TMS 1975)



The Cell Digital Twin

- Gran (1980) represented the digital twin concept while presenting the ASV dynamic model

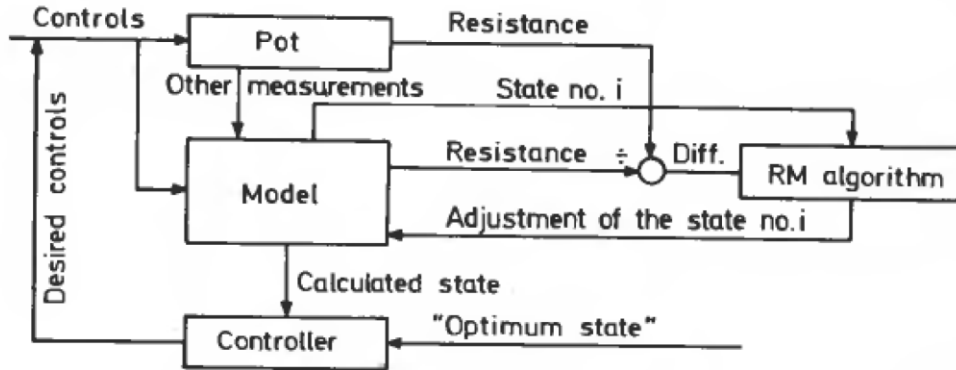
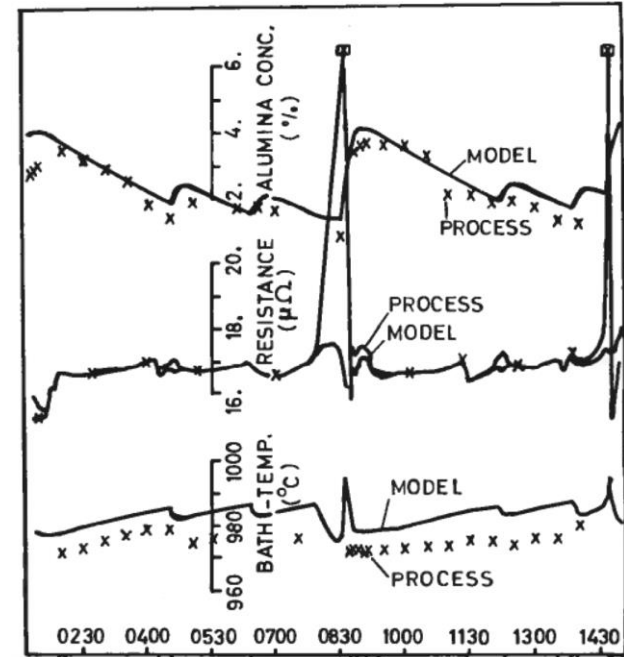
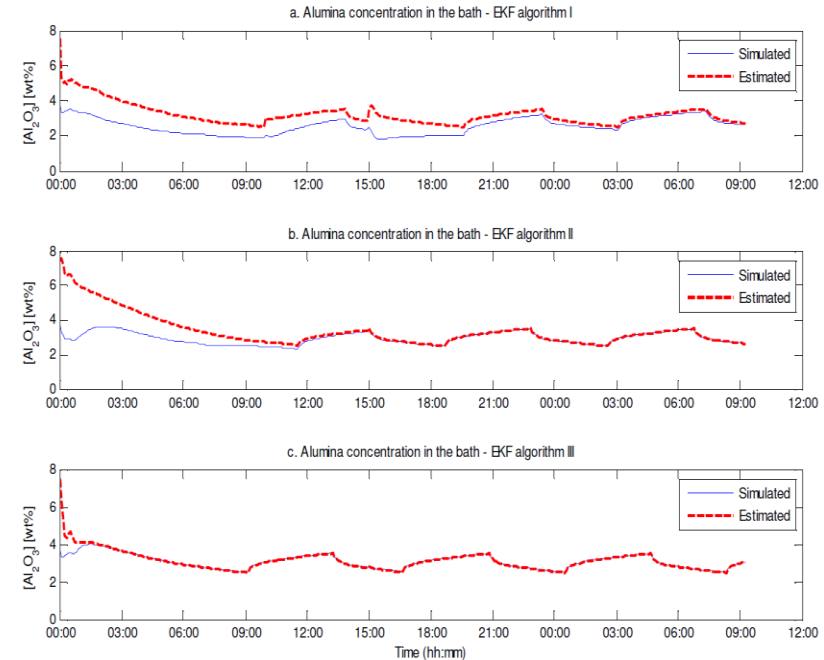
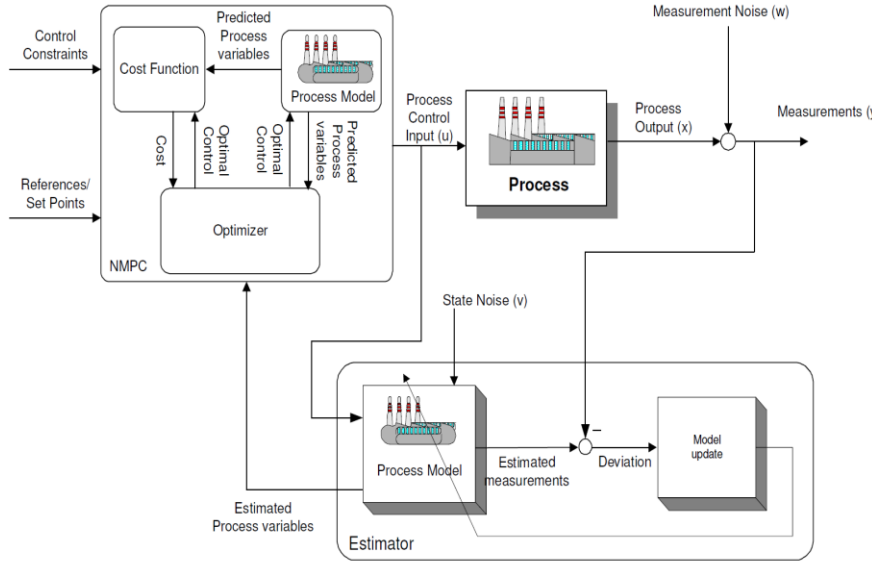


Figure 4. Multivariable control system for aluminium reduction cells.



The Cell Digital Twin

- Kolas (TMS 2010) represented the digital twin concept for a third time

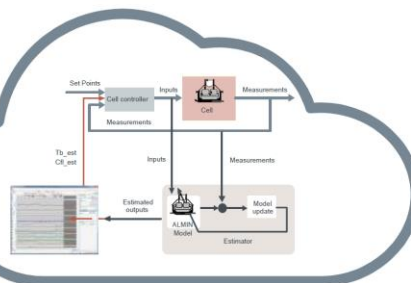


The Cell Digital Twin

- Hydro Aluminium is regularly presenting the digital twin control logic used by the Hal4e and Hal4e Ultra



The concept of digital twins Electrolysis cell as illustration



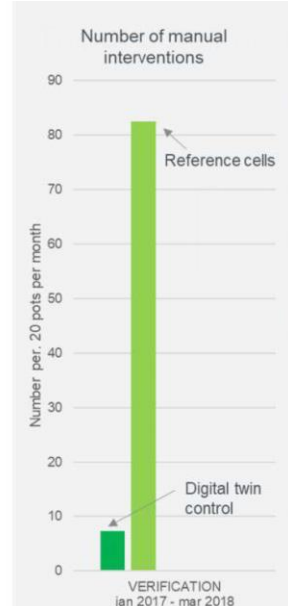
Numerical simulation model based on:

- Physics-based models
- Sensor data from production
- Advanced analytics algorithms

Industrial experience Digital twin for electrolysis cells

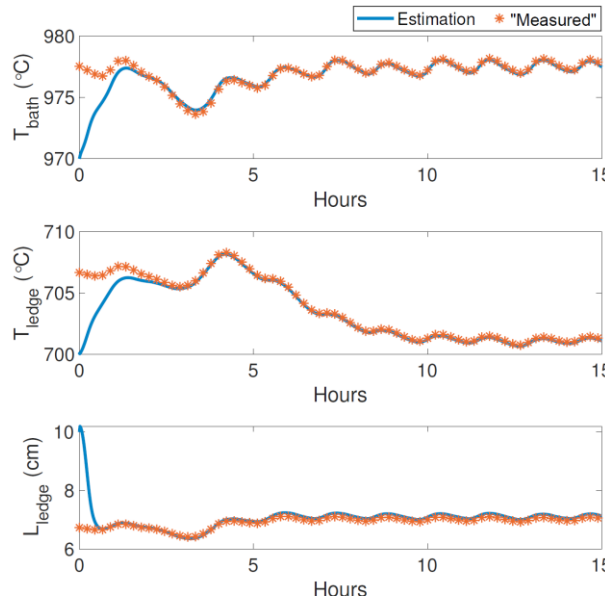
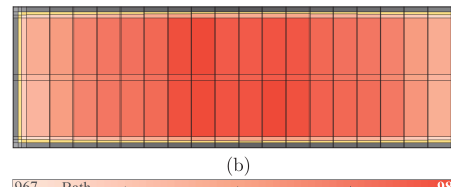
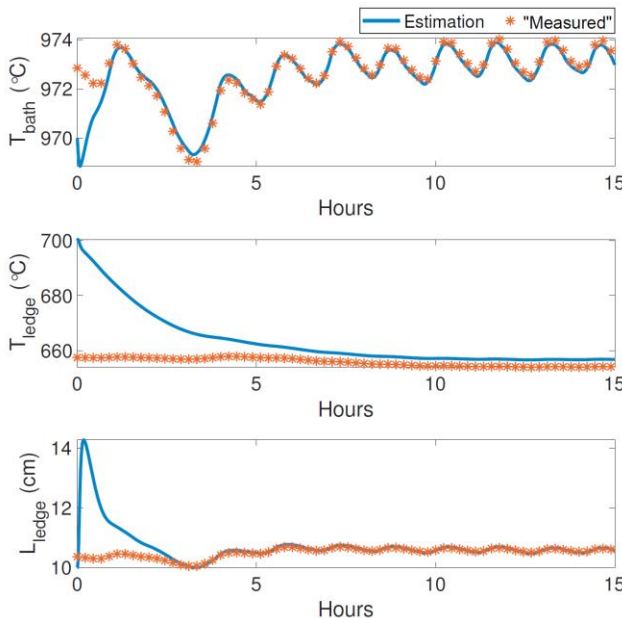
Twin concept:

- A digital twin based on our best models for electrolysis is built into the control system of the cells
- Soft sensor functionality: the twin predicts parameters that are difficult/time-consuming to measure
- Sensor/production data is used to calibrate the digital twin model
- Data analytics so far only for off-line analysis
- Use:
 - The twin automatically controls addition of alumina, temperature and acidity of the cells
 - Implemented in Karmøy technology pilot as well as several industrial smelters
- Effect:
 - More stable production with higher productivity and lower energy consumption



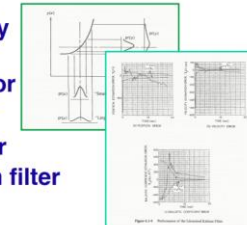
The Cell Digital Twin

- Wong (2021) is planning to use his multi-zones dynamic model as digital twin using EKF (Extended Kalman Filter)



Nonlinear State Estimation
Extended Kalman Filters
Robert Stengel
Optimal Control and Estimation, MAE 546
Princeton University, 2018

- Deformation of the probability distribution
- Neighboring-optimal estimator
- Extended Kalman-Bucy filter
- Hybrid extended Kalman filter
- Quasilinear extended Kalman filter





Thank You



IBAAS-JNARDDC TECHNICAL LECTURE SERIES 2022

